District of Columbia
Exceptional Event Demonstration and Analysis of the June 2023 Nova Scotia Wildfires, New Jersey fires and Their Impact on DC's Air Quality on June 1-2, 2023

January 26, 2024

DEPARTMENT OF ENERGY & ENVIRONMENT
GOVERNMENT OF THE DISTRICT OF COLUMBIA

Prepared by:
Air Quality Division
1200 First Street, NE, Fifth Floor
Washington, DC 20002

(This page is intentionally left blank)

Contents

List of Figures

List of Tables

1.0 Overview

1.1 Introduction

From March 2023, and with increased intensity starting in June, Canada has been affected by an ongoing, record-breaking series of wildfires. Approximately 270 individual wildfires burned across Saskatchewan, Alberta, the extreme southern Northwest Territories, and northeast British Columbia in west-central Canada in mid-May of 2023. While a few fires had commenced in early May, the period from May 13-20 across this domain effectively started the record-breaking wildfire season in Canada, nearly burning the cumulative total of the average annual burn area in Canada and 50-60% of the previous year's total in just these 8-9 days.

A prodigious smoke plume from these fires entered the continental United States (CONUS) on May 20. A potent central US. ridge, also responsible for above-normal temperatures and dry weather across Canada as a persistent blocking pattern, trapped the smoke in the lower troposphere for several days before finally arcing clockwise around the ridge to reach the Mid-Atlantic from the north-northeast in the May 30-June 2 period. While diffuse by this time, the smoke was well-aged and spatially pervasive, with elevated upstream ozone existing and following the path of the smoke and persisting across much of the northeastern quarter of CONUS from May 30th through June 2.

With all this transpiring, several other fires within closer proximity to the District of Columbia were occurring. Fires located in Nova Scotia and New Jersey contributed to the District's June 1-2, 2023, exceedance events. In the north-northeast, transport brought diffuse but regionally aged smoke from west-central Canada, smoke from fires in southern Nova Scotia, and several fires in New Jersey were similarly pushed into the District from May 30 to June 2. These fires further contributed to smoke and precursor concentrations amidst a regional background of aged smoke, exacerbating ozone development.

Regional ozone concentrations, supported by above-average temperatures, were higher by 10-20 parts per billion (ppb) than in similar situations without the smoke on June 1 and June 2, exceeding statistical thresholds of recent years. With the District being a completely urban environment, there was a clear enhancement of surface ozone near NOx sources. Furthermore, enhanced ozone pre-existed within the regional smoke plume and was observed tracking with it long before arriving in the District, indicating a clear causal relationship between the smoke and higher ozone by May 31 (near exceedances over a wide area) and widespread exceedances on June 1-2.

Maximum daily 8-hour average ozone (MD8AO) concentrations exceeded the 2015 ozone National Ambient Air Quality Standard (NAAQS) as the smoke plume migrated into the area, as seen in Figures 1 and 2. These figures depict the Air Quality Index (AQI) from June 1 and June 2. AQI is a tool created by EPA to report air quality in a way that is understandable to the general public. District MD8AO concentrations peaked at 81 ppb on June 1 at the McMillan Reservoir monitor, and at the same location, concentrations peaked at 75 ppb on June 2.

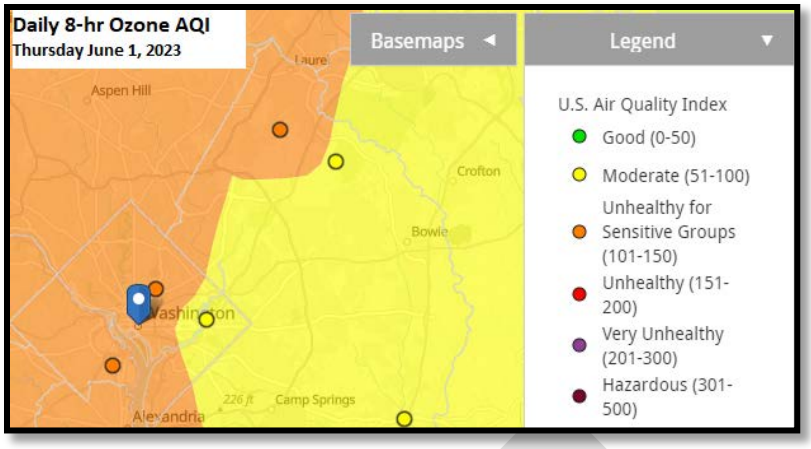

Figure 1: Washington, DC area AQI map on June 1, 2023.

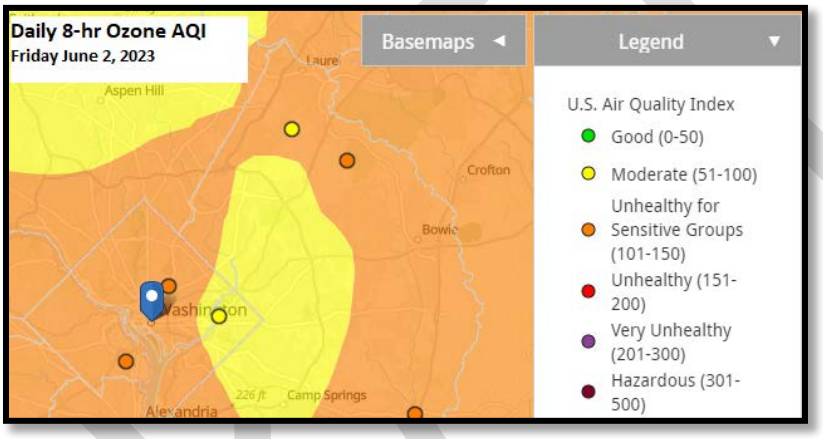

Figure 2: Washington, DC area AQI map on June 2, 2023.

Table 1: Maximum Daily 8-hour average ozone (MD8AO) concentrations on June 1 and 2, 2023, for the McMillan Reservoir reference monitor.

		MD8AO, ppb		2023	
Site Name	**AQSID**	**1-Jun**	**2-Jun**	**Fourth High, ppm**	**Est DV, ppm**
McMillan Reservoir	110010043	81	75	0.075	0.071

*** 2023 data are not certified as of this writing, and therefore, all DVs are estimated.**

Following the US. Environmental Protection Agency's (EPA) regulatory process for the Exceptional Events Rule (40 CFR § 50.14), the District of Columbia's Department of Energy and Environment (DOEE) flagged the data as being influenced by a Canadian wildfire and communicated to EPA, the District's intention of submitting an exceptional event package for ozone on June 1-2, 2023. This analysis demonstrates that the District's 8-hour ozone concentrations that exceeded the 2015 standard meet the requirements for having been influenced by an exceptional event and should, therefore, be excluded from design value (DV) calculations used to determine the District's ozone attainment status.

1.2 Exceptional Events Summary of Approach

The Exceptional Events Rule, as defined in 40 CFR § 50.14, states that an event may be excluded from regulatory use if it had the following characteristics:

1) *There is a clear, causal relationship between the event and the monitored exceedance that affects air quality.*
2) *The event was of human origins, not likely to recur, or was natural in origins.*
3) *The occurrence was not reasonably controllable or preventable.*

The 2016 Exceptional Events Rule at 40 CFR § 50.14(c)(3) states that an exceptional events demonstration must include the following elements:

1) *A narrative conceptual model that describes the event(s) causing the exceedance or violation and a discussion of how emissions from the event(s) led to the exceedance or violation at the affected monitor(s);*
2) *A demonstration that the event affected air quality in such a way that there exists a clear causal relationship between the specific event and the monitored exceedance or violation;*
3) *Analyses comparing the claimed event-influenced concentration(s) to concentrations at the same monitoring site at other times. The Administrator shall not require a State to prove a specific percentile point in the distribution of data;*
4) *A demonstration that the event was both not reasonably controllable and not reasonably preventable;*
5) *A demonstration that the event was caused by human activity that is unlikely to recur at a particular location or was a natural event; and*
6) *Documentation that the submitting air agency followed the public comment process.*

Furthermore, 40 CFR § 50.14(b)(4) states that the EPA:

"… Administrator shall exclude data from use in determinations of exceedances and violations where a State demonstrates to the Administrator's satisfaction that emissions from wildfires caused a specific air pollution concentration in excess of one or more national ambient air quality standards at a particular air quality monitoring location and otherwise satisfies the requirements of this section. Provided the Administrator determines that there is no compelling evidence to the contrary in the record, the Administrator will determine every wildfire occurring predominantly on wildland to have met the requirements identified in paragraph (c)(3)(iv)(D) [item (4) above] of this section regarding the not reasonably controllable or preventable criterion."

The guidance document also recommends following a tiered approach to the analysis, providing evidence of "Key Factors" in each tier. Following the elements suggested in the Exceptional Events Guidance Document[i] outlined above, DOEE contends and demonstrates here-in that transported wildfire smoke had a direct role in amplifying ozone concentrations to a level that would not have been possible in the absence of smoke and constituents and satisfies the three core exceptional event criteria. Based on recommendations from the EPA and the Guidance Document, the District used a Tier

3 weight of evidence approach for this analysis. DOEE addresses each of the necessary elements cited previously in the subsequent sections of this document.

The EPA Guidance Document offers suggestions for appropriate analyses to demonstrate the apparent causal relationship between wildfire and excessive ozone levels. In addition, EPA recognizes that appropriate levels of analysis will vary for particular locations and conditions. EPA does not intend for the guidance to constrain the analysis. DOEE includes some of the suggested analytics and variations on those methods to support our conclusion that the high ozone concentrations throughout the District were caused or worsened by the wildfire smoke from the Nova Scotia and New Jersey fires in June of 2023.

1.3 Regulatory Significance of the Exclusion

1.3.1 June1-2 2023 Exclusion Request

There are three ozone monitors in the District of Columbia (Figure 3) covering the Washington, DC-MD-VA nonattainment area. Those sites are Takoma Recreation Center (in the far north), McMillan Reservoir (central to the District), and River Terrace Education Campus (east of the Anacostia River). DOEE operates all three of these regulatory ozone monitors. On June 1 and 2, 2023, one of these three monitors had both MD8AO observations above 70ppb (Takoma Recreation Center was not operational at the time) exceeding the 70-ppb ozone NAAQS in the District and met the criteria for further analysis and potential exclusion according to those listed in 40 CFR § 50.14(a)(1)(i). Therefore, DOEE asks for the exclusion of both MD8AO observations for June 1 and 2, 2023, that exceeded 70 ppb at the McMillan (110010043) monitor. DOEE requests that these observed ozone concentrations on June 1 and 2, 2023, at the monitor, as listed in Table 1, be classified as an exceptional event and excluded from regulatory use.

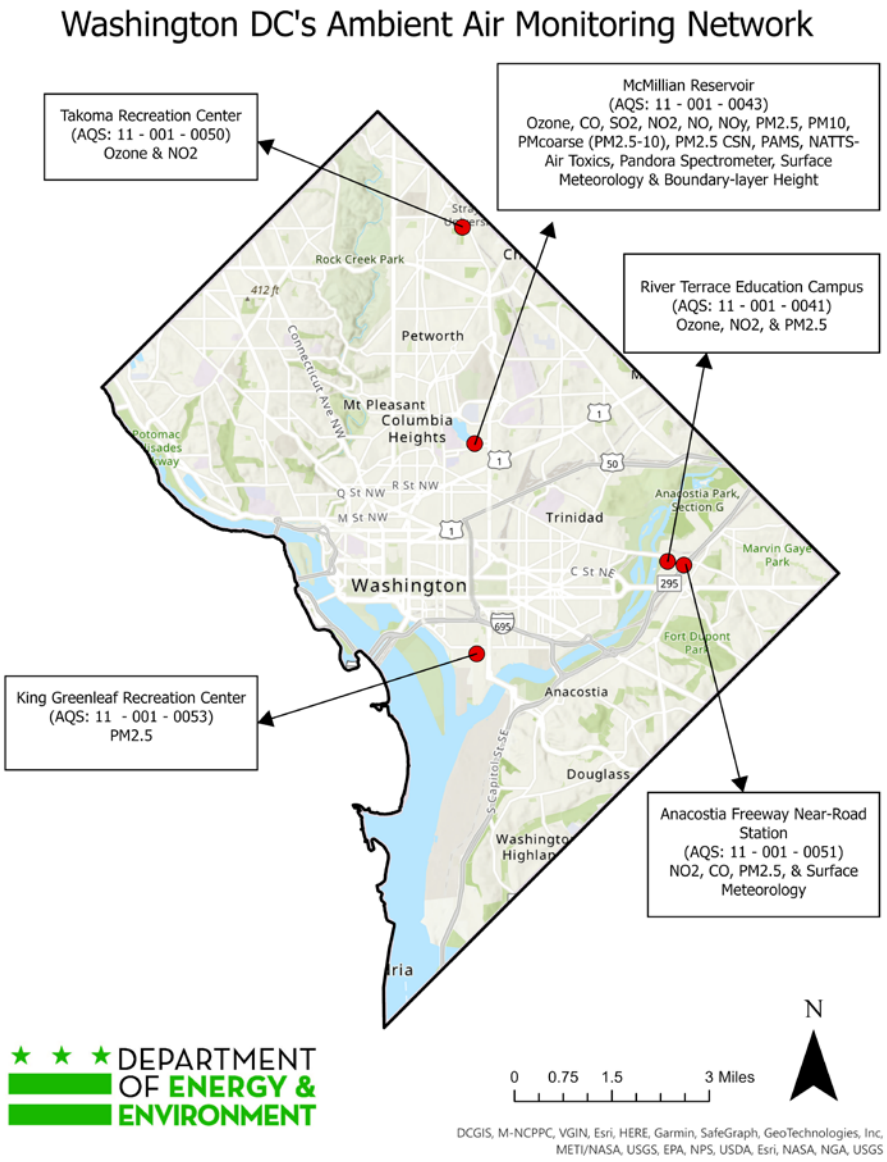

Figure 3: The District of Columbia's ambient air monitoring program as of June 2023. There are three sites that measure ground-level ozone.

		2023					
Site Name	**AQSID**	**MD8AO, ppb**		**Fourth High, ppb**		**Design Value, ppb**	
		1-Jun	**2-Jun**	**Including**	**Excluding**	**Including**	**Excluding**
McMillan	**110010043**	**81**	**75**	**75**	**72**	**71**	**70**

Table 2: Ozone monitors at which DOEE is seeking EPA data exclusion concurrence. Local names and Air Quality System (AQS) identification numbers (AQSID) identify monitors in the text.

Also given are the maximum daily 8-hour average ozone (MD8AO) concentrations in ppb. The final columns indicate the 2023 fourth high and design value with no exclusion of data (Including) and if the requested data from June 1st and 2nd is excluded from the fourth high and design value calculations (Excluding).

1.3.2 Design Value and Fourth High Impacts

Exclusion of MD8AO observations on June 1-2, 2023, will lead to lower DVs for the McMillan Reservoir monitor in the District of Columbia. The June 1-2, 2023, smoke events were two of the strongest smoke events of the year, aiding ozone production across the entire District network. Due to the large amount of smoke during the 2023 season, there were at least four smoke-impacted events at the highest monitor in the District (McMillan).

The EPA designates an area's attainment status of the NAAQS via the DV metric. For 8-hour ozone, each monitor's annual fourth-highest daily 8-hour maximum concentration averaged over the past three years designates the attainment status for that area. Ozone concentrations on June 1 and 2 were within the fourth-highest 8-hour average observations of 2023 at McMillan and Table 1. Excluding the June 1st and 2nd concentrations at the requested monitor

		2023					
Site Name	**AQSID**	**MD8AO, ppb**		**Fourth High, ppb**		**Design Value, ppb**	
		1-Jun	**2-Jun**	**Including**	**Excluding**	**Including**	**Excluding**
McMillan	**110010043**	**81**	**75**	**75**	**72**	**71**	**70**

Table 2 would reduce the design value for the McMillan monitor, which would drop below the 2015 70 ppb NAAQS level (from 71 to 70 ppb). Details of specific site DV with and without exceptional event status, along with changes in the fourth highest concentrations for June 1-2, 2023, are provided in

		2023					
Site Name	**AQSID**	**MD8AO, ppb**		**Fourth High, ppb**		**Design Value, ppb**	
		1-Jun	**2-Jun**	**Including**	**Excluding**	**Including**	**Excluding**
McMillan	**110010043**	**81**	**75**	**75**	**72**	**71**	**70**

Table 2 for the McMillan monitor that DOEE is requesting exceptional event data exclusion.

1.3.3 NAAQS Attainment Considerations

The Washington, DC-MD-VA ozone nonattainment area needs to demonstrate continued attainment of the 2015 ozone standard by August 2024. This continued attainment of the 2015 ozone standard would only occur if EPA concurs with this exceptional event demonstration for June 1-2, 2023.

EPA concurrence of the requested concentrations on June 1-2, 2023, in the District will bring the McMillan monitor (110010043), Washington, DC-MD-VA Non-Attainment Area (NAA) into attainment of the 2015 8-hour ozone NAAQS. At this time only, the McMillan monitor is the only monitor that is violating the NAAQS in the nonattainment area, and the area would be re-classified as in attainment of the 2015 NAAQS should EPA concur with the District's June 1-2, 2023 exceptional event demonstration. However, due to repeated smoke events and their impacts on ozone, this demonstration is one of two in the Washington, DC-MD-VA attainment area. DOEE will be submitting the other demonstrations to have a certain record of the events in the case these monitored values become policy-relevant in future years.

1.4 Summary of Findings

This report demonstrates that:

- There was a clear causal relationship between the smoke and the MD8AO exceedances;
- The wildfire-causing smoke was considered a natural event, and
- The smoke events in question were not reasonably preventable and are unlikely to recur.

Key findings and evidence supporting these assertions include the following:

- Copious, network-wide ozone was generated due to the presence of wildfire-smoke-generated ozone upstream transported into the District with rapid local generation due to smoke augmenting transport;
- Ozone higher than historical norms within an environment of historically low anthropogenic precursors and weak in-situ meteorological support (e.g., low temperatures) for ozone;
- A Q/d analysis which meets EPA thresholds for clear causal influence;
- Fine Particle ($PM_{2.5}$), Carbon Monoxide (CO), and Nitrogen Oxides (NOx) were elevated during the event, consistent with a wildfire smoke plume;
- Elevated $PM_{2.5}$ surface concentrations tracked from the wildfire region; and
- Satellites captured a visual smoke plume transported to the northeastern US, which was also associated with satellite-retrieved CO, both of which tracked from west-central Canada, with Nova Scotia and New Jersey fires adding to the smoke locally.

Several analysis methods were used to develop a weight-of-evidence demonstration that the 8-hour ozone concentrations above 70 ppb in the June 1-2, 2023 event meet the rules for data exclusion as an Exceptional Event. Satellite, meteorological data, trajectory analysis, and emissions data were used to assess whether conditions were favorable for the transport of smoke from west-central Canada wildfires to monitors that showed 8-hour ozone concentrations above 70 ppb. The data also showed that the transported smoke moved over the District, creating a prolonged enhanced ozone period and degraded air quality in the District from May 31 to June 2, specifically June 1 to 2.

Substantial changes in chemistry in the eastern United States due to regional NOx emissions reductions have occurred over the last two decades. The following analysis puts the 8-hour ozone concentrations in the District during this ozone event in the context of these reductions and in comparison to ozone in previous months of June. A comparison of emissions during late June of 2023 shows that aggregate Electric Generating Unit (EGU) NOx emissions were lower than any other year on record during the smoke event. Yet, ozone concentrations in June of 2023 exceeded ozone concentrations in earlier years during meteorology less conducive (cooler, less sunlight reaching the surface) compared to years under heavier anthropogenic precursor emissions. Analysis of the airmass associated with the District's ozone exceedances on June 1-2, 2023, revealed a composition characteristic of wildfires, with an abundance of ozone precursors despite substantial reductions in anthropogenic sources.

DOEE's analysis strongly supports that the MD8AO concentrations above 70 ppb in the District on June 1st -2nd, 2023, meet the rules as an Exceptional Event, and the corresponding MD8AO observations for the McMillan monitor in Table 2 should be excluded from DV calculations.

The following documentation justifies these claims and is outlined as follows:

- Section 2 contains a conceptual model overview of the event, including a synopsis of the meteorological and air quality conditions, emissions, transport, and characteristics defining the event.
- Section 3 demonstrates a clear causal relationship between the exceedance via a tiered, weight-of-evidence approach.
- Section 4 demonstrates that this event fulfills the definition of a natural event that is unlikely to recur.
- Section 5 fulfills the requirements that demonstrate the event was not reasonably controllable or preventable.
- Section 6 documents the public comment process.
- Section 7 summarizes and concludes the analysis.

2.0 Conceptual Model and Overview of the June 26-30, 2023, Smoke and Ozone Event

2.1 District of Columbia Area Description

As part of the Clean Air Act (CAA), both local and state air quality agencies are required to maintain and operate ambient air quality monitoring networks. The Air Monitoring Branch (AMB) in DOEE's Air Quality Division (AQD) operates, maintains, and performs all functions of the ambient air monitoring program required by the CAA. As required by federal air monitoring regulations, the District's monitoring network is designed to study expected high pollutant concentrations, high population density, significant sources, general background concentrations, and regional transport. The District's network currently consists of five monitoring sites. DOEE is proposing to add a new monitoring station in an overburdened environmental justice community in 2024.

Sampling covers criteria air pollutants, $PM_{2.5}$ mass and chemical speciation, and enhanced monitoring for ozone and its precursor pollutants with a photochemical assessment monitoring station (PAMS) for measuring speciated VOCs, NO_x, carbonyls, air toxics, and surface and meteorological parameters. A full description of the various instrumentation used by DOEE is available in the DOEE Ambient Air Monitoring Plan.[ii]

The District of Columbia is an urban area that has a geographic area of 68.3 square miles. It has an estimated population of 671,803 as of 2022, according to the US Census Bureau. The District of Columbia is surrounded by Northern Virginia on its southwest side and Maryland on its southeast, northeast, and northwest sides. The Washington, DC-MD-VA ozone nonattainment area is made up of the District of Columbia, five counties in Maryland, four counties in Virginia, and five independent cities in Virginia, as shown in Figure 4. This figure also shows the location of the 14 air quality monitors used in determining compliance with the ozone NAAQS.

Figure 4: Metropolitan Washington 8-hour Ozone Nonattainment Region (Washington, DC-MD-VA)

2.2 Characteristics of Typical, Non-Event Ozone Formation

In the absence of atypical air mass composition (for instance, extraordinary events or smoke plumes), the primary mechanism driving ozone formation in the District stems from the photolysis of volatile organic compounds (VOCs) and a combination of regionally and locally originated anthropogenic NO_x. This interplay is often accentuated by the densely populated areas and topographical features, leading to concentrated regions that historically have caused ozone-related challenges, particularly to the northeast of the District.

The key contributors to these challenges are human-made emissions from various sources: fixed point sources such as EGUs (electric generating units), mobile sources like cars, trucks, boats, locomotives, and non-road equipment, and area sources encompassing industrial processes and consumer goods. The predominant share of locally generated NO_x, a precursor to ozone, originates from urban pollution plumes that form along the I-95 corridor between the District and Baltimore, along with surrounding point sources, like EGUs. Nonetheless, these emissions alone frequently fall short of generating ozone concentrations exceeding 70 ppb in the District as measured by the MD8AO standard. Photochemical modeling underscores the argument that, excluding instances of light winds and recirculation that result in the accumulation of local emissions, the emissions from EGUs and mobile sources within the

District are insufficient to cause ozone levels to surpass regulatory thresholds. However, the District also lies at the downstream end of the EGU-rich Ohio River Valley (ORV), where a large density of EGU point sources generates a regional NO_x plume upstream, transporting NO_x and/or ozone into the District. Historical instances of ozone exceedances in the District are predominantly associated with this kind of transport phenomenon. Hence, the influx of ozone and ozone precursors, notably NO_x, within the residual layer (the layer of air immediately above the surface, typically situated around 500-2,000 meters above ground level) that enters the District through transport contributes to elevating local ozone levels, often surpassing NAAQS thresholds. In the absence of substantial transport, the District has experienced a reduction in widespread or frequent ozone exceedances of NAAQS standards.

Over the past five years, the District has experienced a dearth of pollution transport cases. In the time frame of 2019 to 2023, the concentration of ozone and its precursors in the residual layer have reached its lowest recorded levels. This reduction has led to a decrease in the maximum daily ozone concentration in the District, resulting in a decline in the frequency of ozone exceedance days. Consequently, local factors such as meteorology and emissions, which used to be overshadowed by regional signals, have gained more significance. Overall, this has led to isolated and infrequent exceedances, as illustrated in Figure 5**.** Emissions of NO_x from point sources in states upstream of and including D.C. (such as Maryland, D.C., Virginia, West Virginia, Pennsylvania, Ohio, and Indiana, represented as "Total NO_x" in Figure 6) during the ozone season have reached historically low levels. In fact, the total 2023 emissions in these upwind states were the lowest ever recorded. This decline has been consistent monthly throughout the season, resulting in a significant regional reduction of almost 50% over the past five years, as shown in Figure 4. NO_x emissions from mobile sources have also decreased during the same period. However, this reduction is overshadowed by the substantial decrease in EGU-related NO_x emissions. It is important to note that while mobile-source NO_x has decreased less compared to EGU-related NO_x, the current emissions from mobile sources in the District, even when combined with additional local EGU emissions, are insufficient to cause anything but isolated and infrequent ozone exceedance days within the state.

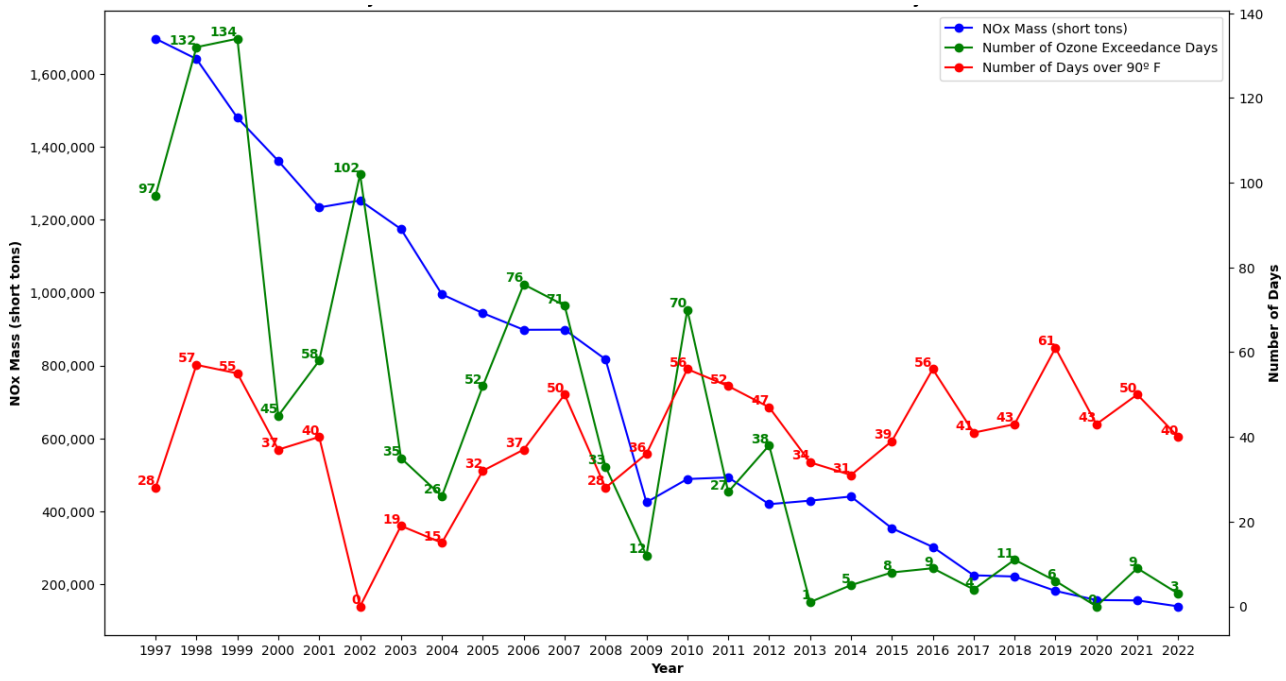

Figure 5: Annual EGU NO_x from the District of Columbia and upwind states, number of days at or above 90°F at National Arboretum (90 DD), and exceedance days at various standards.

2.2.1 Emissions Trends

In the context of a standard scenario involving a District ozone exceedance day, as described earlier, the primary source of NO_x transport into the state stems from upwind EGU point sources. These source emissions can result in elevated ozone concentrations the next day, which compounds the local emissions issue. The Clean Air Markets Database (CAMD) records the NO_x emissions originating from EGU point sources across the nation. Over the past 15-20 years, there have been notable and sustained reductions in NO_x emissions throughout the eastern United States, as illustrated in Figure 6. In 2023, the cumulative NO_x emissions from upstream states had dwindled to a mere 20% of their 2010 levels, marking a substantial decrease of approximately 80%. Furthermore, the collective monthly total NO_x emissions from May to September 2023 were the lowest ever recorded from upwind states, including Indiana, Ohio, West Virginia, Virginia, Pennsylvania, the District of Columbia, and Maryland, as depicted in Figure 6. These states together constitute a significant source region for ozone or ozone precursors transported into the District during typical summer conditions of favorable meteorology. In June 2023, NO_x emissions from these areas were approximately 15% of what was observed in 2010.

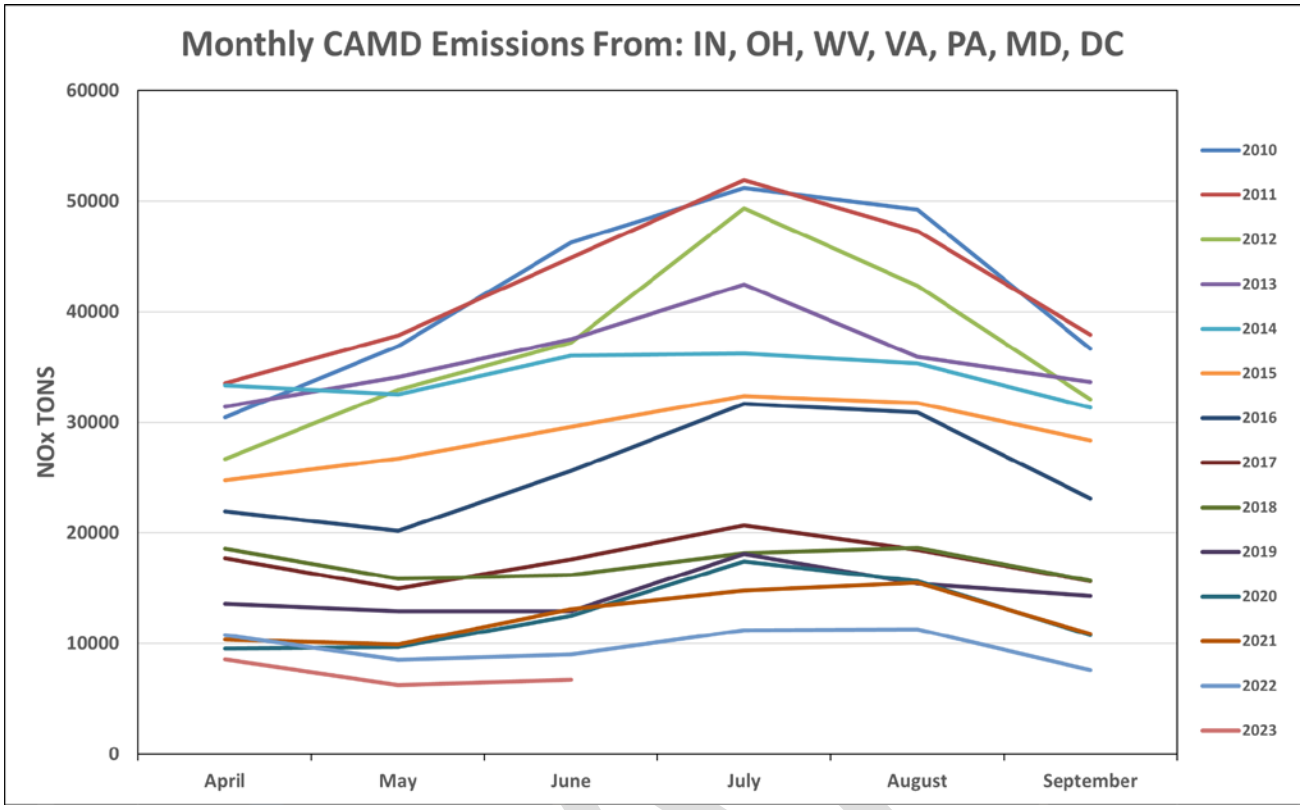

Figure 6: Monthly NO_x-aggregated from the group of upwind states, including the District by Month of ozone season.

The daily emissions data for these same states reflects the same reductions. When we examine the daily combined NO_x emissions from Indiana, Ohio, West Virginia, Virginia, Pennsylvania, Maryland, and the District of Columbia, focusing solely on the month of June from 2017 to 2023 as extracted from CAMD, it becomes evident that the total emissions in June 2023 reached an all-time low. A steady downward trend is observed. Despite these historically low emissions in June 2023, the District experienced one of the worst air quality days in over ten years (June 29th, 2023), with 2 of the District's three ozone monitors exceeding the daily maximum 8-hour ozone standard of 70 parts per billion (ppb) (as represented by the green bars in Figure 7).

Aggregate NO_x emissions from EGU point sources for states upwind of the District (Indiana, Ohio, Pennsylvania, West Virginia, Virginia, DC, and Maryland) from the CAMD database for 2017 – 2023 are shown with the blue points. The maximum 8-hour average ozone at any monitor in the District for each day in June 2017-2023 (orange bars) and the number of monitors exceeding 70 ppb in the District (green bars) is also shown. A downward trend in emissions is noticeable throughout the period, with the lowest emissions in 2023. An increase in NO_x emissions towards the end of June 2023 is apparent, but the increase only matches the mean of the 2022 season, which was the lowest year up to that point.

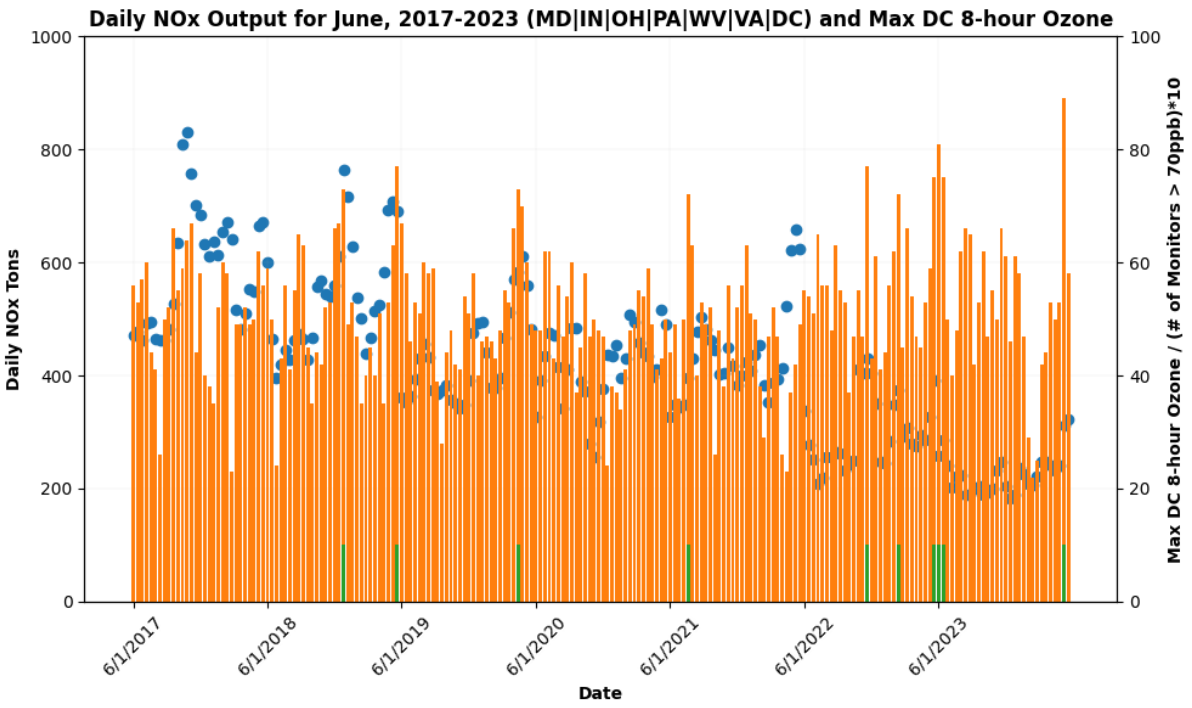

Figure 7: Daily aggregate NO_x, maximum DC ozone, and monitors exceeding 70 ppb in May 2017-2023.

2.2.2 Ozone Production in the District

Research has found that the generation of ozone in the District involves a complex interplay between volatile organic compounds (VOCs) and nitrogen oxides (NO_x), and the atmospheric balance of each required to produce biproducts like ozone. In the past, the balance between these two precursor groups was of little significance compared to their absolute concentrations in the atmosphere. Both precursors were consistently abundant for ozone exceedances and were primarily influenced by weather conditions. For instance, the fluctuations in exceedances depicted in Figure 5 at the 70 parts per billion (ppb) level exhibited a strong correlation with the number of days reaching 90° Fahrenheit between 2000 and 2015. However, in more recent years, this correlation has diminished. The District has now transitioned into a NO_x-limited regime due to regional reductions in NO_x emissions (Roberts et al., 2022). Consequently, the stoichiometry of ozone production is no longer in equilibrium, and daily ozone production depends on the availability of either precursor group and/or the quantity of ozone already formed upstream and transported into the state. As a secondary consequence, high temperatures are no longer a dependable predictor of daily ozone exceedances of the NAAQS.

Ozone production hinges on the availability of NO_x and VOCs, as well as favorable meteorological conditions of ample heat and sunlight. In the District, the VOCs relevant to ozone production encompass both naturally occurring and human-made sources. Although there has been a noticeable reduction in anthropogenic VOCs in tandem with the decrease in NO_x emissions, it's crucial to acknowledge that daily ozone production driven by biogenic (naturally occurring) VOCs cannot be controlled and remains a significant contributor to ozone chemistry in the District. For example, isoprene, a naturally occurring VOC, has the highest maximum incremental reactivity (i.e., easily makes

more ozone) of VOCs tested in the District, and is the highest VOC contributor on high ozone days. Isoprene is emitted by the biosphere, particularly trees, in response to environmental stressors such as elevated temperatures. NO_x emissions from stationary sources also tend to rise on warm summer days due to increased energy demand, while mobile emissions exhibit relative consistency on workdays and diminish over the weekend, unaffected by temperature. Simultaneously, as NO_x output increases relative to temperature, biogenic VOCs are released into the local environment. When exposed to sunlight and heat, these biogenic VOCs facilitate the creation of local ozone. When this locally generated ozone and ozone precursors mix with those transported into the state, the District observes MD8AO above 70 ppb and exhibits its fundamental non-event ozone exceedance. In this NO_x-constrained environment, absent additional transported ozone or ozone precursors, the District's local emissions are insufficient to produce ozone exceedance days.

2.2.3 Weather Patterns Leading to Ozone Formation

The District experiences variable meteorological conditions during the summer. While occasional April days may witness ozone levels surpassing standard limits, many of such instances occur mainly from May to September. Changing weather conditions within the ozone season result in diverse meteorological patterns that favor ozone formation. These include leeside troughing (where downward air movements on the lee side of the Appalachian Mountains create a zone of pollutant convergence along the I-95 corridor). Other such meteorological patterns or processes include airmass and ozone transport and mixing, as well as local recirculation and stagnation, including reverse I-95 corridor flow from the northeast. On the local scale, meteorological factors on which ozone concentrations depend are the amount of available sunlight (ultraviolet range), temperature, and the amount of space (volume) in which precursor emissions mix. Sunlight drives the key photochemical reactions for ozone and its key precursors, and the emissions rates of many precursors (isoprene, for example) are temperature dependent (Ryan and Dickerson, 2000, p2-1).

Ozone production within each pattern depends on favorable local weather conditions, such as warm, sunny days with light to moderate surface winds. The positioning of the Bermuda High ultimately dictates which of these scenarios prevails. During an average summer, the Bermuda High is positioned off the southeast Atlantic coast of the United States, resulting in westerly transport of air towards the District, varying in direction depending on altitude. This creates conditions favorable for cross-Appalachian flow. Leeside troughing relies on weak cross-mountain flow, creating compressional heating and column stretching on the mountains' lee side, often aligning with the I-95 corridor and leading to increased ozone concentration. Both transport and lee troughing can occur simultaneously or independently. In the presence of downward mixing of transported ozone, lee troughing may lead to ozone exceedance days. Over several days, recirculation and stagnation can also elevate local pollution concentrations, exceeding NAAQS levels. These patterns are most likely to occur during the summer months of June through August, historically the peak period for ozone production in the District. Shoulder seasons, like Spring and Fall, are typically cooler, with active weather patterns that prevent the buildup of local or regional emissions. Winter, on the other hand, is too cold for ozone exceedances.

As temperatures rise, there is an increase in the release of super-regional NO_x emissions from power plants located upstream, such as those in the Ohio River Valley (ORV) and western Pennsylvania. This elevated output leads to higher concentrations of ozone and ozone precursor compounds in the residual atmospheric layer. Over time, these substances mix down and blend with locally sourced pollutants, contributing to instances of ozone exceedances in the District.

2.3 Exceptional Event Description: May 2023 West-Central Canada Wildfires, Nova Scotia Wildfires, and New Jersey Wildfires

Abnormally warm and dry conditions during the winter and early spring of 2023 set the stage for a record Canadian wildfire season. Analysis of average temperatures confirms that Nova Scotia's winters are getting warmer. North American snow cover in May was the lowest it has ever been since measurements began being taken in 1966 (over 55 years) (see Figure 8). The little amount of snow that fell across Nova Scotia melted sooner, exposing fire fuels sooner than typical. The Canadian wildfire season typically runs from May through October, peaking in July. However, with snowpack far less than average, wildfires across Canada started considerably earlier, with seasonal fires being detected as early as March.

Numerous wildfires broke out across Canada this wildfire season, with fires out of control over various parts of the country, causing large surges of smoke. Fires burned out of control for the entire month as surges of smoke poured from hundreds of large source regions. Firefighters from as far as Spain, Portugal, and France assisted local teams in battling the flames.[iii] In May, fire concerns were most concentrated around Alberta and Saskatchewan. Early ozone season MD8AO in the District was impacted by fires from these areas in May. A significant increase in the number and area of fires, followed by a period of lightning strikes across Alberta, Saskatchewan, and into British Columbia and the extreme southern Northwest Territories of Canada. NOAA Daily Hazard Mapping System (HMS) smoke and fire analyses (McNamara et al., 2004), as well as the Canadian Wildland Fire Information System (CWFIS), detected an increase in the number and intensity of fires, particularly across Alberta, Saskatchewan, and the Northwest Territories, and British Columbia. Between May 13 and May 20, 270 fires burned across this region (Figure 9). While the fires covered a wide geographical area, meteorological conditions aggregated smoke from these fires into an eventual consolidated smoke plume from the region, pushing into eastern Montana and western North Dakota on May 20, 2023.

Nova Scotia saw the largest recorded wildfires in their history. On average, in Nova Scotia, only about 3% of wildfires are caused by lightning, with the remaining being caused by human activity. By June 1, 2023, there were four out-of-control fires in the province. One of the major wildfires of interest started around May 27, 2023, near Barrington Lake in Shelburne County (Figure 10 depicts satellite data from NASA that shows the area where the wildfire was burning). The top is accumulated hectares burned, reported by the Canadian Wildland Fire Information System (CWFIS), by day over the last ten years. The burn area is estimated by satellite. There was burn area intensification noticed around May 13-21, 2023, leading to an increase in emissions in that time. The area circled highlights the early July period of burning across Canada, with much of the area occurring across west-central regions. Burning across Canada in 2023 is unprecedented compared to any recent year. The bottom is Fire Radiative Power (FRP) in Terawatts (TW) from the satellite. FRP measures the fire intensity and burning temperature. A

steeper slope signifies a greater number or greater intensity of fires. A steep upward increase occurred during the May 13-21 period due to the west central Canada fires, indicating fires of high intensity. The fire burned around 23,015 hectares, and between 30 and 40 structures were destroyed. The response to this included widespread evacuation orders from the surrounding area, displacing 5000 people. This was the largest wildfire recorded in the history of Nova Scotia.

While all this was occurring, there were four fires in New Jersey between May 29th and June 2nd. First, there was the Box Turtle fire that happened on May 29th, burning 158 acres. The next fire in New Jersey was the Allen Road fire, which started on May 31st and was extinguished by June 2nd, burning 2,215 acres, with 1772 acres burnt in June alone (Figure 16 and Figure 17). Then, there was the Fort Dix fire in central New Jersey. It is believed that this had a burn area of about 77 acres. Lastly, the Flat Iron fire on June 2nd, southeast of Philadelphia, with a burnt area of about 86 acres.

In the end, no single fire was responsible for the smoke that was present in the District from May 31st to June 2nd. An aggregation of smoke from two larger, regionally impacting fires (west-central Canada and Nova Scotia) created a background environment with diffuse, chemically aged smoke associated with a regional extent of ozone-enhanced air, to which localized additional fires along the I-95 corridor in New Jersey added additional smoke to create an airmass richly supportive of ozone generation. Together, the impact of the combined smoke resulted in 2 ozone exceedances on June 1 and 2. Figure 11: May 2023 Nova Scotia Wildfire. Satellite data from NASA on May 28, 2023, shows the area where the wildfire is burning in Shelburne County.

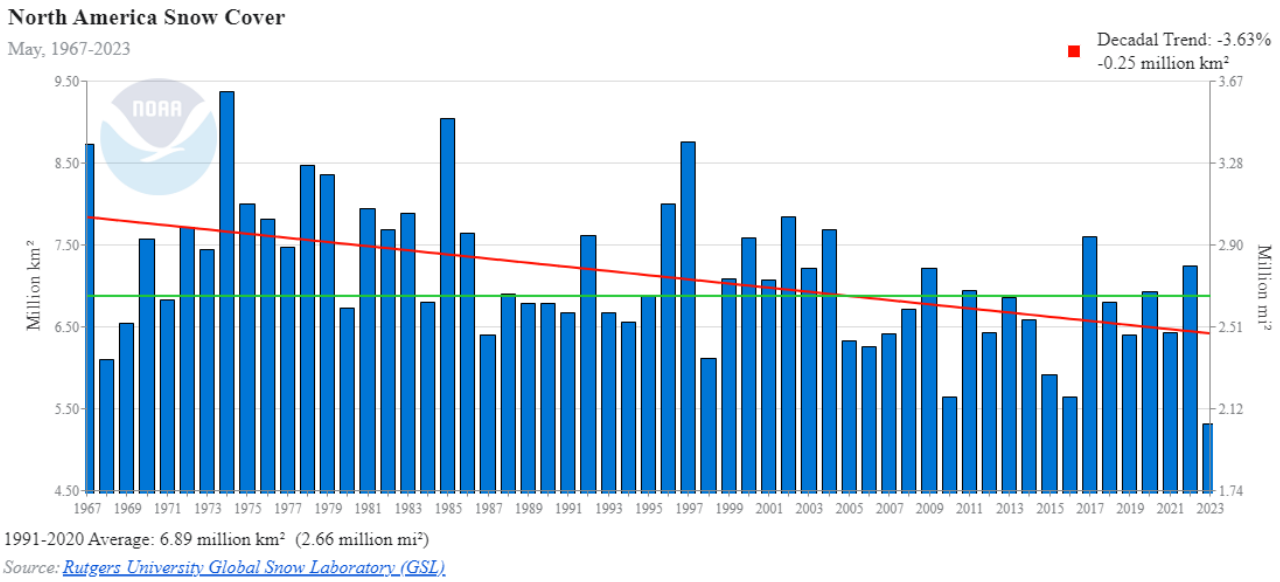

Figure 8: North American Snow Cover (Millions km^2) each May between 1967 and 2023. Average line in green and decadal trend line in red.

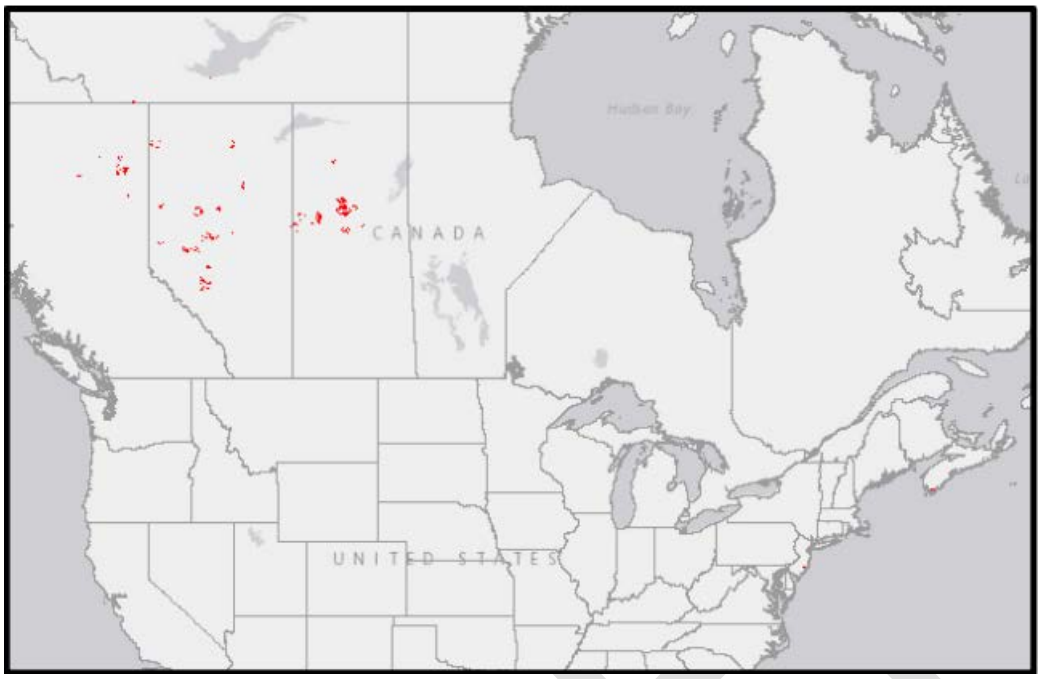

Figure 9: May 13-20, 2023, fire locations relevant to this demonstration.

Fire areas burned (red) derived from the CWIFS from satellites such as GOES Imager, the POES AVHRR and MODIS satellites, and expert ground reports and analysis are shown for the period from May 13-20, 2023. Note the fires in southern Nova Scotia and New Jersey, as well as west-central Canada.

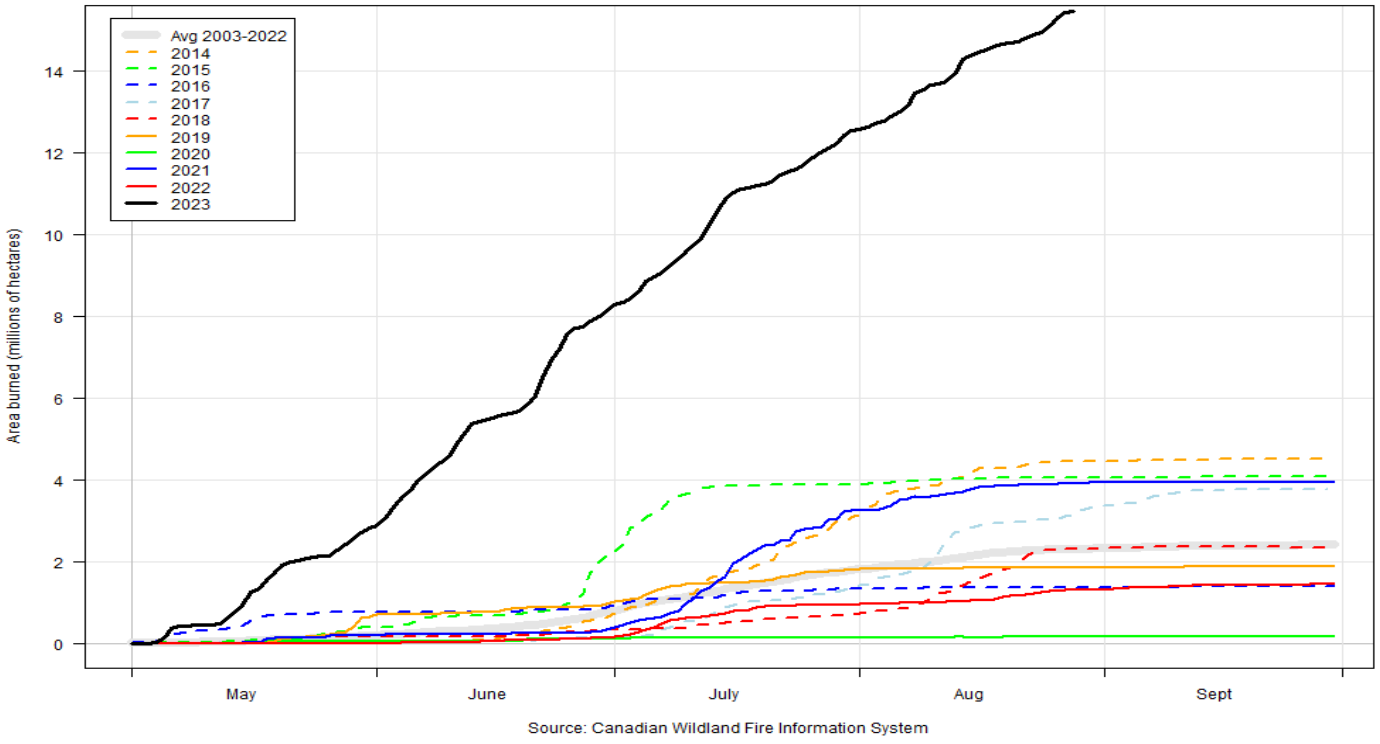

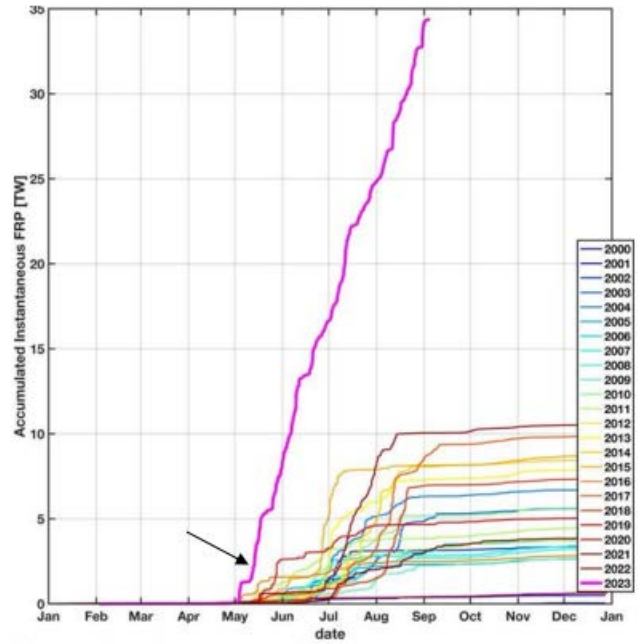

Figure 10: Top: Accumulated hectares burned, Bottom: Fire Radiative Power. Source: https://cwfis.cfs.nrcan.gc.ca/downloads/hotspots/burnarea_chart_10yr.png Source: Dr. Neil Lareau, X (Twitter) feed: https://twitter.com/nplareau/status/1699815550078390706. Used with Permission.

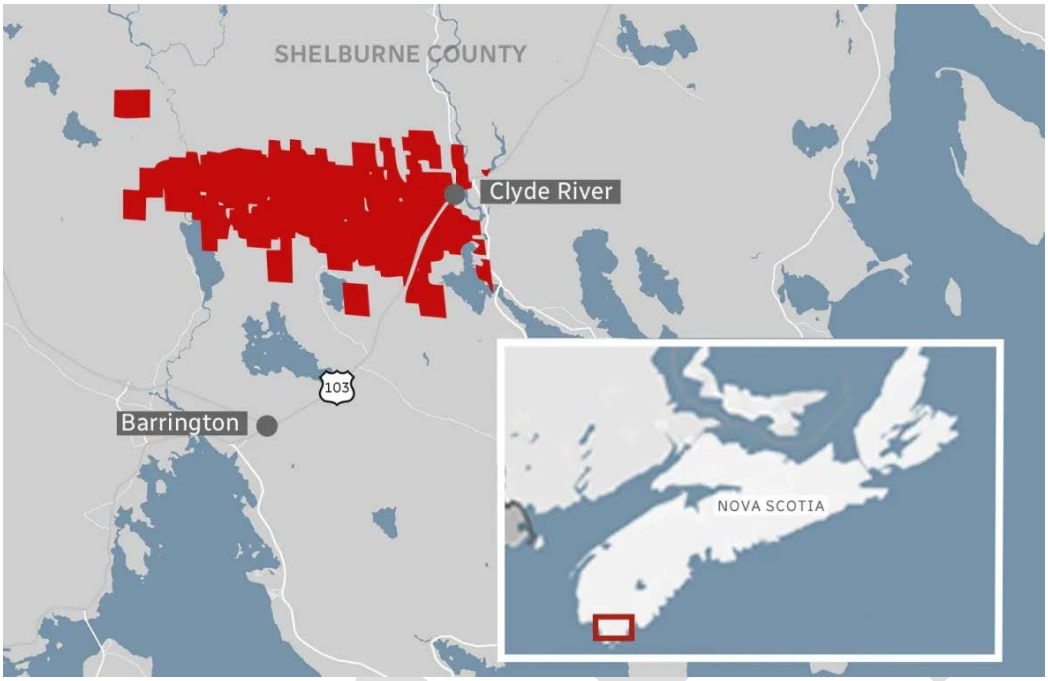

Figure 11: May 2023 Nova Scotia Wildfire. Satellite data from NASA on May 28, 2023, shows the area where the wildfire is burning in Shelburne County.

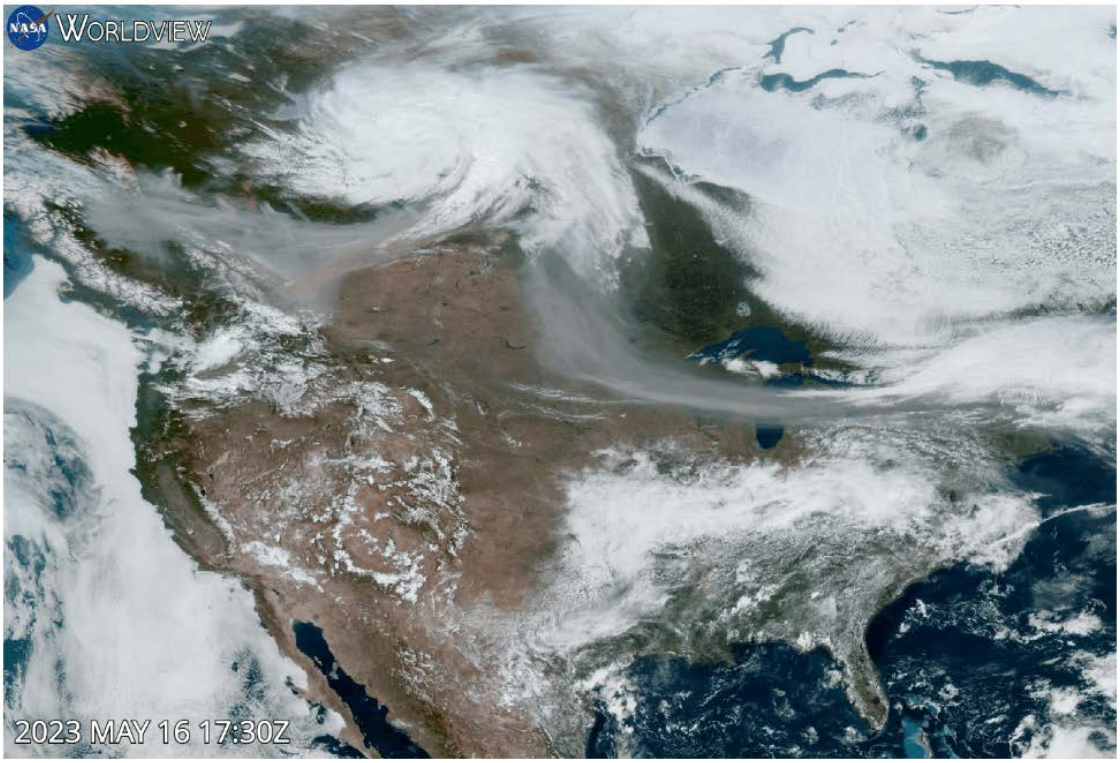

Figure 12: Smoke from fires in Alberta and British Columbia, Canada, 5/16/2023 (ABI instrument/GOES-East satellite).
https://www.earthdata.nasa.gov/worldview/worldview-image-archive/canada-fires-16-may-2023

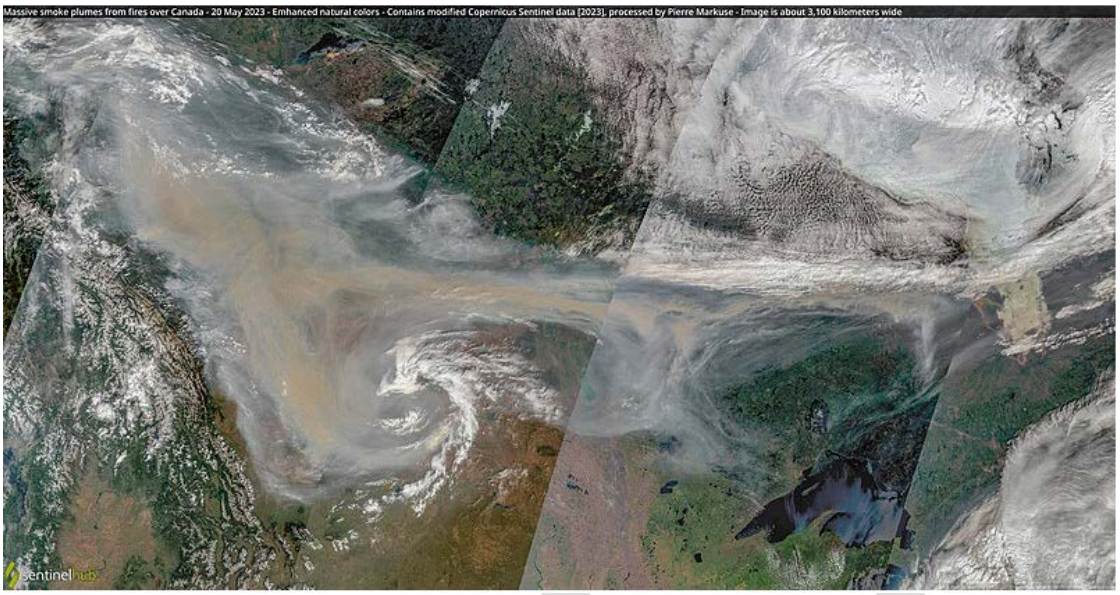

Figure 13: Massive smoke plume from fires over Canada, 5/20/2023. https://en.wikipedia.org/wiki/File:Massive_smoke_plumes_from_fires_over_Canada_-_20_May_2023_%2852913795290%29.jpg

Figure 14: May 15, 2023 (Alberta, Canada). https://www.reuters.com/pictures/wildfires-choke-alberta-skies-air-quality-deteriorates-2023-05-17/DQALRQTGAJKLNL2QBANXPJMJR4/

Figure 15: May 16, 2023 (Alberta, Canada). https://www.reuters.com/pictures/wildfires-choke-alberta-skies-air-quality-deteriorates-2023-05-17/DQALRQTGAJKLNL2QBANXPJMJR4/

Figure 16: Allen Road Wildfire in Bass River State Forest, New Jersey, 6/1/2023. https://www.inquirer.com/news/new-jersey/new-jersey-wildfire-pinelands-bass-river-state-forest-20230601.html

Figure 17: Allen Road Wildfire in Bass River State Forest, New Jersey, 6/1/2023. https://www.inquirer.com/news/new-jersey/new-jersey-wildfire-pinelands-bass-river-state-forest-20230601.html

Figure 18: New Jersey officials said the Allen Road Wildfire within the Bass River State Forest, which has burned over 5,000 acres, is 50% contained. (Courtesy of 6abc) Allen Road Wildfire in Bass River State Forest 50% contained - WHYY

2.4 Conceptual Model of Ozone Formation from June 2023 Quebec Fires

2.4.1 Overview and Literature Review

Wildfires are known sources of emissions responsible for both primary and secondary pollutants, including CO, PM2.5, NOx, VOCs, as well as ozone (Andreae and Merlet, 2001; McKeen et al., 2002; Bytnerowicz et al., 2010). Similar to the study presented here, Canadian wildfires have increased ozone concentrations in Houston, TX (Morris et al., 2006) and as far away as Europe (Spichtinger et al., 2001). Evidence of Canadian wildfire smoke and biomass burning affecting the Mid-Atlantic's particulate matter (PM) air quality was also previously reported (Adam et al., 2004; Colarco et al., 2004; Sapkota et al., 2005; Dreessen et al., 2016) but wildfire smoke has also been recognized in high-ozone events on the East Coast (Fiore et al., 2014). DeBell et al., (2004) presented a chemical characterization of the July 2002 Quebec wildfire smoke plume and its impact on atmospheric chemistry in the northeastern United States. More recently, Dreessen et. al., (2016) presented a case where a Saskatchewan, Canada wildfire smoke plume amplified ozone in Maryland in June of 2015.

While historically infrequent in the Mid-Atlantic, wildfire smoke has been an increasing fractional contribution to high-ozone exceedance days, particularly in light of increased fire frequency in a warming climate (Flannigan and Wagner, 1991; Marlon et al., 2009; Westerling et al., 2006; Spracklen et al., 2009; Pechony and Shindell, 2010), decreasing regional NOx emissions (Gégo, et al., 2007) and tighter ozone NAAQS (https://www.epa.gov/ground-level-ozone-pollution).

2.4.2 Ozone Generation from the Fire

Wildfires generate precursors that may directly lead to ozone formation or indirectly foster ozone through atmospheric composition that disproportionately generates ozone when impacted by anthropogenic precursors. Dreessen et al. (2016) previously showed that smoke plumes from Central Canada are capable of transporting ozone to the Mid-Atlantic and causing NAAQS exceedances, even in the contemporaneously low NO_x emission environment. As in the June 2015 ozone case covered in Dreessen et al. (2016), the June 2023 ozone events across the Northeast and Mid-Atlantic US were characterized by smoke plumes associated with ozone, increasing in concentration as the smoke plume aged.

During the late June 2023 Quebec wildfire event, ozone was transported into the District after being produced in a modified airmass upstream of the District. Furthermore, active chemistry within the plume exacerbated any local de minimis emission contributions (in relation to the plume concentrations) to foster rapid ozone chemistry. In other words, in addition to 'already formed ozone' transported in the smoke, chemistry in the smoke enhanced local ozone production beyond expected concentration outcomes. In the 2015 case study examined by Dreessen et al. (2016), it was hypothesized that once the smoke-sourced VOC-rich plume interacted with anthropogenic NO_x sources, that copious ozone production began, which was capable of being transported long distances as either ozone or within ozone reservoir species.

Dreessen et al. (2016) also acknowledged NO_x contribution from the fire itself, though focused on the plume's interaction with anthropogenic sources. In that 2015 study, smoke subsided across the eastern Midwest and northern Mid-Atlantic and took over 24 hours of aging before ozone above 70 ppb was widespread across the region. This delay in ozone production while the airmass aged is consistent with previous studies such as Putero et al. (2014), which observed the largest increases in ozone from fires five days (120 hours) after the initial pollutants were emitted from the fire (Figure 19).

In the current June 1-2 case, the FRP increased proportionally greater than the area burned (compare Figure 9 top and bottom, annotated area, compared to other burn periods), suggesting hot fires in addition to evident smoke. Increased RFP suggests more NO_x output than normally would be expected; this will be explored in subsequent sections. The ozone content of the plume built steadily over the week leading up to June 1, with an observed ozone concentration of 81ppb, and June 2, with an observed ozone concentration of 75ppb. Buildup was balanced with air mass diffusion, dispersion, and ozone deposition. Nevertheless, ozone expanded in spatial coverage with relatively consistent concentrations. This was generally consistent with increased ozone with aged smoke.

Smoke arrived at the surface in the District behind a cold front on May 29th. Cool temperatures and cloud cover on May 30th prevented significant ozone production, but an increase in particles noted the smoke's arrival. This was evident on May 31st, as we saw a notable increase in ozone concentrations. Additional fires in Nova Scotia and New Jersey contributed to the smoke in the area. On June 1st, we saw an MD8AO of 81ppb in the District. The following day, we saw an MDA8O of 75ppb in the District. All are consistent with the presence of smoke. Thus, sufficient precursors were generated by the fires in May/June of 2023 for ozone production over the NAAQS standard as the plume aged and mixed with anthropogenic NOx. In so doing, ozone concentrations were augmented to and above levels exceeding the NAAQS, not possible without the smoke.

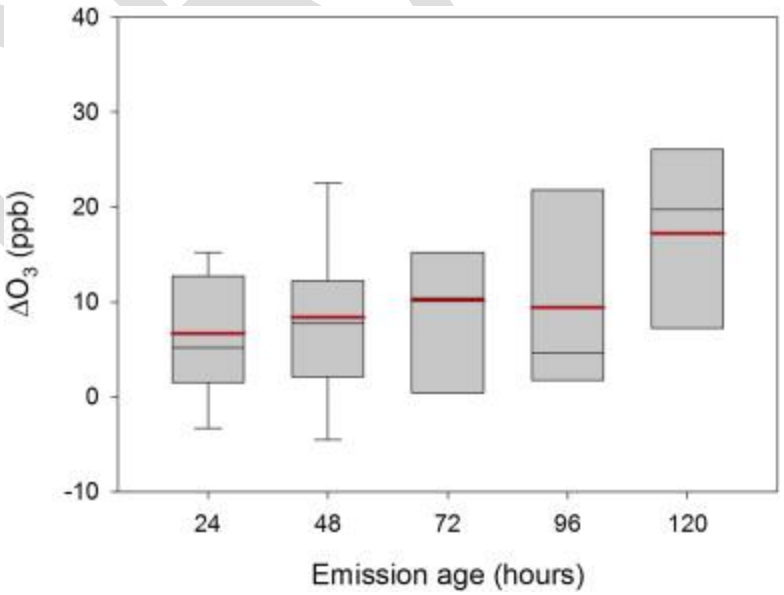

Figure 19: Ozone enhancement with smoke plume age.
(from Putero et al. (2014), Figure 7)

DOEE contends that the abundance of recirculated, age smoke from west-central Canada created a pool of ozone across a vast expanse of northeastern CONUS. This pool of ozone stuck beneath a persisting area of high pressure was augmented further by smoke from the Nova Scotia and New Jersey fires, all of which caused additional smoke to arrive in the District around May 30th through June 2nd. These latter fires were in closer proximity to the District and caused an influx of denser smoke atop the regional background. The resulting chemical composition of the air was thereby highly reactive with favorable chemistry for ozone, which led to exceedances on June 1-2 in the District.

While anthropogenic NOx emissions were not absent, EGUs, for example, had NOx emissions lower than the previous years of emissions during the same period. Any influx of new NOx emissions from local anthropogenic sources acts rapidly in these reactive atmospheres, exacerbating local conditions well beyond contemporary concentrations. The magnitude and spatial scale of widespread ozone, stretching from the Great Lakes to the East Coast, was beyond contemporary norms. Therefore, it is unlikely such a widespread area of ozone exceedance could have occurred in the contemporaneously low emissions without additional supportive atmospheric chemistry (ozone precursors) provided by the wildfire smoke. Below, the event is described in detail.

2.4.3 Meteorological Conditions Driving Smoke and Ozone Transport

2.4.3.1 Conceptual Model Overview

Fires were already ongoing in Alberta, Canada, in early May 2023 due to an early start. An immense increase in the number of fires and areas burned occurred as widespread lightning strikes ignited hundreds of additional fires in Alberta, Saskatchewan, nearby areas of British Columbia, and even the extreme southern Northwest Territories. Over 200 fires burned over 1.4 million hectares between May 13 and May 20 (Figures 8-9). A brief day or two period of recirculation occurred over the fire on roughly May 18 and May 19 before northerly flow pushed a thick, conglomerate smoke plume southward on the west side of a weak low-level, low-pressure system and ridging upstream. This smoke plume entered northern CONUS on May 20 and stagnated for a day or two along the north-central US and Canadian border before being pulled into and trapped under an immense (in spatial extent) and strong ridge of high pressure, effectively trapping the smoke in a clockwise recirculation for the next week (Figure 20). Some smoke at higher elevations managed to disperse farther southwards along the Canadian front range. The result was smoke from the Gulf of Mexico to the Great Lakes, covering the entire western half of the high-pressure system encompassing central CONUS.

Over the course of about a week, smoke remained trapped within the high-pressure system centered across the northern tier of CONUS, to arcing around the Great Lakes by May 31-June 2. Clockwise flow around this high-pressure system took smoke northward into Canada before the pattern would bring smoke back southward. However, north transport on the east side of the low kept bringing cleaner air from polar regions across the far eastern US, pushing the smoke back towards the high center repeatedly. Eventually, as the center of high pressure moved eastward to be centered over southern Ontario, eastward transport aloft pushed smoke into and behind another cold front on May 29, passing

through the District. The subsiding dynamics of this system pulled smoke to the surface, inundating the entire northeastern US in diffuse smoke from May 30 - June 3.

Concurrent with this large-scale transport, significant fires developed in Nova Scotia on May 28-June 2. Part of the smoke from these fires, particularly from burns occurring May 29-May 30, was pulled toward the Mid-Atlantic behind the cold front, further exacerbating the smoke concentration at the surface. Finally, local fires in New Jersey occurred May 31-June 2; at least one of these fires was significant in size, with all three or four fires in New Jersey providing further smoke into the region due to north-northeast flow behind the cold front moving through on May 29, with persisting smoke through June 2.

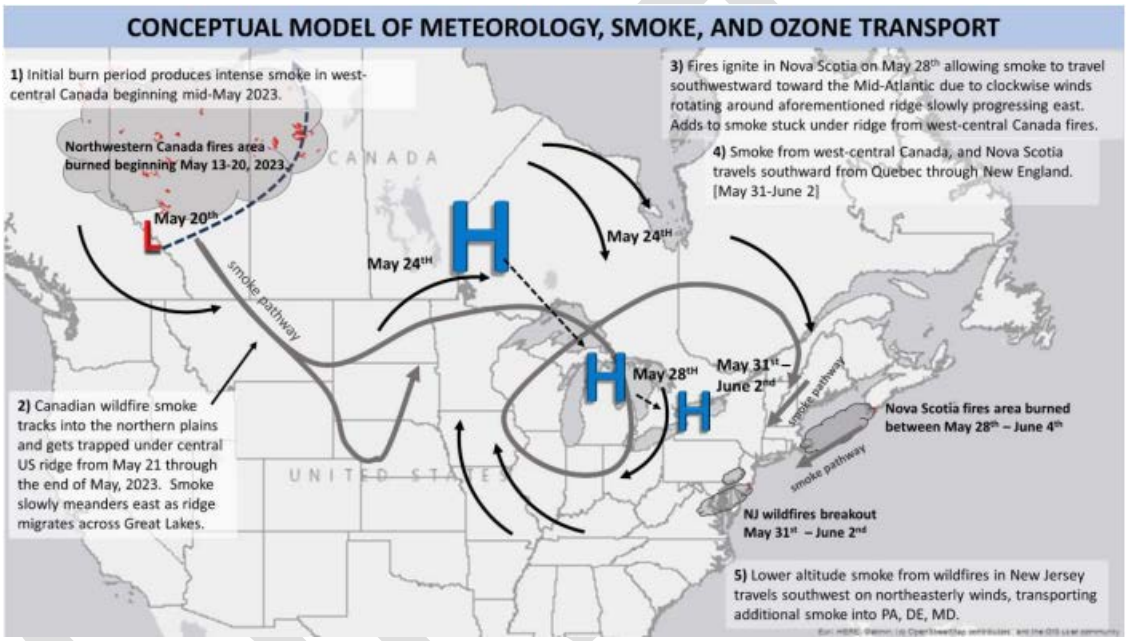

Figure 20: A simplified, illustrated conceptual model of the June 1-2, 2023, wildfire-influenced ozone event.

2.4.3.2 Upper-Level Pattern Overview

The 850 millibar (mb) level (approximately 1500 m above sea level) sits near the top of the planetary boundary layer (PBL), the atmospheric layer in which ozone pertinent to surface observations and human health develops. The 850 mb height level can serve as a guide for the transport of pollutants. The analysis of this atmospheric level is given for May 20 - June 2 in Figures 21 a-t.

High pressure over western Canada existed in mid-May, driving warm and dry conditions over the fire regions from Saskatchewan to British Columbia. Lightning strikes across the region had previously ignited the fires some days prior. As of May 14, high pressure was centered just south of the fire area, providing southerly winds subsiding off higher terrain, fueling lower humidities in an already dry area (Figure 21a). The center of the high slid southeastward on May 15, though southerly winds persisted (Figure 21b). A cold front (tightening green isotherms to the north of the fires) approached from the

north, but strong southwesterly winds continued across the fire area. On May 16, a low-pressure system formed and propagated along the cold front noted on May 15 (Figure 21c). This changed the wind direction across the fire region and intensified speeds, fanning the flames and increasing the fire size. By May 17, the low had moved slightly farther east, but all the fires remained in strong northerly flow (Figure 21d), with the bulk of the smoke transported from the fires pushing southward. Much of this smoke pushed into the United States and impacted air quality across a wide region of central CONUS several days prior to the main smoke plume associated with the June 1-2 events in the District.

By May 18, the area of low pressure had moved eastward, and the resulting pressure gradient across the fire and smoke region had significantly diminished (Figure 21e). As such, winds across the area were light, with little mean transport directly defined at 850 mb. Ridging quickly developed on May 19 to the south of the fire region, resulting in persisting light transport winds in the area (Figure 21f). Since 850 mb winds are nearly geostrophic, it can be inferred that light smoke transport occurred towards the southeast for western fires and back towards the north-northeast for smoke and fires farther to the east and south, following the lines of geopotential heights, but at very slow speeds. As such, this may have acted to recirculate smoke on May 19, allowing smoke concentrations to build. This buildup culminated on May 20 as the ridge moved southeastward on the previous day, with the ridge axis tilting northeastward from eastern Colorado towards Ontario (Figure 21g).

This is important to note as this positive tilting was also reflected in the approaching trough and associated cold front coming out of Canada. The resulting orientation of the height field was to push all smoke southwards from the fire region together in front of the approaching cold front. As the cold front was noted at 850 mb, it would also be connected to the surface. As such, it essentially acted as a bulldozer of transport of the smoke towards the south in the mean northerly flow. This pattern, along with some recirculation the previous days, likely accounts for the very dense plume of smoke noted on satellite on May 20 moving out of the fire region and into northern Montana (see title figure).

The pattern rapidly changed on May 21 (Figure 21h); the cold front moving out of Canada did not continue to push southwards. The overall pattern of the atmosphere acted to push the front east-southeastward across Canada towards Quebec instead of sweeping the smoke southward. Instead, a significant closed ridge developed from southern Saskatchewan and Manitoba, extending southeastward towards another closed ridge (high pressure) center in Missouri. As this occurred in the absence of a strong frontal passage over this region, the thick smoke plume across northern CONUS was now "captured" within the ridge. Due to the strength of the ridge and because the ridge was "closed," smoke was now essentially trapped in at least the 850 mb layer.

The center of the southern portion of the ridge, previously located over Missouri, moved eastwards to be centered over Ohio on May 22 (Figure 21i). Weak winds exist within closed high-pressure systems, particularly within the vicinity of the center of the high. However, the closed center of the high pressure over Ohio was vast, extending northwestward, arguably as far as southern Alberta, where another closed area of high pressure existed. Marginal eastward transport across the northern part of CONUS was supported by this setup, which was consistent with smoke movements at the time. The east-central CONUS ridge was pushed further eastward on May 23 (Figure 21j). It should be noted that ridges and centers of high pressure are associated with subsidence or sinking motion. As such, smoke

may be transported vertically downwards where high-pressure "reforms." Said another way, a pressure system should not be thought of as a rigid object that moves in the wind but rather as constantly reforming, much like a wave in the ocean. As such, smoke may not move as far east as the high-pressure forms. This seemed to be the case, as the center of high pressure moved to New York, but the smoke was only as far east as western New York by this time due to the weak southerly and westerly winds impacting the smoke region between May 21 and May 23. Concurrently, a cold front moved out of Canada, keeping smoke from moving northward back into Canada. In fact, this front eventually pushed the entirety of the smoke back southward across central CONUS, resulting in continental-scale recirculation of the plume into May 24 and beyond.

Incredible height gains were realized across southern Canada on May 24 (Figure 21k). Heights within the developing closed high were measured at 1590m, an increase of over 60 m in 24 hours in some areas. This indicates incredible amounts of subsidence and strengthening of the ridge across central North America. The cold front sweeping south out of northern Ontario on May 23 continued its trek southeastward, weakening at least at 850mb. However, the trough associated with the cold front acted to pinch off the high pressure, which was previously located over New York. This resulted in northeasterly flow across northeast CONUS and the Great Lakes as the high center retreated west. As such, the eastward progress of the smoke was again tempered and instead pushed back westward. Furthermore, the cold front, while weak at 850 mb, can be effective at delivering new air masses to large regions, removing air in front of it from the region. Behind the cold front on May 24, clean air moved into northeast CONUS, while the front swept smoky air south and southwestward with clockwise flow around the high across the Great Lakes. Said succinctly, the west-central Canadian smoke was recirculated across the Great Lakes and upper Ohio River Valley to the Central Plains under the developing high pressure located across Canada and central CONUS on May 24 as it was swept southwest by cleaner air arriving from northeastern Canada.

Smoke contained within the high pressure continued to be recirculated from May 25 to June 2. In essence, the smoke remained trapped within the slowly moving clockwise flow around the center of high pressure. On May 25, the center of high pressure moved southward out of Canada to be located over Lake Superior (Figure 21l). On May 26, the center of high pressure was located over Wisconsin (Figure 21m), and by May 27 was centered over southern Ontario (Figure 21n). Note the slowing day-to-day progression. Farther to the west, just east of the Rocky Mountains, stronger winds indicative of a low-level jet in the lee of the Rockies were observed. This acted to transport smoke northward into Canada more quickly. While most smoke was located under the ridge, the low-level jet on the periphery acted to pull smoke located under the ridge out and push it northward, expanding the area under the influence of smoke northward. A similar pattern persisted for May 28 (Figure 21o), May 29 (Figure 21p), and May 30 (Figure 21q). A cold front approached the Mid-Atlantic from the north on May 29 but had not yet reached the District. On May 30, the cold front passed through and was able to bring an airmass laden with smoke across the District. This occurred as the continued presence of high-pressure west of the Mid-Atlantic started to "arc" smoke from within or west of the high pressure through Canada and then southwards towards the Mid-Atlantic region. The persistent pattern then delivered diffuse smoke to the District by May 30, with weak but northeasterly flow with subsidence behind the front, bringing the smoke to the surface. The northeast flow continued on May 31, with the center of high-pressure strengthening, though not moving (Figure 21r).

Between May 29 and May 31, winds between Nova Scotia and the District were favorable for transport of smoke from that region to the Mid-Atlantic. Smoke from the Nova Scotia fires was caught behind the cold front, and northeasterly winds present on May 30-31 would have delivered smoke from that fire to the District from May 31 to June 1. On June 1, the center of high pressure had strengthened further but retrograded westward to over southern Ontario (Figure 21s). The movement away balanced by intensification consequently did not impact the District's absolute surface pressure but did thereby maintain northeast flow for the first day of ozone exceedance on June 1. The Northeast flow at 850 mb continued on June 2, resulting in similar conditions as June 1 with resulting ozone exceedances in the smoky air (Figure 21t).

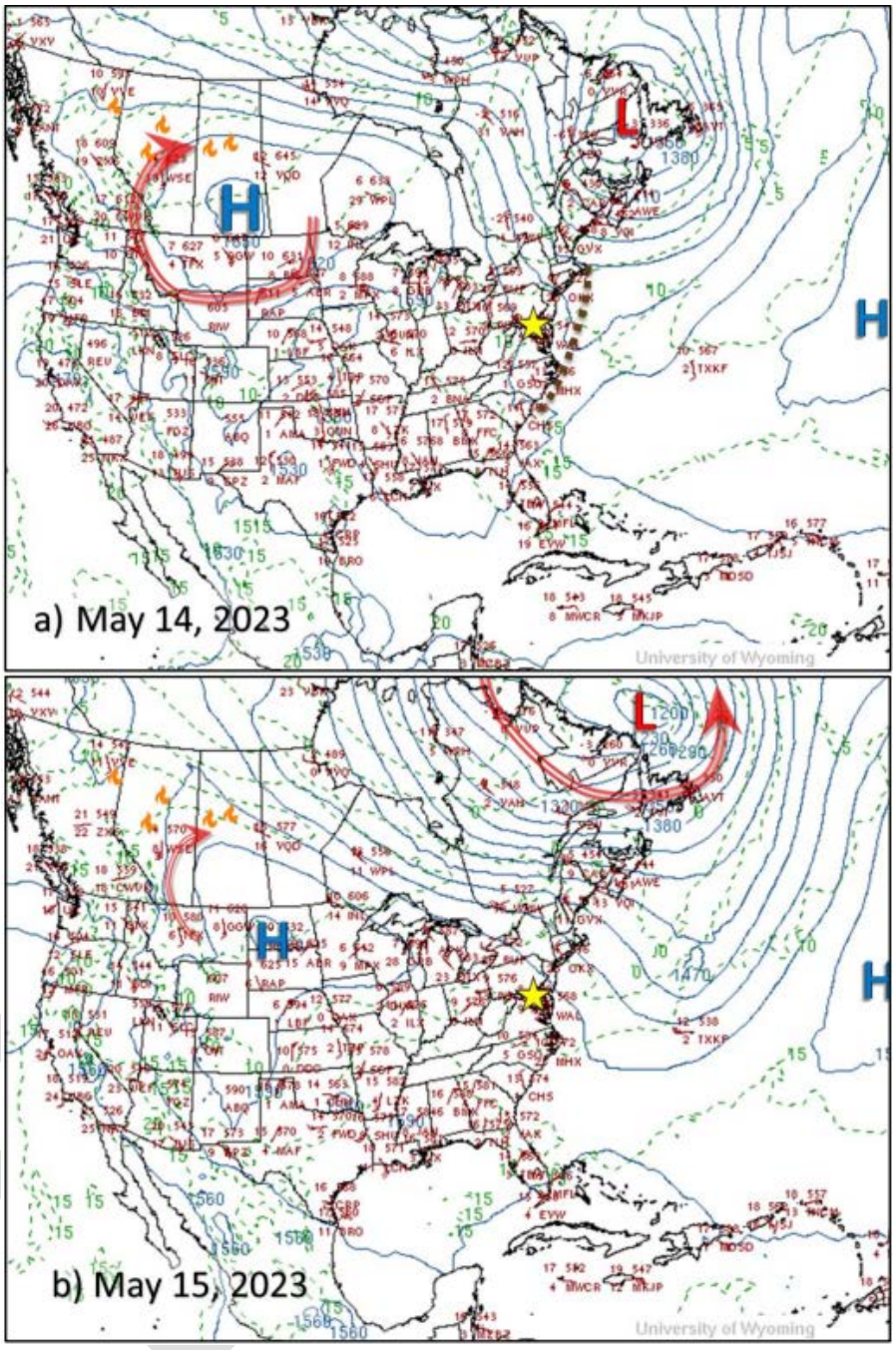
a) May 14, 2023
b) May 15, 2023
University of Wyoming
University of Wyoming

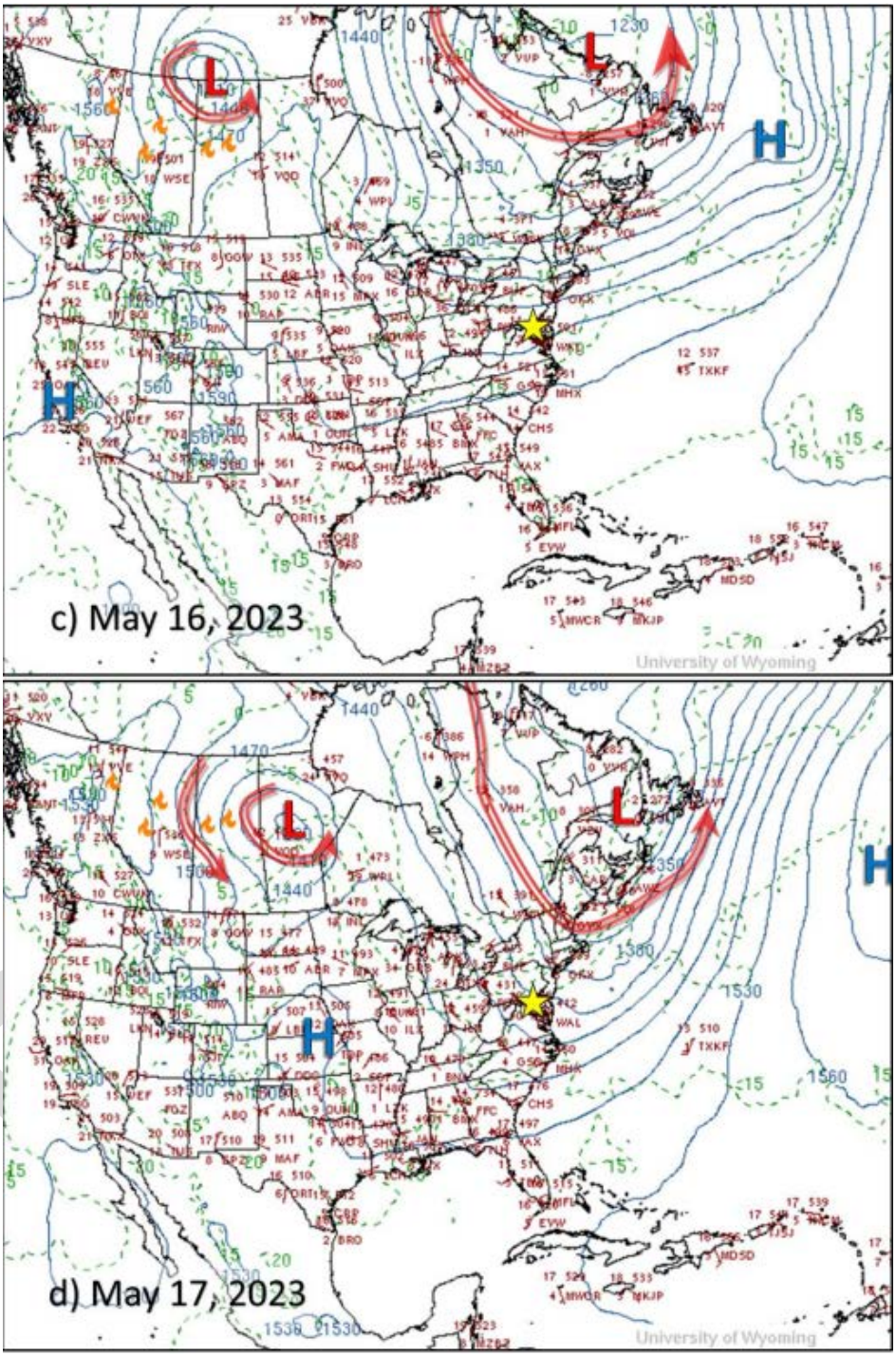
c) May 16, 2023
University of Wyoming
d) May 17, 2023
University of Wyoming

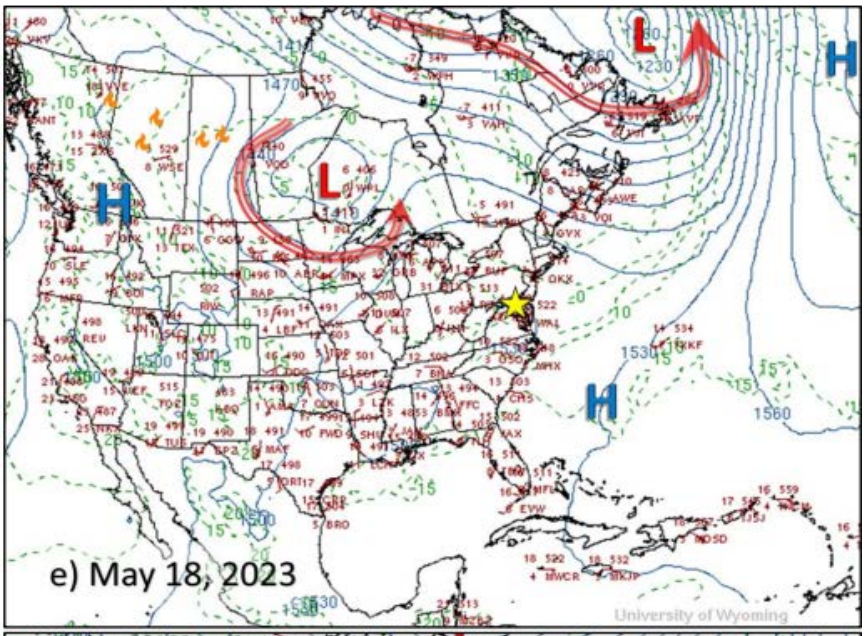
e) May 18, 2023
University of Wyoming

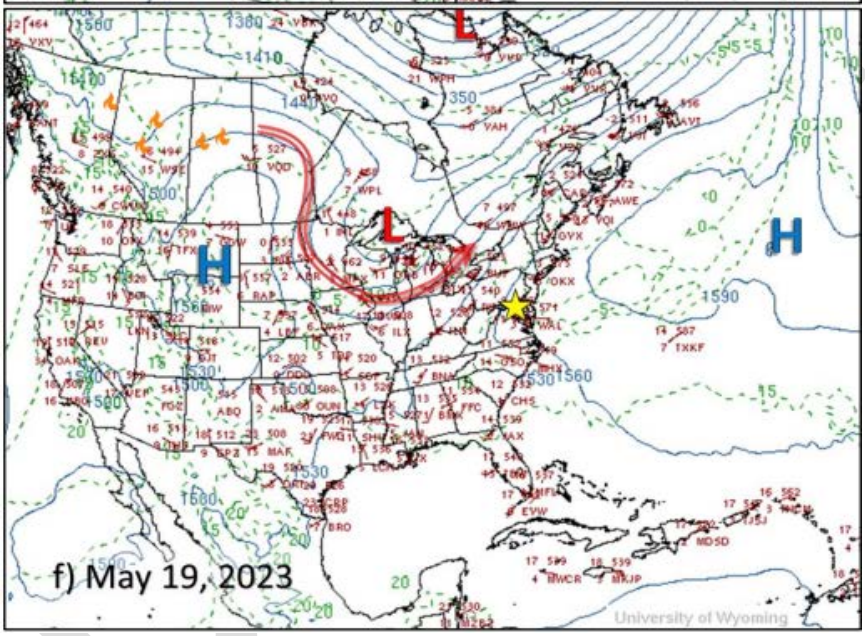
f) May 19, 2023
University of Wyoming

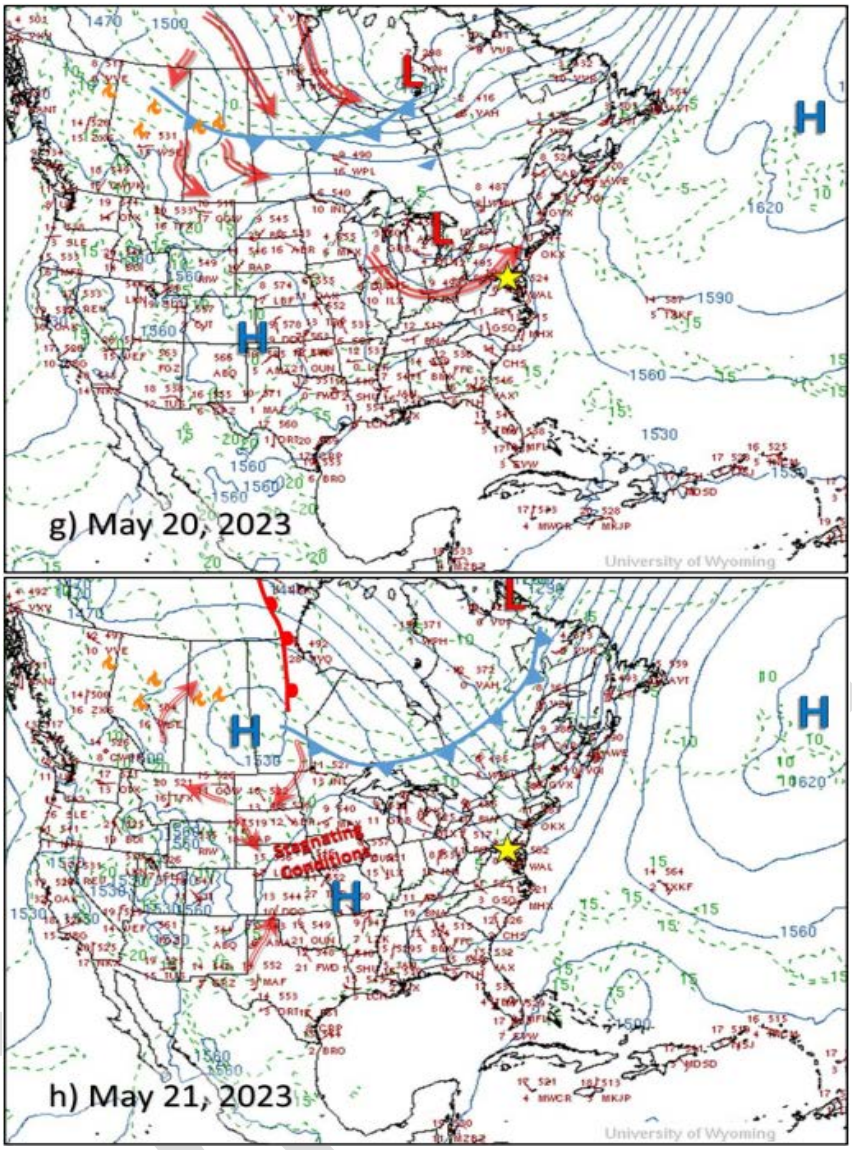
g) May 20, 2023
University of Wyoming
h) May 21, 2023
Stagnating Conditions
University of Wyoming

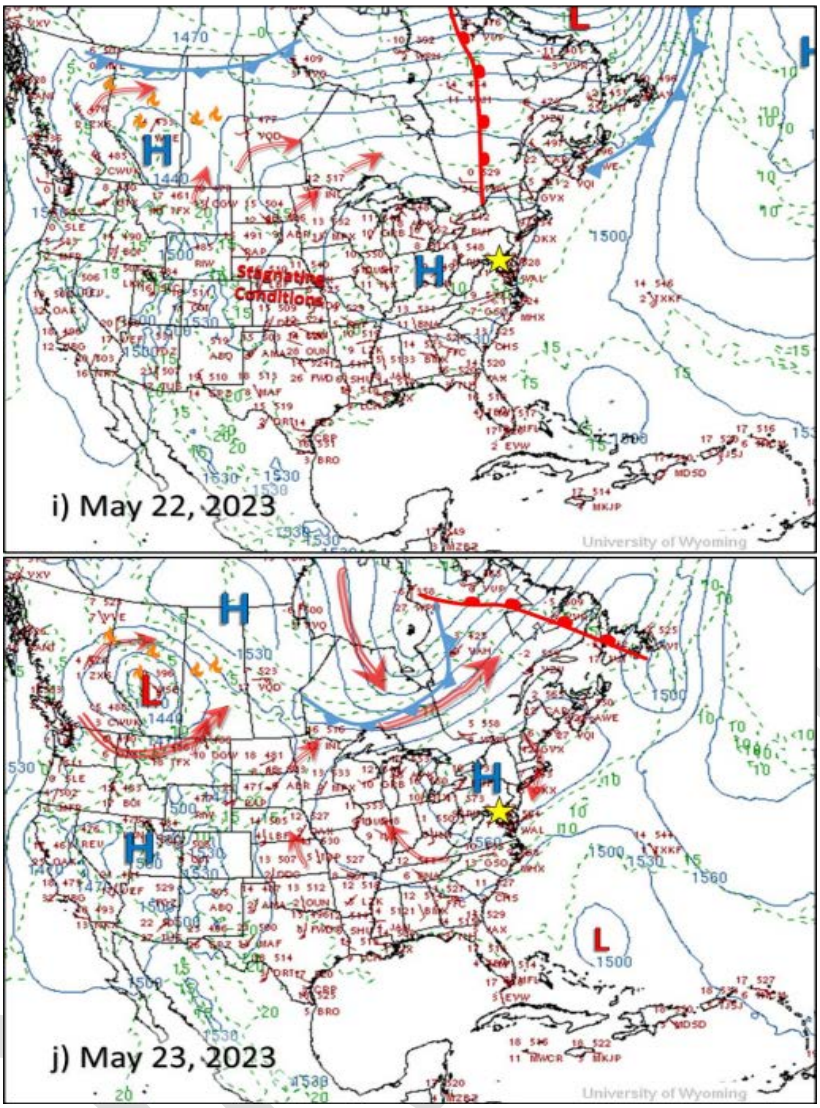
i) May 22, 2023
University of Wyoming
j) May 23, 2023
University of Wyoming

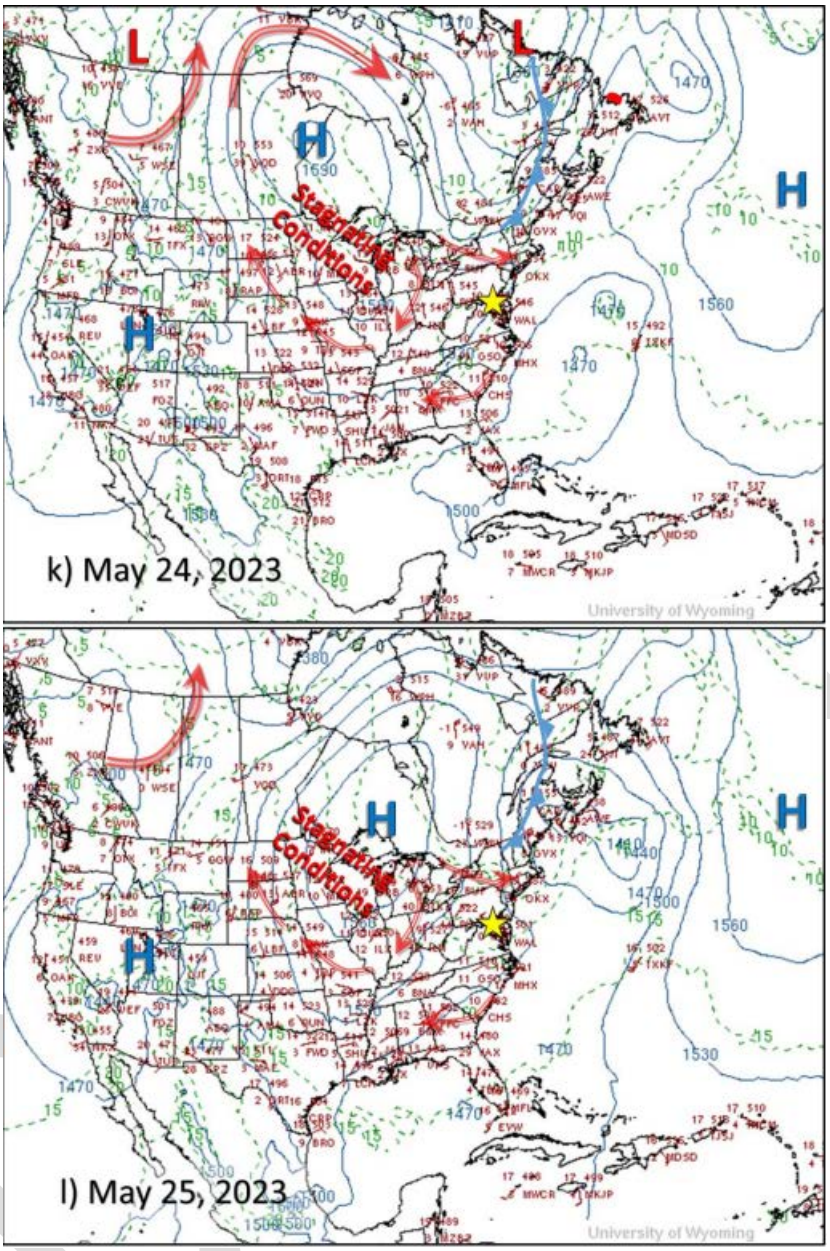
L
L
H
H
H
Stagnating Conditions
k) May 24, 2023
University of Wyoming
H
H
H
Stagnating Conditions
l) May 25, 2023
University of Wyoming

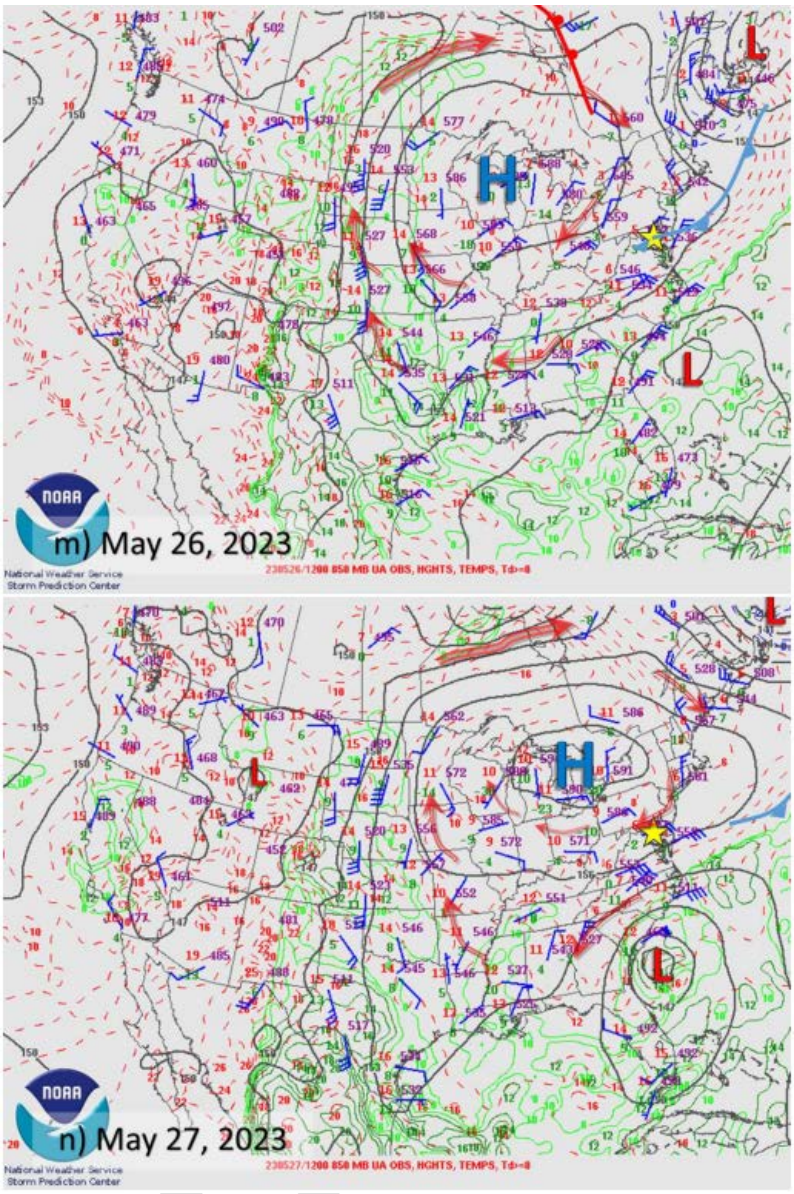
m) May 26, 2023
National Weather Service
Storm Prediction Center
230526/1200 850 MB UA OBS, HGHTS, TEMPS, Td>=0
n) May 27, 2023
National Weather Service
Storm Prediction Center
230527/1200 850 MB UA OBS, HGHTS, TEMPS, Td>=0

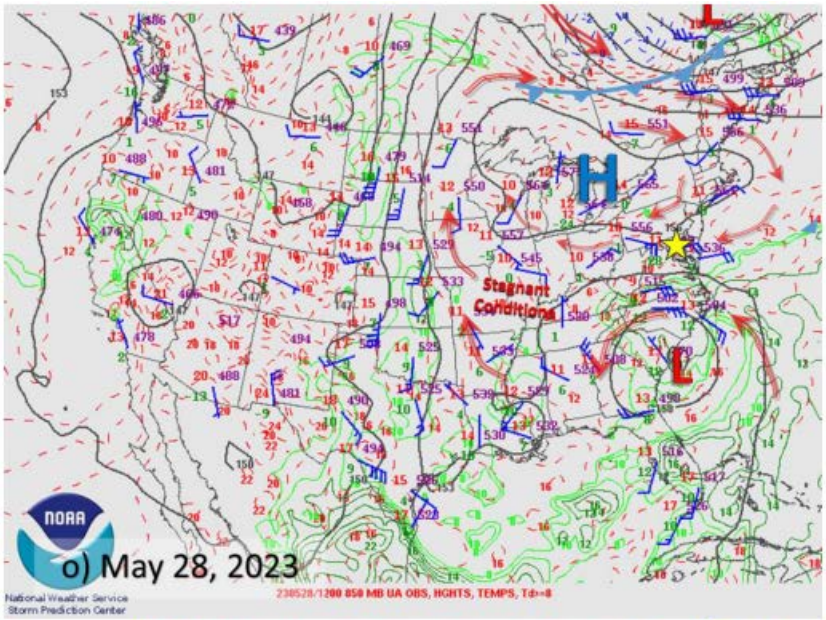
H
L
Stagnant Conditions
o) May 28, 2023
National Weather Service
Storm Prediction Center
230528/1200 850 MB UA OBS, HGHTS, TEMPS, Td>=8

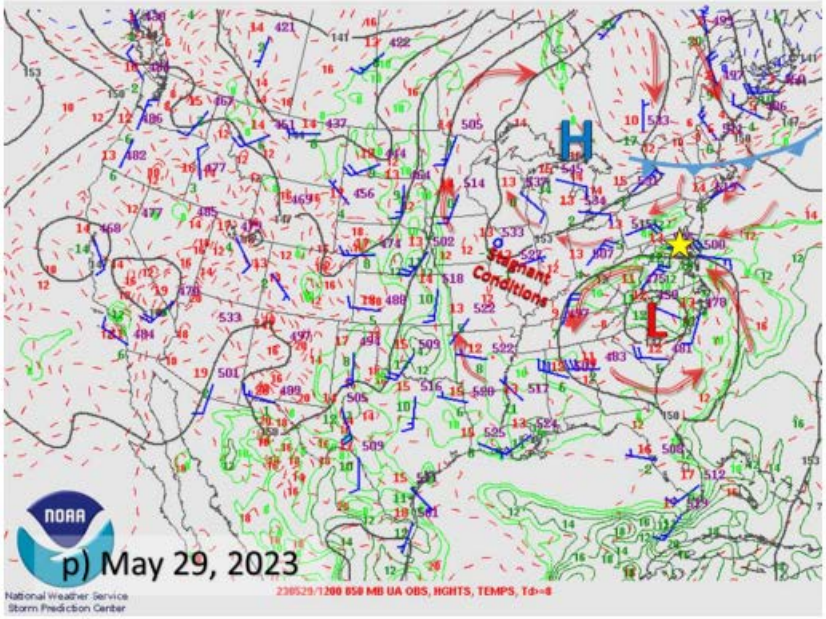
H
L
Stagnant Conditions
p) May 29, 2023
National Weather Service
Storm Prediction Center
230529/1200 850 MB UA OBS, HGHTS, TEMPS, Td>=8

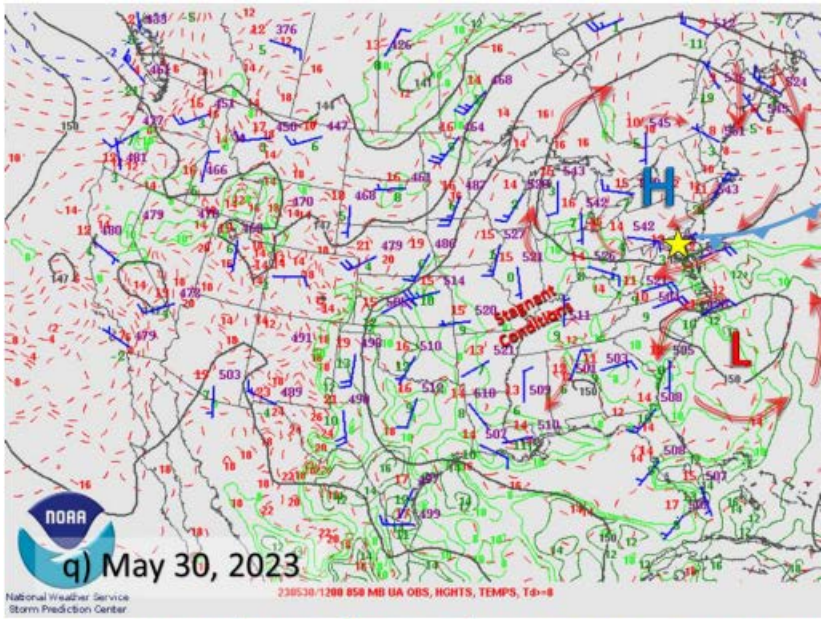

q) May 30, 2023

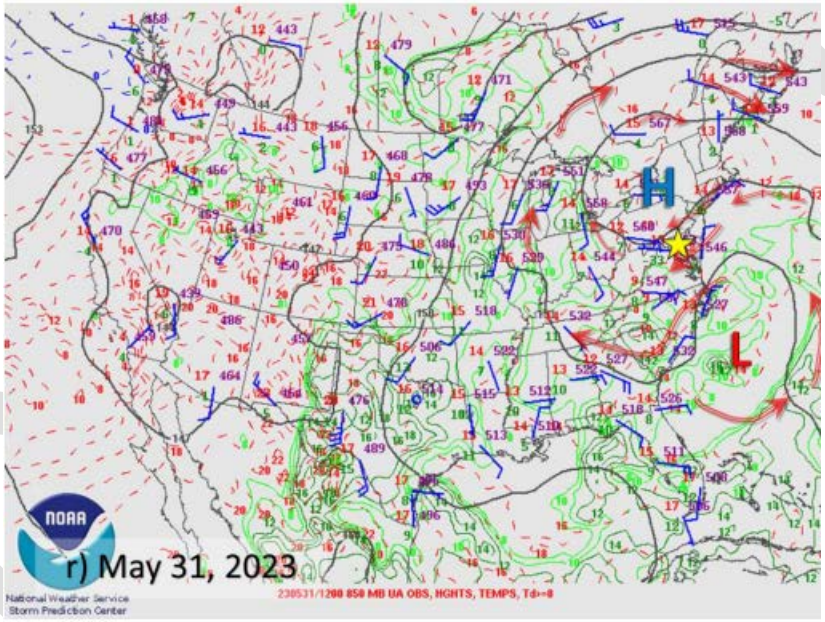

r) May 31, 2023

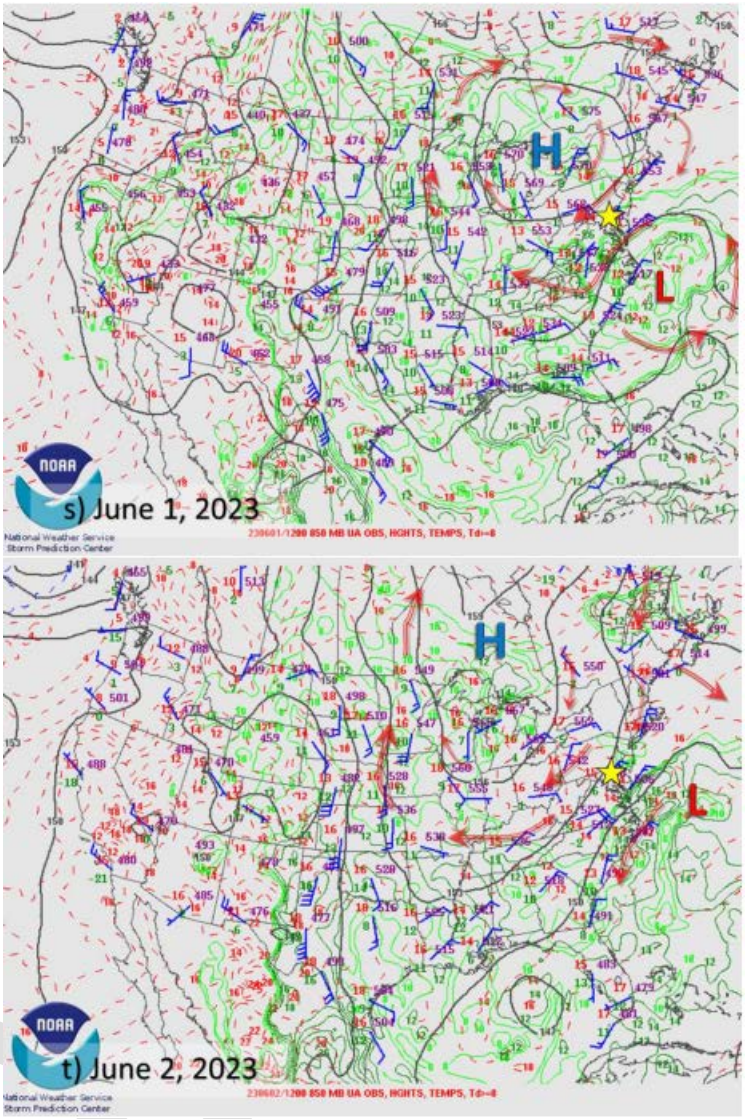

Figure 21: The 1200 UTC 850 mb pattern for CONUS, from May 13 - June 2, 2023 (Figure a-t).

Red arrows show the general transport pattern and are generally sized by wind speed. The letter "H" is high pressure, and the letter "L" is low pressure. The base images switched sources on May 26 from the University of Wyoming to the Storm Prediction Center to better capture northern Canada and/or details of CONUS. In the North American figures (a-l), heights (m) (blue lines), temperature (°C) (green dashed lines) and station plots (red), which include temperature (°C), dewpoint depression (°C), height (+1000m), wind barb and station identifier, are all included. Similar features with slightly altered color configurations are presented in figures m-t. The yellow star identifies the District's location. Frontal boundaries are noted as cold fronts (blue lines with triangles) and warm fronts (red lines with semi-circles)

2.4.3.3 Surface Pattern Overview

Gross transport in the atmosphere is generally representative at 850mb but lacks detailed information on features such as surface fronts that provide insight into the evolution of events at specific locations and which impact the concentrations relevant to human health. Analysis of the surface pattern followed similar trends as those seen at 850mb.

The smoke plume from the conglomeration of fires across west-central Canada entered CONUS on May 20, 2023 (Figure 22a). This was driven by transport level winds discussed above and the associated surface cold front pushing across the region, as well as a weak low-pressure system over southern Saskatchewan. While this low pressure across southern Saskatchewan was weak, it had a noted influence in the smoke field, which had a spiral pattern consistent with counterclockwise flow associated with low-pressure systems and was collocated with analyzed low pressure in Figure 22a. While this weak low may have helped to pull smoke into northern CONUS, the southward progress of the smoke was immediately met with southerly winds around the spatially massive area of high pressure dominating eastern CONUS on May 21 (Figure 22b). As a result, a narrow corridor of smoke existed by May 21 across north-central CONUS, into the Great Lakes, pinched from the north by a cold front and pushed northward from the south by southerly winds around the west side of high pressure centered over Missouri. At higher altitudes (even above the upper air analysis), smoke drifted southward along the Rockies underneath upper-level ridging.

The smoke plume was pulled into the ridge of high pressure centered over central CONUS on May 22 and May 23 (Figures 22c and 22d). By May 24, subsidence and surface divergence within the high had spread the regional extent of smoke eastward from the Colorado Rockies to the East Coast (Figure 22e). On May 25, a strong cold front moved through the District from the northeast (Figure 22f). The airmass behind the front was devoid of smoke, improving air quality in the District by removing smoke and providing cooler temperatures. Under surface high pressure over the Great Lakes, clockwise circulation around the high, working with the cold front that moved through northeast CONUS, placed clean air over areas east of the high and put smoke on the western periphery of the surface high (still centered over the Great Lakes) from the Gulf Coast all the way into Canada. Cleaner air continued to push westward around the southern portion of surface high pressure across the lower Ohio River Valley on May 26 (Figure 22g). However, by this point, the surface front had essentially washed out, and the cleaner air was losing its character, mixing well with smoke still contained within the central high-pressure system. By May 27 (Figure 22h), smoke began to become visible again farther east in central CONUS, with smoke noted to be wrapping around the high center over northeast CONUS (aloft).

On May 28 (Figure 22i), another cold front pushed south out of northern Quebec. This removed much of the smoke initially evident via satellite. However, westerly winds aloft across southern Ontario brought additional smoke over the airmass behind the front, smoke that was recirculated several times around the high-pressure system. In a rare circumstance, a warm front / cold front pair developed under the high-pressure center located over southern Ontario on May 28. Fronts of this nature are typically associated with low-pressure systems. However, in this instance, as a cold front moved southward out of northern Quebec 54 and Ontario, it was acted on by surface high pressure, causing

the north and western portion of the cold front to return north and eastward as a warm front while the south and eastward portion continued southward as a cold front. Furthermore, additional smoke continued to be locked immediately under the high-pressure center, and as the May 28 cold front swept southward (the eastern portion), subsidence and entrainment associated with high pressure caused smoke to fill in behind the front as it moved towards the District. Said another way, the smoke backfilled behind the front, evident by May 29 (Figure 22j). Acted on by high pressure increasingly northwest of the front's progress, the cold front continued to push south but with a greater southwestward inclination into May 29, arcing with an apex approaching the District by midday on May 29. By May 30, the front pushed further south, further moving the smoke (Figure 22k). Easterly flow due to slow-moving low pressure off the Carolina coasts and high pressure centered over the eastern Great Lakes kept clouds and cooler temperatures in the area at the time, mitigating the smoke impact.

Light east to northeast flow persisted on May 31 (Figure 22l). While smoke had moved into the District, clouds continued to cover southeastern areas of the state due to the easterly flow of low pressure off the coast of North Carolina. However, slightly more northeasterly than easterly flow allowed a return of sun to the northwestern half of the state. On June 1, the low off the coast of the Carolinas moved east, bringing additional areas of Sunshine for most of the state save the far southeast (Figure 22m). Winds remained northeast, with the regional circulation now mainly dictated by the location of high pressure over the Great Lakes and the resulting clockwise flow around the high. A similar atmospheric state existed for June 2, with continued northeast flow dictated by the center of high pressure over the Great Lakes (Figure 22n). A weak trough of low pressure was analyzed in the northeast.

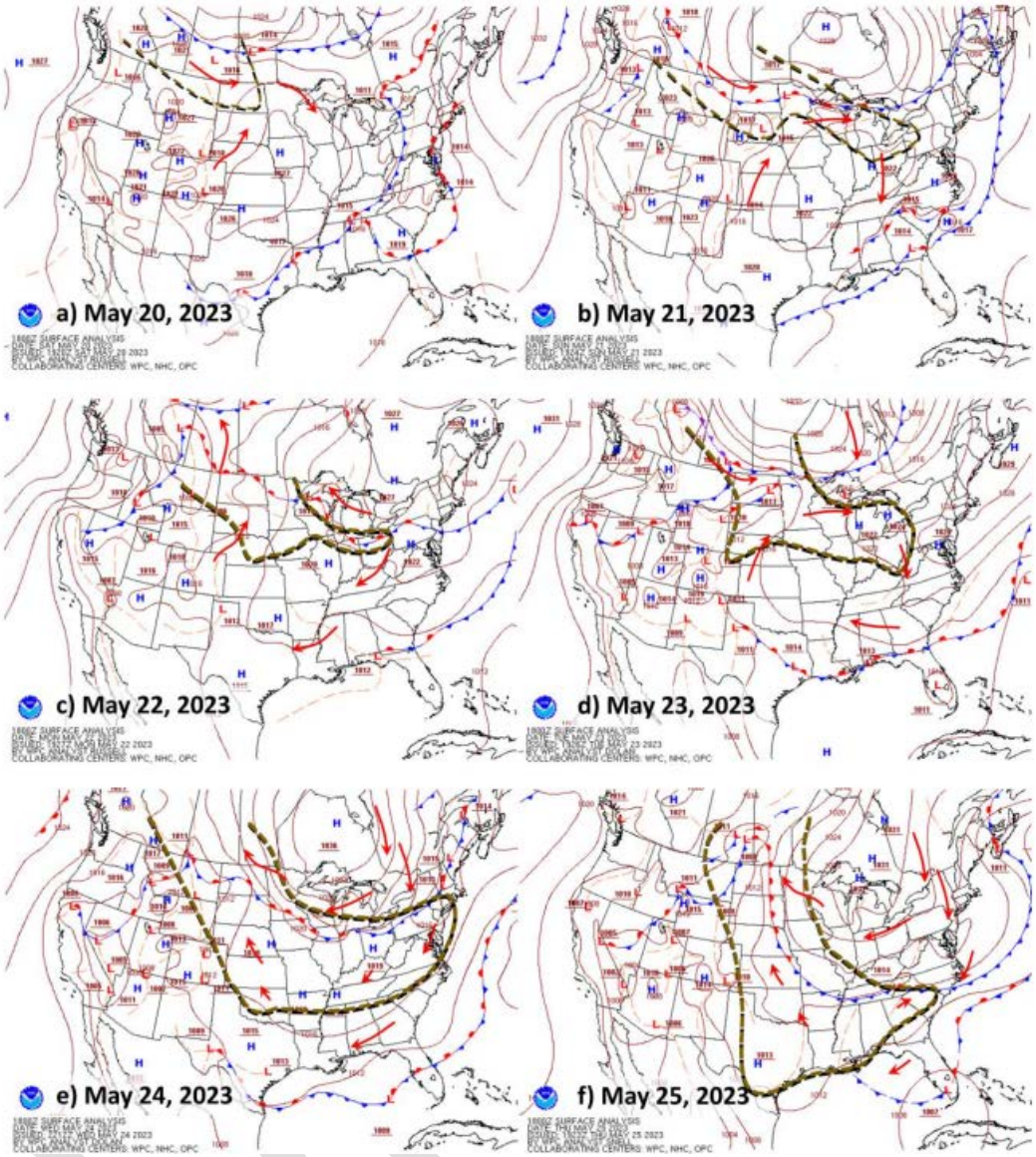
a) May 20, 2023
b) May 21, 2023
c) May 22, 2023
d) May 23, 2023
e) May 24, 2023
f) May 25, 2023

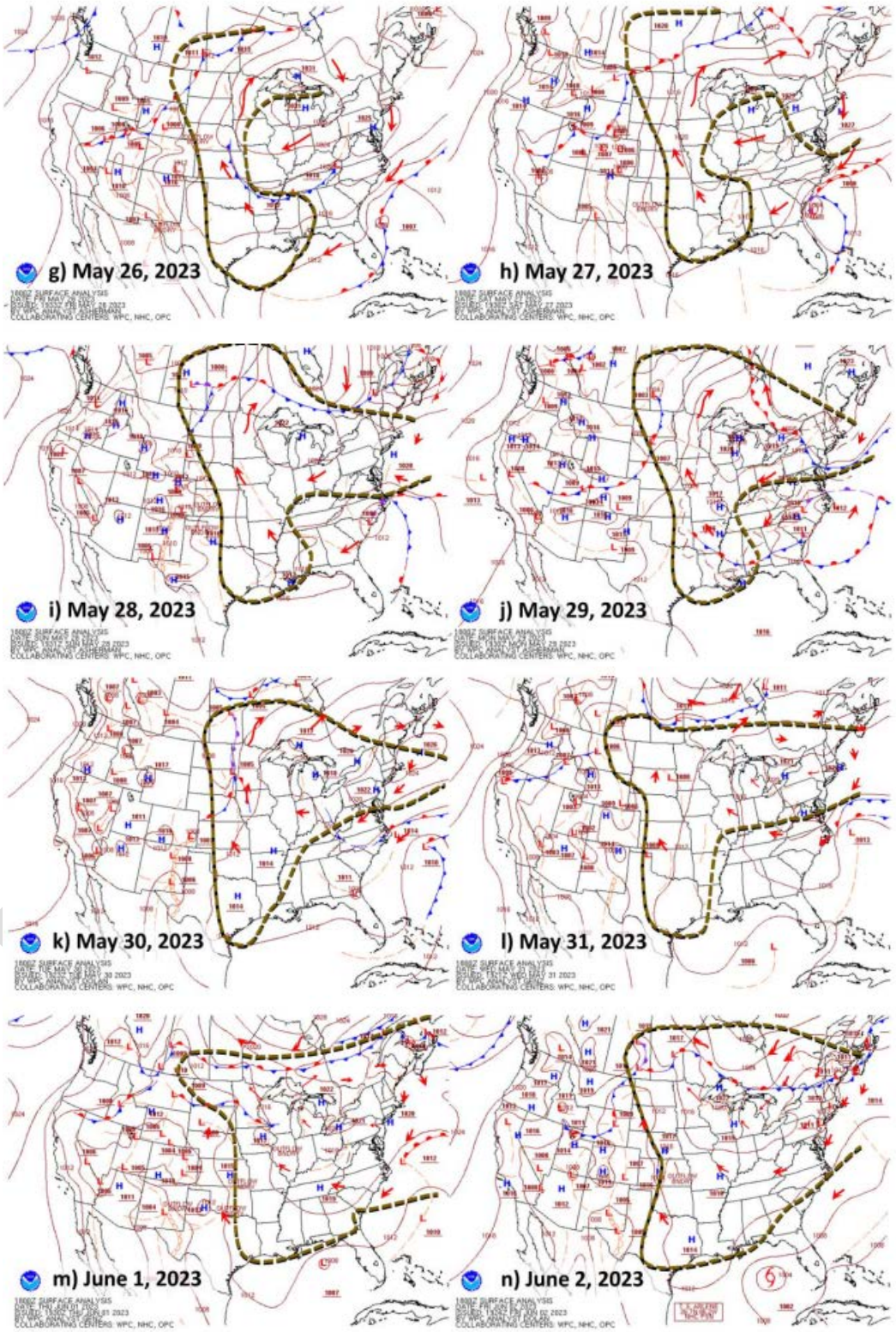

Figure 22: Surface analysis at 1800 UTC (2 pm. LDT in the District) for May 20 - June 2 (a-n), 2023. Red arrows show the general surface wind pattern/direction and are approximately scaled by wind strength. The letter "H" highlights high pressure, and the letter "L" is low pressure. Heights (brown lines) and fronts are also analyzed. The thick, shadowed, dashed lines represent the visible smoke plume on the satellite.

2.4.3.4 Temperature

Consistent with the theme of 2023, heightened ozone concentrations, specifically reaching near or beyond 70 ppb, were associated with periods of smoke. Smoke was initially observed across the Midwest beginning May 21, 2023. MD8AO greater than 70 ppb was first observed centered over the Minneapolis region. In the presence of smoke, MD8AO concentrations climbed from 51 to 74 ppb on May 20 vs 21, a 23-ppb increase (Table 3). Temperatures did climb slightly, but only to 79°F on May 21 from 73°F on May 20. Though roughly 8°F above normal, the absolute temperature is not alone ozone conducive.

Smoke continued to be a presence across the Midwest, stretching to the Great Lakes region on May 22-23 and even a brief stint of diffuse smoke pushing to the East Coast on May 24. Temperatures over this period were warmer than normal but not conducive to ozone exceedance. On May 23, Minneapolis, despite only reaching a high temperature of 84°F, saw an MD8AO of 82 ppb. A similar story occurred on this day at Chicago's O'Hare Airport, where MD8AO reached 80 ppb despite a high temperature of just 86°F (Table 3).

Beginning May 24, a cold front began to slowly push south and west through the Great Lakes and through the Ohio River Valley. Drops in temperature were first observed over Minneapolis, MN, and Chicago's O'Hare. A near 20°F drop in temperature was seen in Chicago, Illinois, between May 23 and 24 (Table 3). Aside from temperatures, this front also helped to provide a reprieve from the smoke as clean air behind the front dropped ozone concentrations. Significant drops in ozone were observed on May 24 at both Minneapolis, Minnesota. and Chicago, Illinois, with a 21 and 26 ppb MD8AO drop at these two locations, respectively (Table 3). On May 25, this front was able to stretch all the way south through St. Louis, Missouri, where a similar drop in ozone was noted. Temperatures were not seen as significant a drop at St. Louis, however, due to the front washing out by this point.

High pressure became centered over the Great Lakes beginning May 25 and 26, persisting in that region for the remainder of this event. Clockwise flow began to wrap the smoke and warmer temperatures back over eastern CONUS. This warming trend and eventual onset of smoke were observed across all four Midwest and Great Lakes area cities (Minneapolis, Minn., Chicago, Ill., Cleveland, Ohio, and St. Louis, Mo.) between May 25 and 30, varying slightly on the exact days for each location given their orientation in reference to the high pressure (Table 3). Across the Mid-Atlantic over this period, temperatures remained at or slightly below seasonal norms, as smoke remained west of the region. Upper 70°F to low 80°F were observed during this time at both Philadelphia, Pennsylvania and at National Airport in Virginia, with MD8AO generally in the Good to low Moderate AQI range (Table 3).

By May 31, the smoke had wrapped all the way around the Great Lakes high-pressure system and was impacting Mid-Atlantic states. Surface temperatures on May 31 at both Philadelphia and BWI Airport in the District were near seasonal norms at 80°F. An uptick of roughly 10-15 ppb ozone was observed versus May 30, despite temperatures only being a few degrees warmer (Table 3). At least part of the difference between May 30 and 31 was the availability of sunshine, with more available on May 31. Smoke continued to filter into the Mid-Atlantic on June 1 and 2 while slightly warmer air aloft wrapped

around the high-pressure system. Temperatures saw an increase at both Philadelphia, BWI, and Regan, climbing from the upper 80s°F on June 1 to the 90s°F by June 2. By this point in time, smoke was covering a large stretch of eastern CONUS, with numerous locations and regions recording MD8AO greater than 70 ppb.

The temperature trends across these seven cities impacted by smoke indicated that while warm temperatures support ozone production, they were not a primary deterministic factor of high values in this case. As asserted earlier and exemplified over this period of warm weather, temperatures no longer necessarily predict ozone production, and the most recent years of data have shown that warm temperatures are no longer sufficient for ozone exceedances in the District.

Date	**20-May**	**21-May**	**22-May**	**23-May**	**24-May**	**25-May**	**26-May**	**27-May**	**28-May**	**29-May**	**30-May**	**31-May**	**1-Jun**	**2-Jun**	**3-Jun**	**4-Jun**
Minneapolis, MIN	73	79	82	84	76	77	81	84	84	88	90	90	91	87	90	92
Normal	70.7	71.1	71.4	71.7	72.1	72.4	72.7	73.1	73.4	73.7	74.1	74.4	74.7	75	75.4	75.7
Departure	2.3	7.9	10.6	12.3	3.9	4.6	8.3	10.9	10.6	14.3	15.9	15.6	16.3	12	14.6	16.3
MD8AO (ppb)	51	74	74	82	51	59	68	74	75	73	65	69	62	67	77	68
Chicago, IL	73	81	83	86	67	62	70	74	80	86	91	91	91	91	87	77
Normal	71.9	72.3	72.6	73	73.3	73.7	74	74.3	74.7	75	75.4	75.7	76	76.4	76.7	77
Departure	1.1	8.7	10.4	13	-6.3	-11.7	-4	-0.3	5.3	11	15.6	15.3	15	14.6	10.3	0
MD8AO (ppb)	44	63	69	80	54	43	56	65	66	74	78	65	79	85	78	55
Cleveland, OH	63	74	76	79	75	58	66	74	77	80	87	84	86	84	81	73
Normal	72.3	72.6	72.9	73.2	73.5	73.8	74	74.3	74.6	74.9	75.2	75.5	75.8	76.1	76.4	76.7
Departure	-9.3	1.4	3.1	5.8	1.5	-15.8	-8	-0.3	2.4	5.1	11.8	8.5	10.2	7.9	4.6	-3.7
MD8AO (ppb)	38	46	50	62	60	39	47	55	66	65	67	68	82	84	53	48
St. Louis, MO	73	78	81	85	88	81	77	81	82	87	90	91	92	93	94	93
Normal	78.2	78.5	78.8	79.1	79.4	79.7	80	80.4	80.7	81	81.3	81.6	81.9	82.3	82.6	82.9
Departure	-5.2	-0.5	2.2	5.9	8.6	1.3	-3	0.6	1.3	6	8.7	9.4	10.1	10.7	11.4	10.1
MD8AO (ppb)	41	60	68	65	82	61	62	68	71	76	82	77	69	75	88	69
Philadelphia, PA	71	77	79	75	81	71	75	80	79	82	76	80	88	95	76	77
Normal	75.4	75.7	75.9	76.2	76.5	76.8	77.1	77.3	77.6	77.9	78.2	78.5	78.8	79.1	79.4	79.7
Departure	-4.4	1.3	3.1	-1.2	4.5	-5.8	-2.1	2.7	1.4	4.1	-2.2	1.5	9.2	15.9	-3.4	-2.7
MD8AO (ppb)	37	51	50	43	65	49	50	60	53	63	49	63	72	105	40	44
BWI, MD	79	80	82	75	84	74	75	78	77	78	77	80	87	97	85	80
Normal	76.4	76.6	76.9	77.2	77.4	77.7	78	78.3	78.6	78.9	79.2	79.5	79.8	80.1	80.4	80.8
Departure	2.6	3.4	5.1	-2.2	6.6	-3.7	-3	-0.3	-1.6	-0.9	-2.2	0.5	7.2	16.9	4.6	-0.8
MD8AO (ppb)	47	54	53	46	65	54	58	58	48	51	52	64	74	87	53	48
National Airport	81	79	82	76	82	74	76	78	75	77	76	79	85	94	86	76
Normal	77	78	78	78	78	79	79	79	80	80	80	80	81	81	81	82
Departure	4	1	4	-2	4	-5	-3	-1	-5	-3	-4	-1	4	13	5	-6
MD8AO (ppb)	53	51	54	48	67	57	61	56	48	42	49	63	81	75	50	40

Table 3: Maximum daily temperature, average maximum daily temperature, a departure from normal (observation minus normal/average), and MD8AO at various locations along the smoke trek to the District.

2.4.4 Smoke and Ozone Discussion and Analysis

Spatial analysis of contoured MD8AO concentrations and HMS-analyzed smoke was done for the period of May 30 – June 4 (Figure 24). Thick smoke had already begun to make its way into the Mid-Atlantic and Great Lakes areas on May 30 (Figure 24a). Temperatures along the East Coast were not ozone-conducive, with high temperatures only reaching the mid-to-upper-70s°F on May 30, resulting in little ozone at this time (See Table 5). Across the Southeast, widespread cloud coverage associated with a low-pressure disturbance also limited ozone production. By this point, the smoke plume was significantly aged. More favorable meteorology across the Midwest resulted in an anomalously large area of MD8AO above 70 ppb centered over Wisconsin and Illinois.

Ozone concentrations began to rise across the Mid-Atlantic states on May 31 because of slightly warmer temperatures, pushing into the low-80s°F. Widespread MD8AO above 70 ppb were again noted over Wisconsin and Illinois, with a few other pockets developing over Ohio and New York (Figure 24b). The highest ozone concentrations across CONUS match up very well with HMS smoke of medium density except for the southeastern states, where general cloud coverage lingered from the previous day.

By June 1, surface temperatures climbed into the upper-80s°F for the District and the rest of the Mid-Atlantic states. Plentiful sunshine in the presence of aged smoke resulted in widespread MD8AO greater than 70 ppb for a large area, stretching from DC-Maryland-Virginia northeastward to New England and northwestward to Wisconsin (Figure 24c). Ozone concentrations were further compounded on June 2, with a further uptick in temperatures across the region (Figure 24d). Apart from the Appalachian Mountain range region, MD8AO above 70 ppb were observed from Massachusetts south to North Carolina and extending westward to Iowa.

The aged smoke and associated ozone began to gradually shift westward on June 3 and 4 (Figure 24e & 24f). As a result, the airmass associated with ozone exceedances also shifted mostly (though not entirely) away from the Mid-Atlantic to the Midwest to the Northern Plains. Once again, there was a very close correlation between the aged smoke and surface ozone concentrations during this spatial evolution. The heavy smoke analyzed by HMS, primarily over Quebec and Ontario on June 3 and 4, is tied to fresh wildfire emissions from central Quebec. Given the age of this secondary smoke plume, it had not yet had a chance to increase surface ozone concentrations over where it is located. The elevated ozone is strictly tied to the initial aged plume. By June 4, the clearing of this aged smoke plume across the District and the Mid-Atlantic brings the return of good air quality.

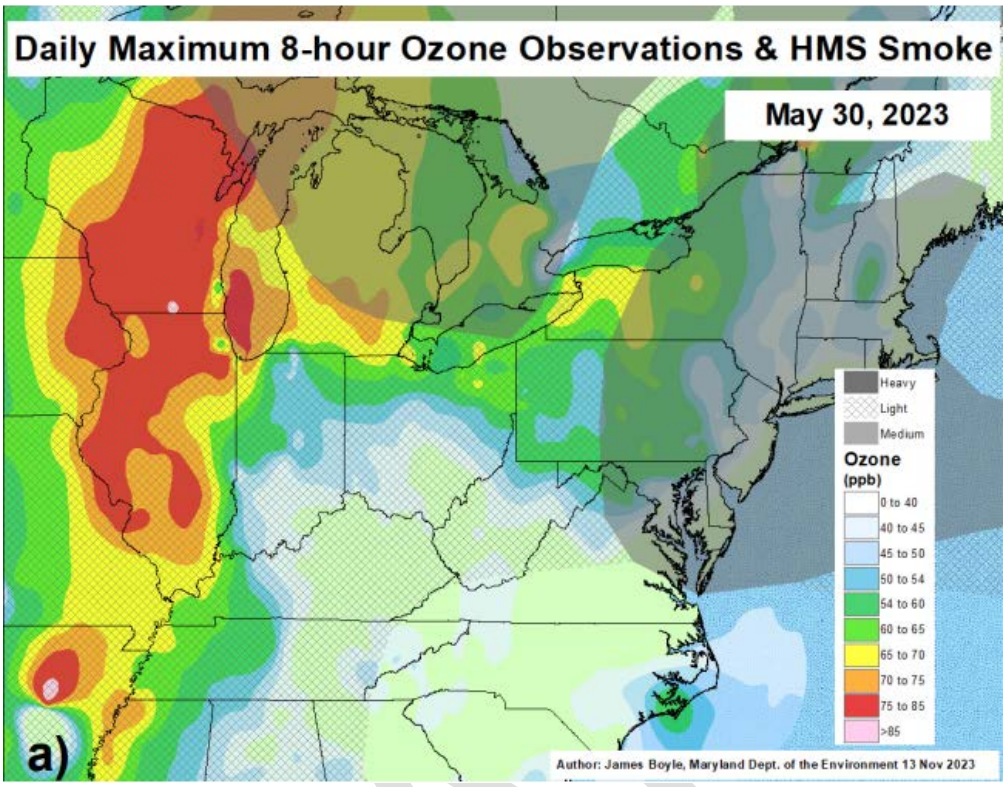
Daily Maximum 8-hour Ozone Observations & HMS Smoke
May 30, 2023
Heavy
Light
Medium
Ozone
(ppb)
0 to 40
40 to 45
45 to 50
50 to 54
54 to 60
60 to 65
65 to 70
70 to 75
75 to 85
>85
a)
Author: James Boyle, Maryland Dept. of the Environment 13 Nov 2023

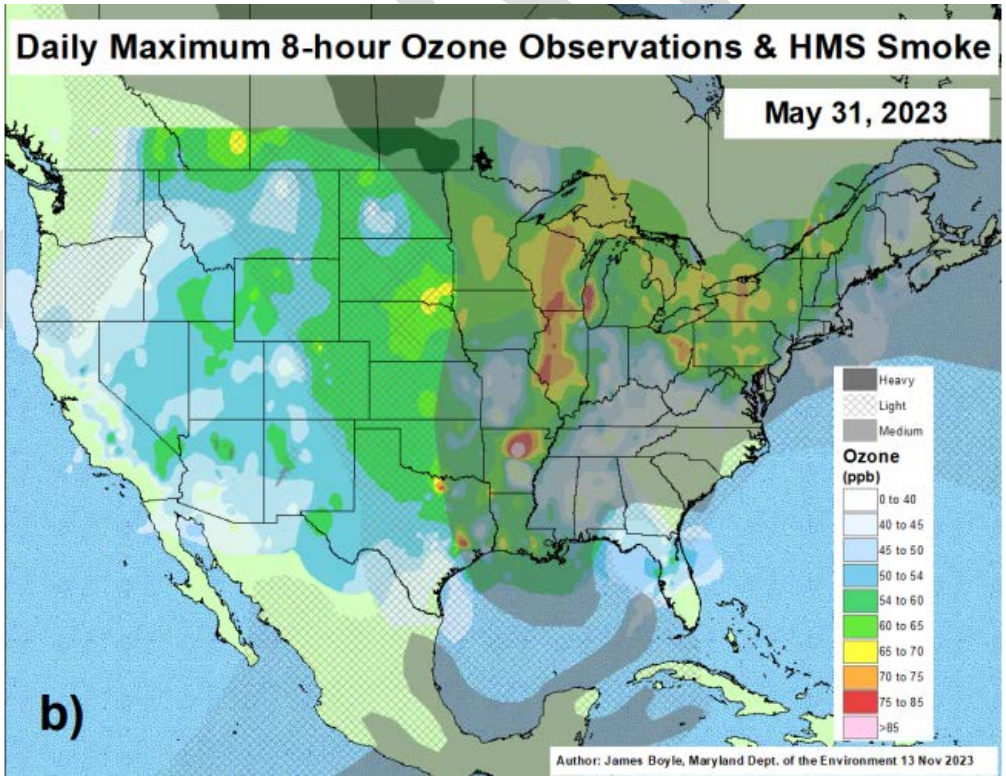
Daily Maximum 8-hour Ozone Observations & HMS Smoke
May 31, 2023
Heavy
Light
Medium
Ozone
(ppb)
0 to 40
40 to 45
45 to 50
50 to 54
54 to 60
60 to 65
65 to 70
70 to 75
75 to 85
>85
b)
Author: James Boyle, Maryland Dept. of the Environment 13 Nov 2023

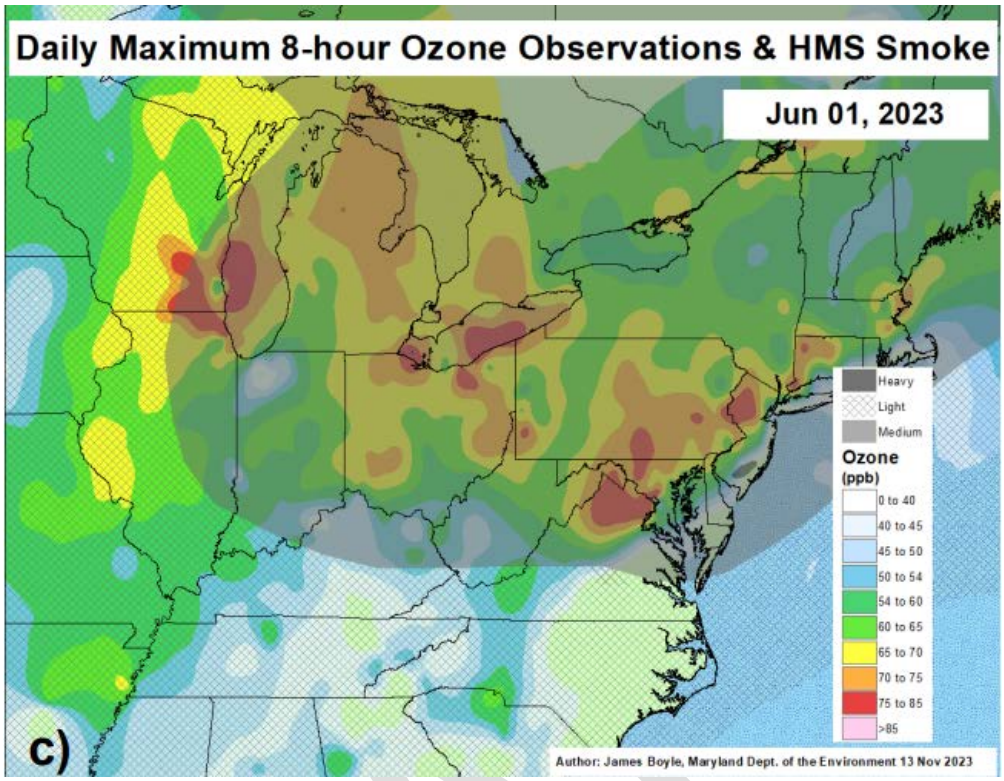
Daily Maximum 8-hour Ozone Observations & HMS Smoke
Jun 01, 2023
Heavy
Light
Medium
Ozone
(ppb)
0 to 40
40 to 45
45 to 50
50 to 54
54 to 60
60 to 65
65 to 70
70 to 75
75 to 85
>85
c)
Author: James Boyle, Maryland Dept. of the Environment 13 Nov 2023

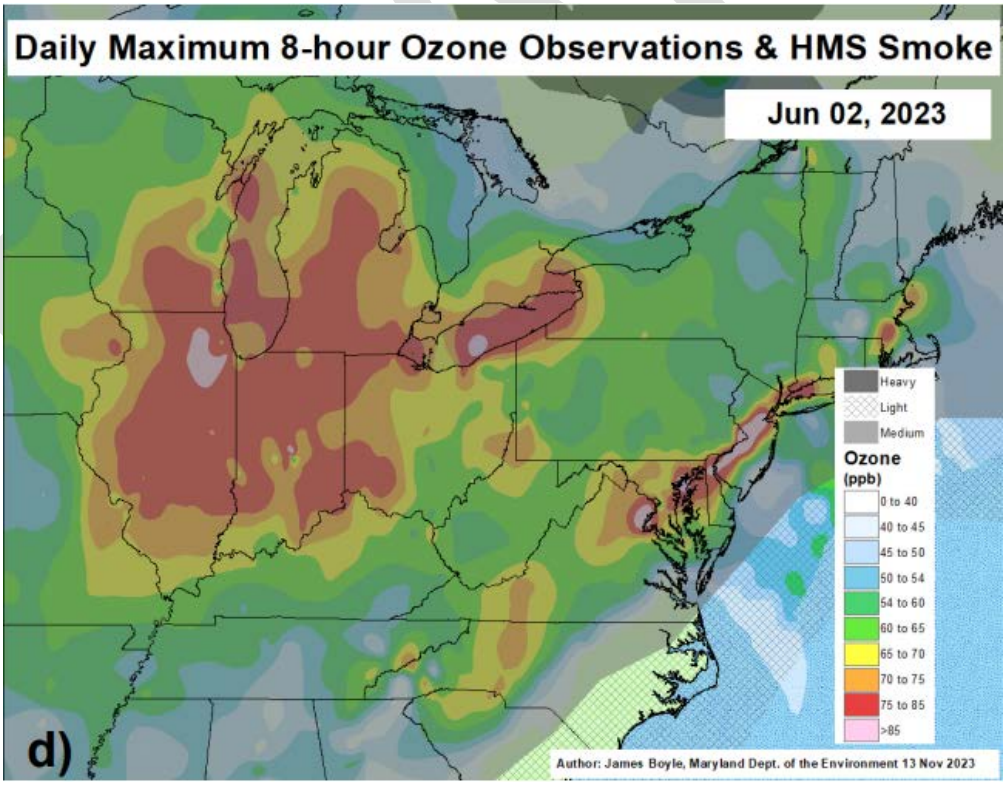
Daily Maximum 8-hour Ozone Observations & HMS Smoke
Jun 02, 2023
Heavy
Light
Medium
Ozone
(ppb)
0 to 40
40 to 45
45 to 50
50 to 54
54 to 60
60 to 65
65 to 70
70 to 75
75 to 85
>85
d)
Author: James Boyle, Maryland Dept. of the Environment 13 Nov 2023

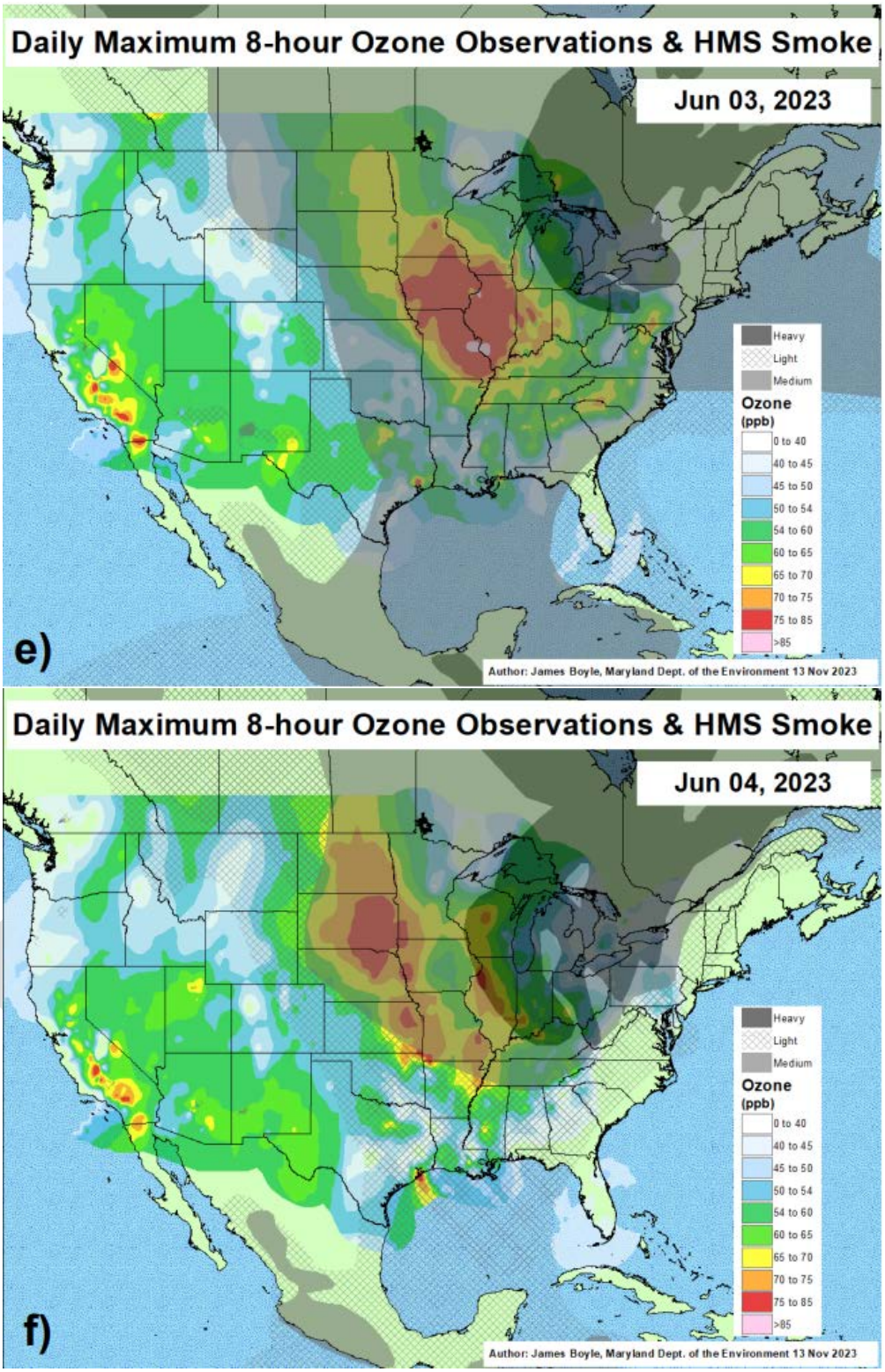

Figure 23: May 31 - June 4 maximum 8-hour average ozone concentrations and Hazard Mapping System (HMS) analyzed smoke (hatching and shading). Figures A, d, e, and f show the CONUS view, while b and c show a regional, zoomed-in view of the Mid-Atlantic area for greater detail. Transported smoke was closely associated with ozone in the District beginning on June 1.

3.0 Clear Causal Relationship Between the Event and Monitored Ozone Concentrations

The case presented in this analysis illustrates an example of the impact of smoke on ozone concentrations via the transport of smoke-augmented, ozone-laden air into the District. DOEE here presents necessary evidence to show the smoke event affected air quality in the District and clearly was associated with ozone concentrations beyond what otherwise is expected in the absence of smoke and/or that smoke caused the exceedance days.

Comparisons to historical concentrations and a Q/d analysis (Tier 1 and 2 steps) are provided. While DOEE believes these analyses alone show a causal relationship between the ozone and smoke, the complicated nature and long transport of the event may not clearly demonstrate a clear causal relationship. However, it was deemed that further analysis was necessary to further establish and demonstrate a clear causal relationship was prudent. Therefore, a weight of evidence (Tier 3) approach is used to build an irrefutable case that smoke transport was responsible for the ozone concentrations and the ozone exceedance days in the District.

3.1 Historical Concentrations

Scatter plots of MD8AO at the McMillan monitor exceeding the 70 ppb NAAQS on June 1st and 2nd showed the exceptional nature of the exceedances (Figure 24). All ozone data from 2019-2023, during the months of April to September, were plotted for each monitor against that monitor's multi-season and June only 99th percentile. Recall that significant and sustained reductions in ozone precursors across the eastern US have occurred in the past ten years. These reductions have been particularly evident in NO_x, leading to lower ozone concentrations. Consequently, this has led to a noticeable decrease in ozone exceedance days despite an increasing number of hot days; four of the lowest five years based on exceedance days have occurred in the 2018-2022 period. COVID lockdowns lowered exceedance frequency in 2020, but 2022 had an equal number of exceedance days as 2020.

June 2023 had the lowest aggregate EGU emissions ever (Figure 6 and Figure 7). While June 1st and 2nd, 2023, had a notable increase in 2023 aggregate NO_x emissions, the total NO_x on June 1st and 2nd (311 tons) was close to the mean of 2022 (300 tons), which as a year had only three total exceedance days in the District. Therefore, amplified MD8AO concentrations in late June 2023 represented substantially more ozone generated from available NO_x than in 2022 or a more historical scenario, when emissions were substantially higher. For comparison, mean aggregate emissions in June 2019 were 430 tons. Even so, 2022 EGU emissions experienced a substantial decrease of 30% compared to the 2019-2021 daily average (per Figure 5). The 2023 average daily output for June was 225 tons per day, or 47% lower than the 2019-2021 average (428 daily tons). Since 2019-2021 is within the previous five years of data that EPA requests for historical comparisons, DOEE feels the data from 2019-2021 raises the 99th percentile higher than what is otherwise now representative of the District's ozone. Thus, DOEE also offers two additional 99th percentiles to compare the McMillan monitor MD8AO on June 1st and 2nd.

These additional 99th percentiles are calculated using data from only June in 2022 or June 2022 and 2023 combined. DOEE believes this increases the robustness of the historical comparison.

This can be seen in Figure 24; the days that exceeded the NAAQS on June 1 or 2, 2023, and for which DOEE is seeking exclusion of the data are colored red. Textual annotations give the MD8AO for the red-colored data points. Along with the 70 ppb NAAQS (red solid line), four additional lines provide the 99th percentiles to account for the changing NO_x emissions and ozone levels in D.C. over the past five years. The 99th percentile for all ozone season data, 2019-2023, is given in dashed purple. All June ozone data from 2019-2023 is given in green dash. Data from June 2022 is only given in dashed orange, while all June ozone data from 2022 and 2023 combined are given as a blue short-dashed line.

The McMillan monitor exceeded the June 99th percentile threshold on June 1st. It exceeded the 99th percentile for 2022 and the 99th percentile from 2019 to 2023. It is safe to say these events caused one of the highest ozone concentrations at all monitors, which exceeded the standard (and even at those that did not – see Appendix B). The following scatter plot from the McMillan monitor shows the below data (Figure 24). Along with the 70 ppb NAAQS, four additional lines show the 99th percentiles for all ozone season data from 2019-2023, all June ozone data from 2019-2023, only ozone from June 2022, and ozone from June of 2022 and 2023 combined.

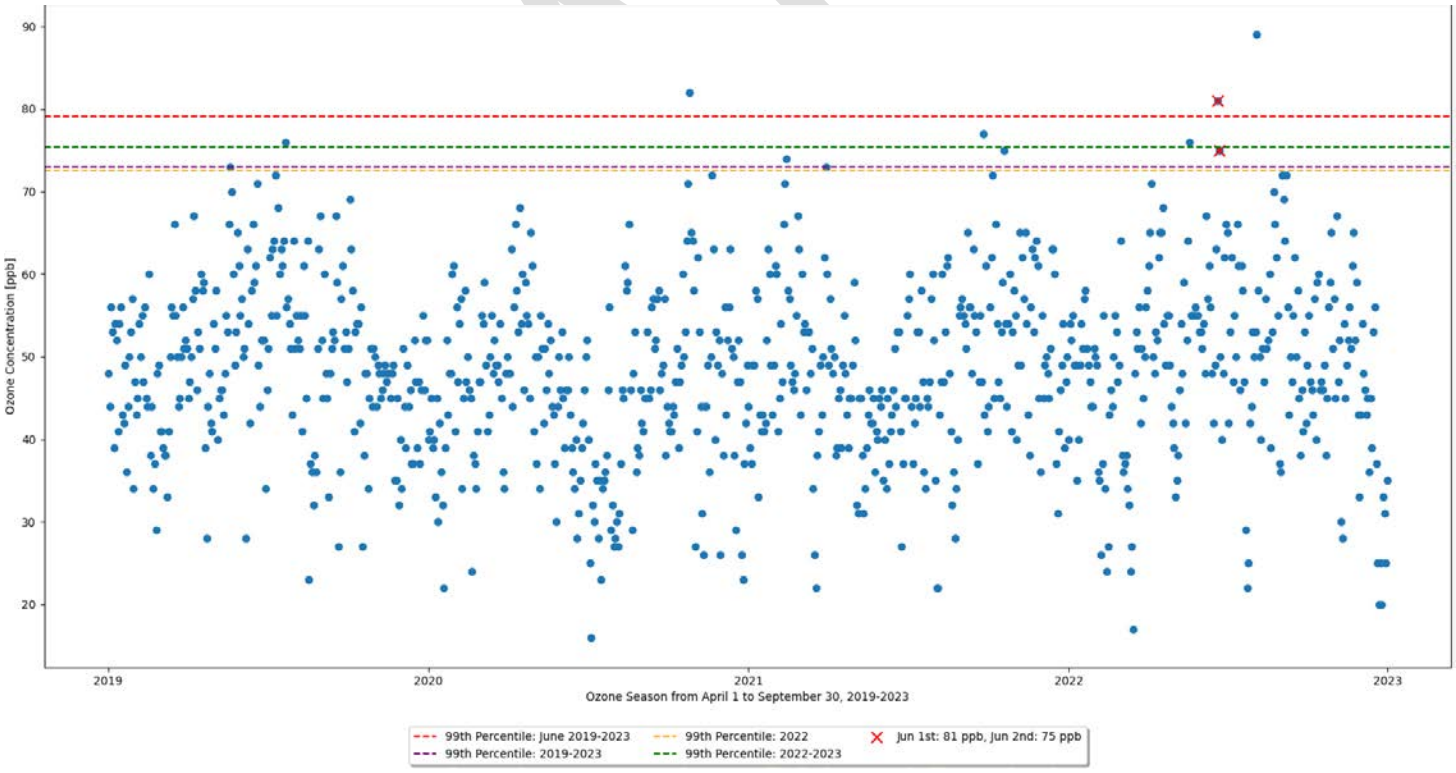

Figure 24: Scatterplot of Maximum Daily 8-hour Average Ozone (MD8AO) concentrations at McMillan (blue dots), April 1 – September 30, 2019-2023.

3.2 Evidence that Fire Emissions were Transported to the District

Here are trajectory modeling results to support that smoke from west-central Canadian fires reached the District after more than a week. Note that weakly forced meteorological conditions (e.g., winds), such as occur under high pressure, tend to be associated with relatively poor meteorological transport modeling performance due to weak winds. The Hybrid Single-Particle Lagrangian Integrated Trajectory (HYSPLIT; Rolph, 2017; Stein et al., 2015) model was used to calculate backward trajectories originating from within the District on June 2. Meteorological data driving these trajectories was from the Global Forecast System (GFS) model (0.25 degree) dataset.

Backward trajectories from the District starting at 2:00 pm. EDT on June 2 were run at three heights: 1500 m, 1000 m, and 500 m (Figure 25). The trajectories were allowed to run backward for 13 days, which would be 2:00 pm. on May 20, or approximately when smoke was seen entering CONUS. While the evolution of this smoke has already been conveyed extensively above, these trajectories support the same conclusions. The trajectory at 2000 m arcs around the Great Lakes eventually recirculate over the greater Wisconsin area. Note that while this origin does not match the location of smoke on May 20, this trajectory crosses the path of smoke by May 24-26 from plume "B."

The general pattern of recirculation around the high of the 2000 m trajectory was also consistent with the narrative already put forth. The entirety of the 1000 m trajectory is not as important as the first few days. Note that this trajectory goes directly to the location of the Nova Scotia fire during the first 72 to 96 hours of the trajectory run, in line with the burn period of that fire, again supporting the supposition of multiple smoke plumes for the June 2 event. The 750 m trajectory was also pulling in air from the north of the region. Symbols on the trajectories provide 6-hour intervals of the trajectory path. The 750 m trajectory was very slow to progress southward from trajectory "kink" near Lake Superior, taking 8-9 days to reach the District from that location, meaning any smoke introduced to this layer between May 24 and June 1 along the path would have found its way to the District.

Indeed, abundant smoke was noted by May 27 and 28 over this area as it was pulled around the high and subsided. This further substantiates the introduction of smoke behind the cold front via subsidence aloft to the surface, as the 750 m trajectory had substantial subsidence (lowering in height) approaching the District on June 1. Together, these trajectories confirm the narrative model and highlight the complexity of the event.

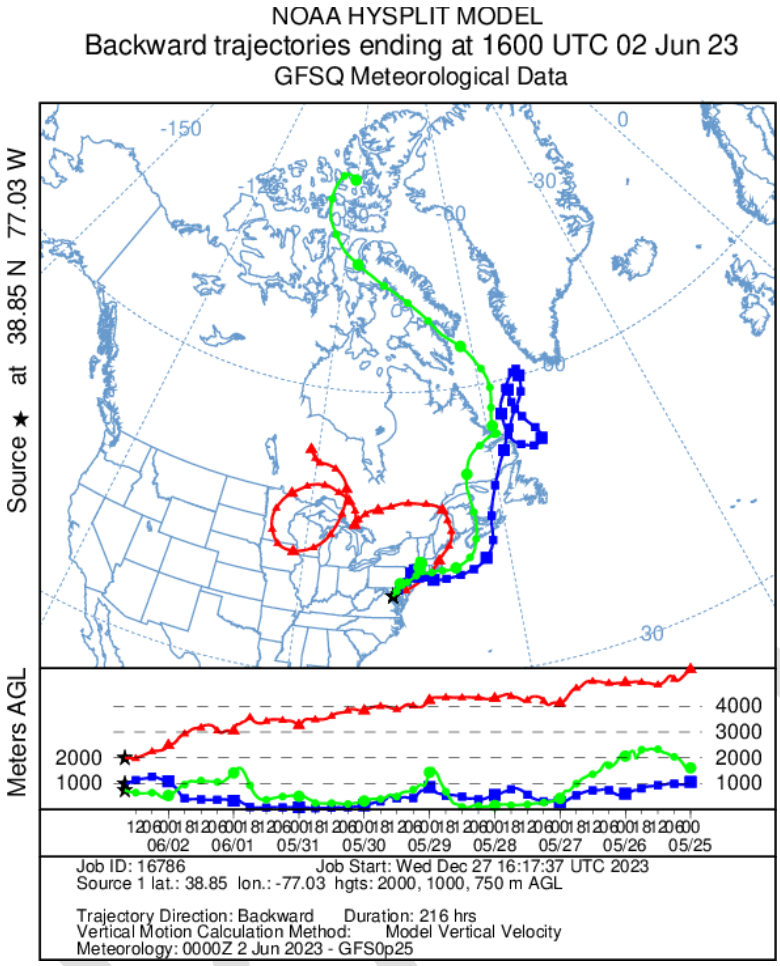

Figure 25: Three-height Backward 312-hour (13 days) GFS (0.25 degree) Transport Trajectories. GFS back trajectories at three heights (2000 m green, 1000 m blue, 750 m red) from the District, beginning on June at 2:00 pm EDT.

3.2.1 Visibility

Aside from the surface observations of PM2.5, smoke impacted visibility in a dramatic fashion in the District. The images below were taken in both Northern Virginia and in the District.

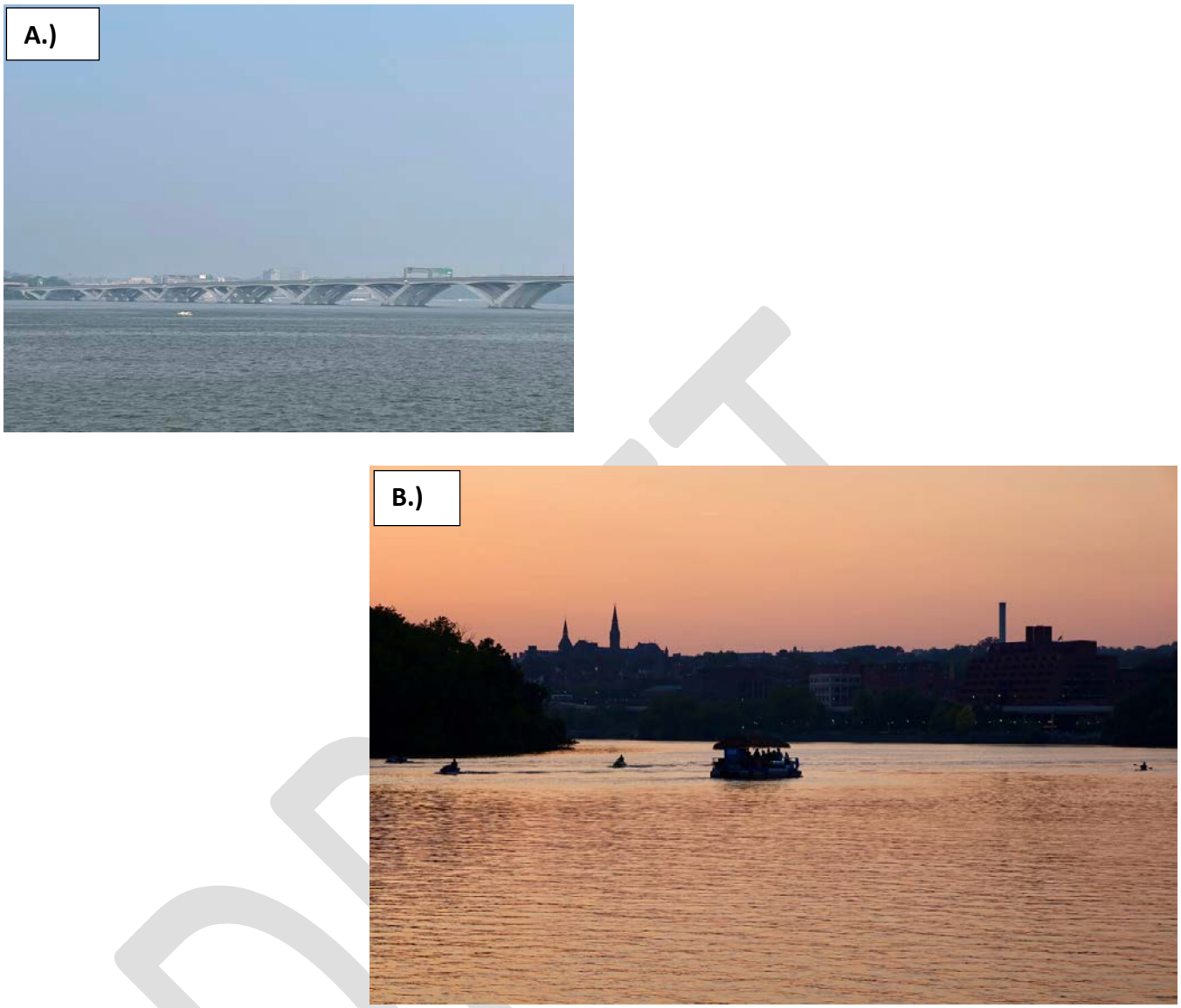

Figure 26: Pictures from June 1-2, 2023, at various times and locations around the District. A.) Image taken of the Woodrow Wilson Bridge. B.) Image taken of a hazy sunset taken along the Potomac River.

3.2.2 Evidence of Ozone Transport via Ozonesondes

DOEE was able to obtain ozonesonde data from launches conducted by the Maryland Department of Environment (MDE) in partnership with Howard University Beltsville to measure the morning and afternoon vertical profiles of the exceptional event on June 2. Ozonesondes are used to measure stratospheric ozone. Howard University has a contract with the Maryland Department to perform these sonde launches during ozone season and other times on an as-needed basis. All ozonesondes were launched from the Howard University Beltsville site just northeast of Washington, DC. Ozonesondes were successfully launched during the pre-dawn hours (2:16 am. EDT; Figure 27) and

peak heat period in the afternoon (3:13 pm. EDT; Figure 29). At night, ozone is removed from the layer of air a few tens of meters from the surface in the absence of sunlight as it interacts with other molecules or objects. However, the layer of air immediately above the surface at night "preserves" ozone overnight, making it the "transport relevant" or "carry-over" layer simply known as "the residual layer." The residual layer is usually found from around 500 m to 1,500-2,000 m above ground level at night. Therefore, surface ozone may be at or near zero at night, while just a few hundred meters above the ground, ozone may still be 50-80 ppb. The pre-dawn ozonesonde on June 2 observed ozone concentrations in the residual layer reaching as high as 85-86 ppb in a layer of ozone between 0.5 and 1.5 km (Figure 27)! Note the height consistency of this layer compared to the ceilometer at McMillan (Figure 30, first vertical white line), which had an aerosol layer of smoke between approximately 800 m to 1600 m at the time of the ozonesonde, essentially showing the ozone layer on the ozonesonde was associated with a deep laminar layer of smoke. The ozonesonde also confirms that Beginning just below 3 km AGL, another layer of ozone greater than 70 ppb was apparent with a depth through 3.5 km AGL. This was noteworthy given the afternoon mixing depth discussed previously and explored next.

The afternoon ozonesonde (3:13 pm. EDT launch) observed ozone concentrations consistently at 75 ppb through 2.5 km in depth, though above 70 ppb to heights greater than 3 km (Figure 28). This was important to note because the temperature profile in the afternoon showed adiabatic lapse rates (the red line was tilted towards the left with height in a consistent 9.8°C/km trend), a sign of boundary layer mixing through 3 km. In practical interpretation, this was an extremely deep mixed layer, which may otherwise typically dilute pollutants. However, as seen in the early morning profile and in the ozone lidar, ozone was plentiful above 2 km in height due to the abundance of regionally diffuse smoke. As such, instead of diluting pollutants in the boundary layer (thereby decreasing ozone load), continued mixing brought additional residual ozone towards the surface, persisting ozone concentrations there. This also explained the consistent 70-75 ppb ozone concentration with height through 3 km on the afternoon ozonesonde. Given the residual layer represents a regional concentration or "burden" on the air quality (particularly in this extreme case as ozone above 2 km becomes considered), the primary reason for greater concentrations was due to the buildup of ozone within the aged, smoky airmass that had propagated around the central CONUS ridge.

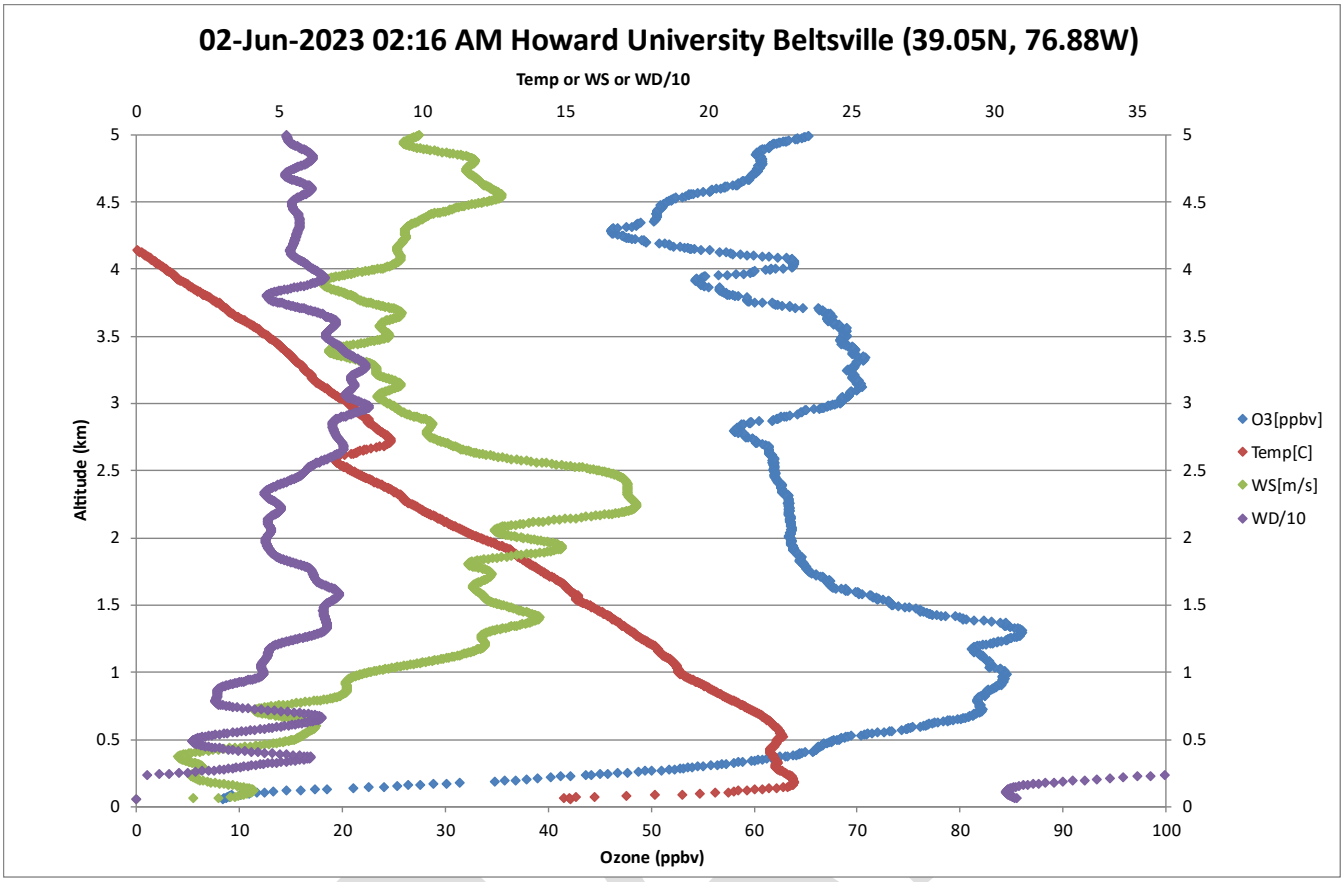

Figure 27: Ozonesonde launched from Howard University Beltsville on the morning of June 2, 2023. 2:26 am. is equivalent to 06:26 UTC. Temperature (red, squares), wind direction (green, triangles), wind speed (blue, diamonds), and ozone (purple, dashes) are shown from the surface through 5 km AGL. Ozone concentration is given on the top horizontal axis. Temperature and winds are given by the bottom horizontal axis.

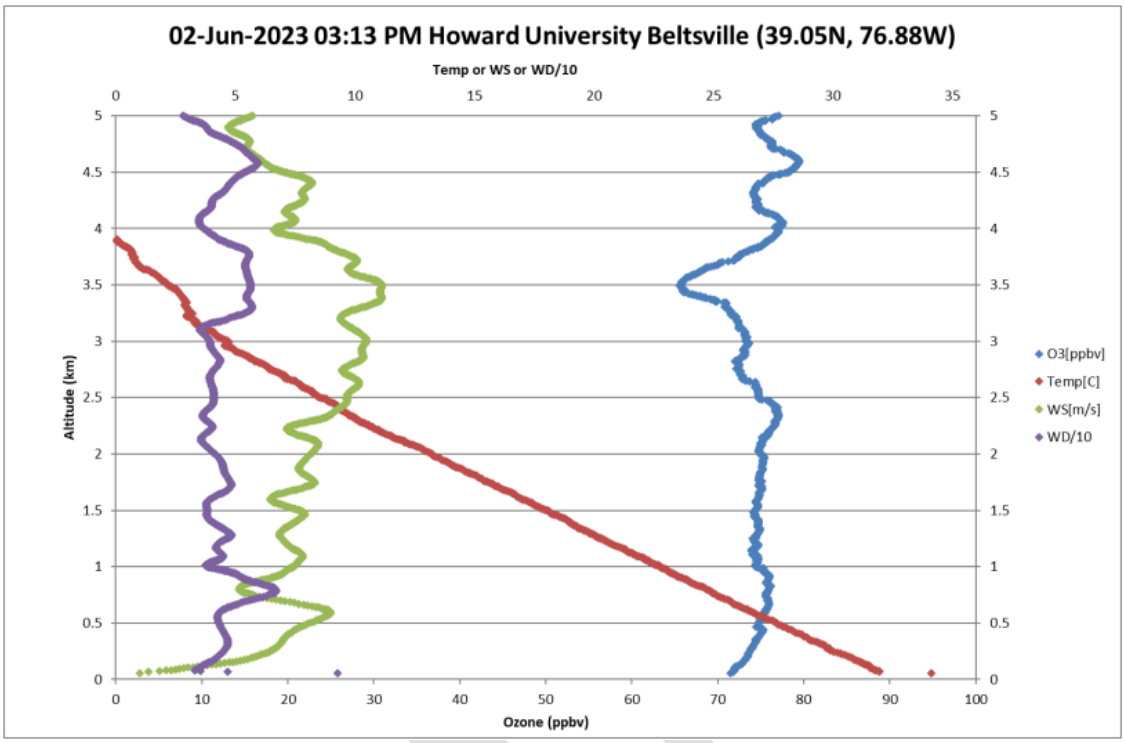

Figure 28: As in Figure 18, except for June 2, 2023, at 3:13 pm. EDT.

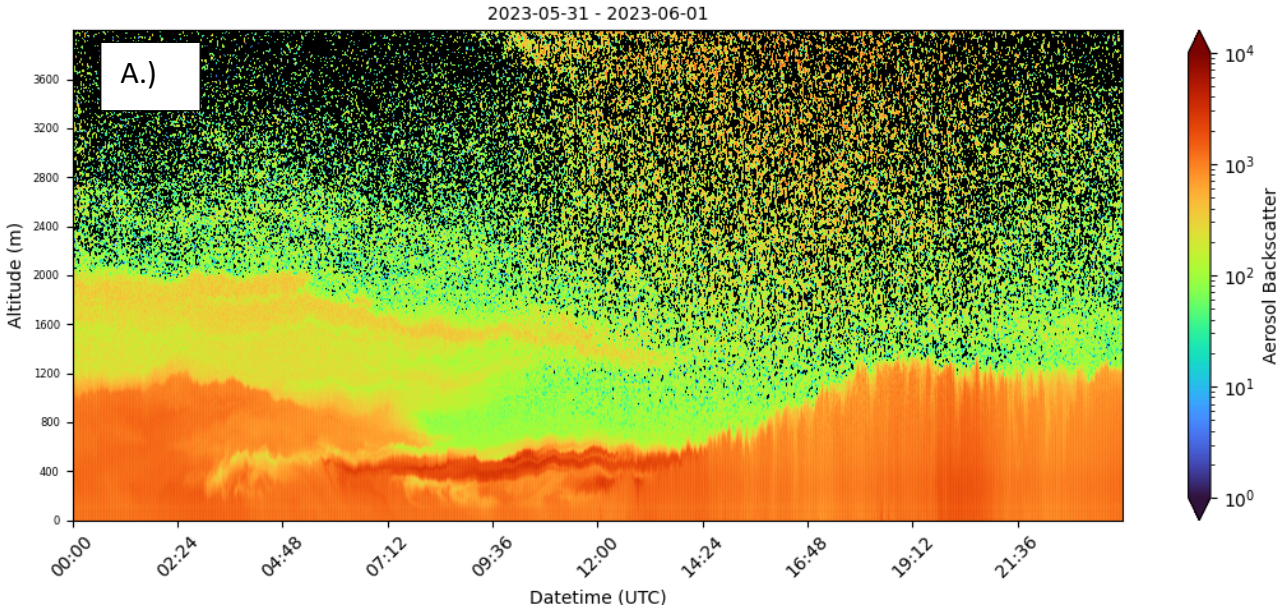

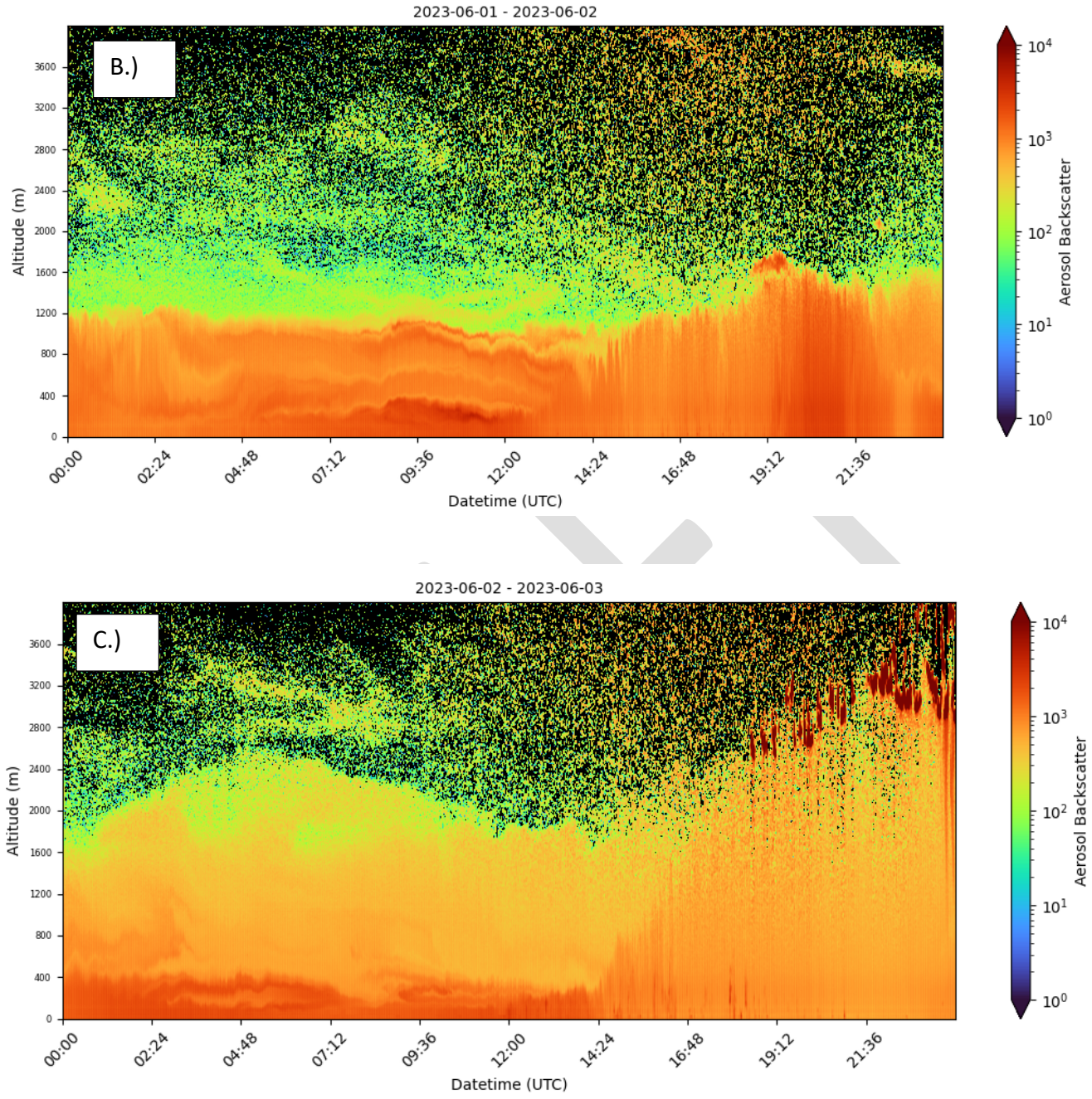

Figure 29: Ceilometer backscatter (colors). The McMillan Reservoir site on May 31- June 2, figures a-c.

Ceilometer data provided the highest multi-dimensional temporal resolution of the arrival of smoke. The ceilometer at the McMillan location shows the presence of smoke starting May 31. The ceilometer on May 31 continued to show surface air burdened with aerosol. Particularly prominent from roughly 0448 to 1424 UTC were layers of aerosols (smoke) that formed due to nocturnal stability within the atmospheric boundary layer (Figure 29a). These layered features illustrate the presence of smoke well and how smoke carried over from day to day, then mixed back into the boundary layer the following morning. On May 31, mixing was completed around 1424 UTC (10:24 am. EDT) as the layered structure

disappeared; for the remainder of the day, aerosol concentrations ebbed and flowed, as seen in the varying shades of red in Figure 31.

Background smoke and aerosol from May 31 carried over to June 1 as noted by the layered aerosols overnight from roughly 0224 to at least 1200 UTC (10:24 pm. EDT May 31 to 8:00 am. EDT June 1; Figure 29b). Around 1400 UTC (10:00 am. EDT), dark red returns were observed. This was smoke from the Allen Road fire in New Jersey, impacting the site directly. The smoke after that time diffused the rest of the day over the District and as the boundary layer grew.

During the overnight hours on June 2, smoke persisted. Smoke layers during nocturnal stability were again evident (Figure 29c). Note that on most days, the boundary layer depth was well below 2 km based on aerosol returns. Boundary layer depth is best not assessed on aerosols alone but still may be used as a qualitative proxy, and as such, it may be noted that on all the previous days, much of the aerosol returns on the ceilometers remained below ~1500 m. On June 2, even during the overnight and early morning hours, a coherent residual layer of aerosol to at least 2400 m in depth was observed, indicating a greater depth of pollutants available for the next day. As on previous days, layering of aerosols (smoke) was observed in the sub-1000 m depth till roughly 1300 UTC (9:00 am), after which mixing washed out this characteristic. Mixing during the afternoon of June 2 achieved a boundary layer height similar to that overnight, reaching a higher daytime depth than the previous days.

3.3 Q/d Analysis

EPA guidance[iv] recommends conducting a Q/d analysis as a rough assessment of the ability of a wildfire to cause increased ozone concentrations. The Q/d analysis is a simple comparison of the ratio of Q, the daily tons of VOC and NO_x emitted from the fire, to d, the distance in kilometers from the fire to the point of concern. If the Q/d value compares favorably to analytical data from other fires, then the fire can be presumed to have had a causal effect on ozone concentrations at the point of concern. The comparison to other fires is a key point that will be brought up again.

EPA guidance[v] indicates that a fire should have a Q/d of more than 100 tons per day per kilometer (tpd/km) to be considered to have a clear causal impact on ozone. EPA developed this value based on analyses of four fires that occurred in 2011. Due to the large distances that Canadian wildfire plumes must travel to the District, the Q/d analysis will regularly fail to achieve the 100 deemed acceptable by the EPA guidance. Therefore, DOEE feels the 100 value is not representative of long-range east-coast smoke events. DOEE instead presents several alternatives based on this analysis.

3.3.1 Estimate of Q

The emissions from the fire can be estimated using information from EPA's AP-42 Compilation of Air Emission Factors Section 13.1 Wildfires and Prescribed Burning. The equations given are as follows:

Fi = Pi * L (Equation 1)
Ei = Fi * A (Equation 2)

Fi = emission factor (mass of pollutant/unit area of forest consumed)

Pi = yield for pollutant "i" (mass of pollutant/unit mass of forest fuel consumed)
= 12 kg/Mg (24 lb/ton) for total hydrocarbon (as CH4)
= 2 kg/Mg (4 lb/ton) for nitrogen oxides (NOx)

L = fuel loading consumed (mass of forest fuel/unit land area burned)
A = land area burned
Ei = total emissions of pollutant "i" (mass pollutant)

Combining equations 1 and 2, we have:

$$Ei = Pi * L * A$$

Pi is given above for total hydrocarbons and for nitrogen oxides. The fuel loading is given in AP-42 for different regions of the United States and ranges from 9 to 60 tons per acre. Conservatively, we will estimate a low-end emission rate using 10 tons per acre, which is associated with North Central US. conifer forests. Note that our results could increase by a factor of 6, which was the high end of emissions expected.

Information provided by the Canadian Wildland Fire Information System (CWFIS) reported that between May 13 and May 20, 2023, fires across northwestern Canada consumed 1,400,000 hectares (3,459,475 acres), with a slight lull around May 17 amid an otherwise extremely intense eight-day period (Figure 30). On May 16 alone, 311,360 hectares (769,387 acres). For reference, the total land area of Rhode Island is approximately 314,000 hectares. It appeared that smoke lingered and built up over parts of that region during this period before a passing low-pressure system "released" a thick plume of smoke into the Central United States. This appears to be the primary plume that meandered around central CONUS under the stout Omega-block ridge before moving around the Great Lakes to approach the Mid-Atlantic from the north and northeast.

There may be some additional contribution from additional enhanced burning near the 15. A contextual comparison to the State of Rhode Island makes the fires' size more comprehensible. [https://www.ri.gov/facts/trivia.php] 123 end of the month. However, initial analyses seemed to indicate that this may have drifted northward. Smoke at this latitude is harder to track due to limited satellite overpasses (the latitude is too far north for geostationary retrievals) and cloud cover during polar orbiting overpasses. To that end, we focus on the recirculated smoke emanating from the burning period between May 13 and 20, 2023, across west-central Canada.

As complicated as the smoke transport from the west-central makes the event on its own, several additional fires occurred closer to the Mid-Atlantic. These fires were smaller in scale but, due to their increasing proximity to the District, provided further amplification of airborne precursors (Figure 31). The first fires of note and chronology were the Nova Scotia fires. These occurred on the southernmost tip of the province between May 28 and June 2. Fires burned 24,840 hectares (61,381 acres) over this time period. Much of the burning took place on May 29, when 9,154 hectares (22,620 acres) were burned. Smoke from these fires appeared to move towards the Mid-Atlantic on north-northeasterly

flow from May 29-31, burning a total of 19,670 hectares (48,605 acres) over that period, resulting in residual smoke in the District for the June 1-2 event.

Several fires also occurred in New Jersey leading up to the June 1-2 ozone exceedance in the District. Note that these fires were also north of the District, further contributing to precursor concentrations in the atmosphere from the "background" smoke from west-central Canada and Nova Scotia (Figure 31). The first fire, chronologically and by size, was the Allen Road fire in southern New Jersey. This fire burned a total of 2,215 acres between May 31 and June 2. Most of the burn occurred on June 1, when 1,772 acres burned. This smoke came thickly in the District in June, leaving another source of residual smoke for June 2. In this analysis, we consider only emissions from May 31 (332 acres; relatively inconsequential but happening very late and thus considered June 1 as well) and June 1. Two other known smaller fires were also reported or observed across New Jersey. The first occurred on the Fort Dix military installation in central New Jersey on June 1, directly east of Philadelphia. Little information is available from military burns. However, an estimation done by satellite area-of-detection put the magnitude of the fire around 77 acres.

While small, a copious, visible plume was apparent from the fire heading towards the eastern Greater Philadelphia area on June 1 (Figure 32). There was an additional fire on June 2, called the Flatiron Fire, in Medford Township, New Jersey. This fire was reported at 86 acres and burned only on June 2. A third fire was reported on May 29 called the Box Turtle Wildfire, which occurred in Monroe Township of Gloucester County, southeast of Philadelphia. This fire consumed 158 acres. The timing of this fire would have allowed smoke to push into the District behind the cold front. Unfortunately, due to cloud cover, little visible evidence can be extracted from this burn, and thus, it has been left out of further analysis here. Still, collectively, despite the smaller fire sizes, the close proximity to the ozone exceedance region suggests an additional contributing direct causal relationship.

Assuming a lower threshold of emission per area burned, the total hydrocarbon emissions from the period can be estimated to be:
Ehc = 24 lbs of HC / ton of forest fuel consumed * 10 tons fuel / acre * 3,879,755 acres
Ehc =931,141,200 pounds of HC
Ehc = 465,571 tons of HC emitted during the period from June 21 to June 26, 2023

Similarly, for NO_x:
Enox = 4 lbs of NO_x / ton of forest fuel consumed * 10 tons fuel / acre * 3,879,755 acres
Enox = 155,190,200 pounds of NO_x
Enox = 77,595 tons of NO_x emitted during the period from June 21 to June 26, 2023

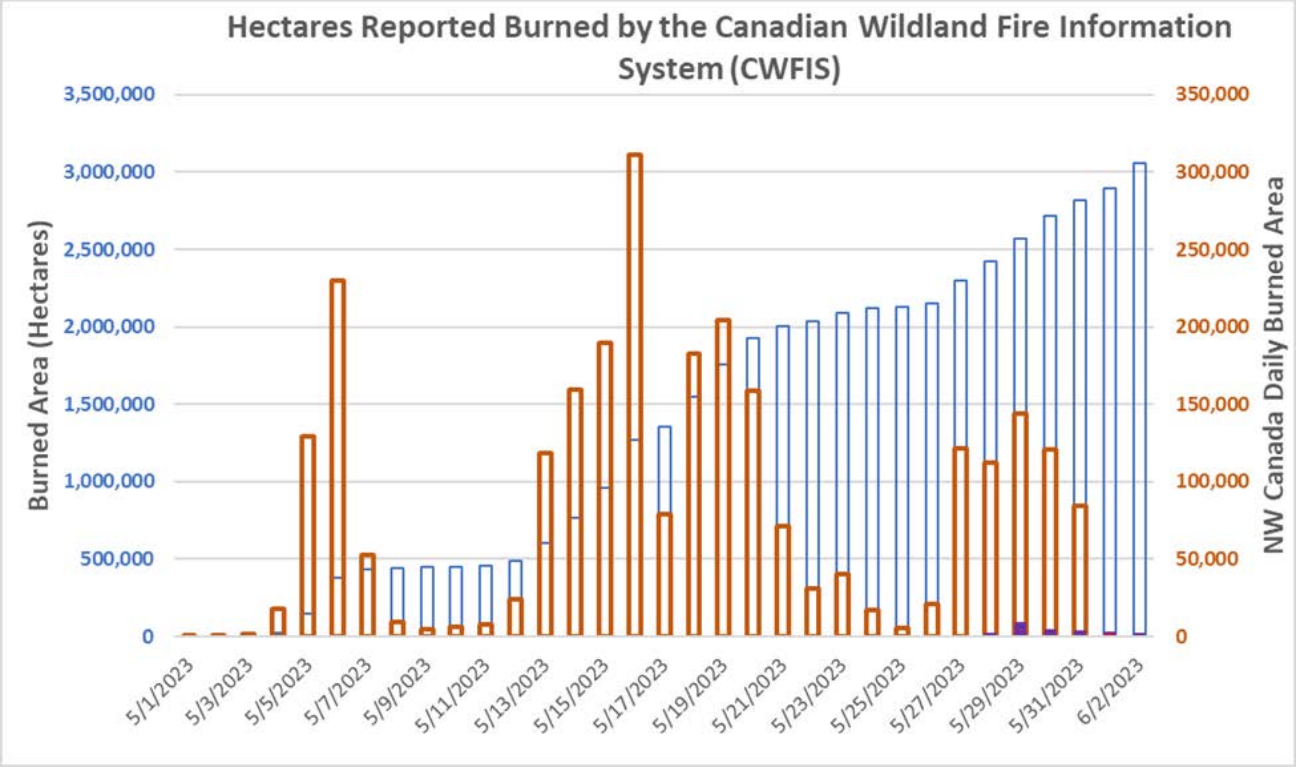

Figure 30: Hectares burned reported by the Canadian Wildland Fire Information System (CWFIS).

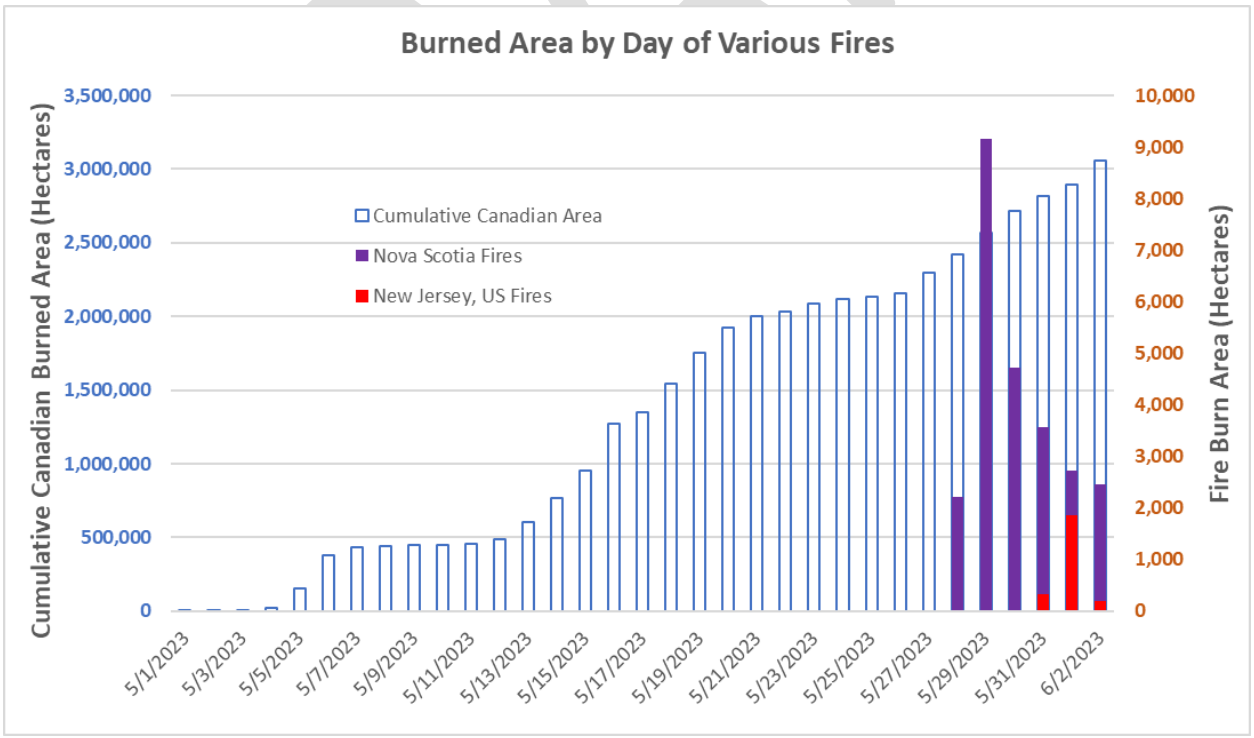

Figure 31: Like Figure 43 but with emphasis on Nova Scotia and New Jersey fires. Daily hectares of land burned across Canada May 1 - June 2, 2023.

Q is the total daily emission rate in tons per day of reactive hydrocarbons and nitrogen oxides. EPA recommends in the exceptional events guidance that only 60% of the hydrocarbons should be considered reactive. Therefore, the reactive hydrocarbon emissions become rHC = 0.6 * Ehc or 0.6 * 465,571 = 279,343 tons of reactive HC emitted during the period of interest. No adjustments are suggested for the NO_x emissions. Total rHC and NO_x emissions over the period would therefore be 279,343 + 77,595, or 356,938 tons over the six days. On average, this results in a daily emission rate, or Q, of 59,490 tons per day.

3.3.2 Estimate of d

BDue to the large distance and the widely dispersed nature of the fires across west central Canada, individual analyses will not be completed for each monitor in the District, but an estimate of the distance from the McMillan monitor will be calculated. The centroid of the fire region was along the border between Alberta and Saskatchewan (roughly 55.8835°N, 110.1683°W). Using this location supplies a representative distance the smoke traveled to the District ozone network. The travel distance was complicated due to residence time across central CONUS for several days. As such, a significant distance has been added to the path of the smoke to account for sub-continental scale recirculation across the Central Plains. As such, the flight distance followed a "spiraled" trajectory path between these two locations, giving an approximate value of 5,170 km for d.

Successive fires closer to the Mid-Atlantic will essentially use a direct line to determine the distance traveled by the smoke.

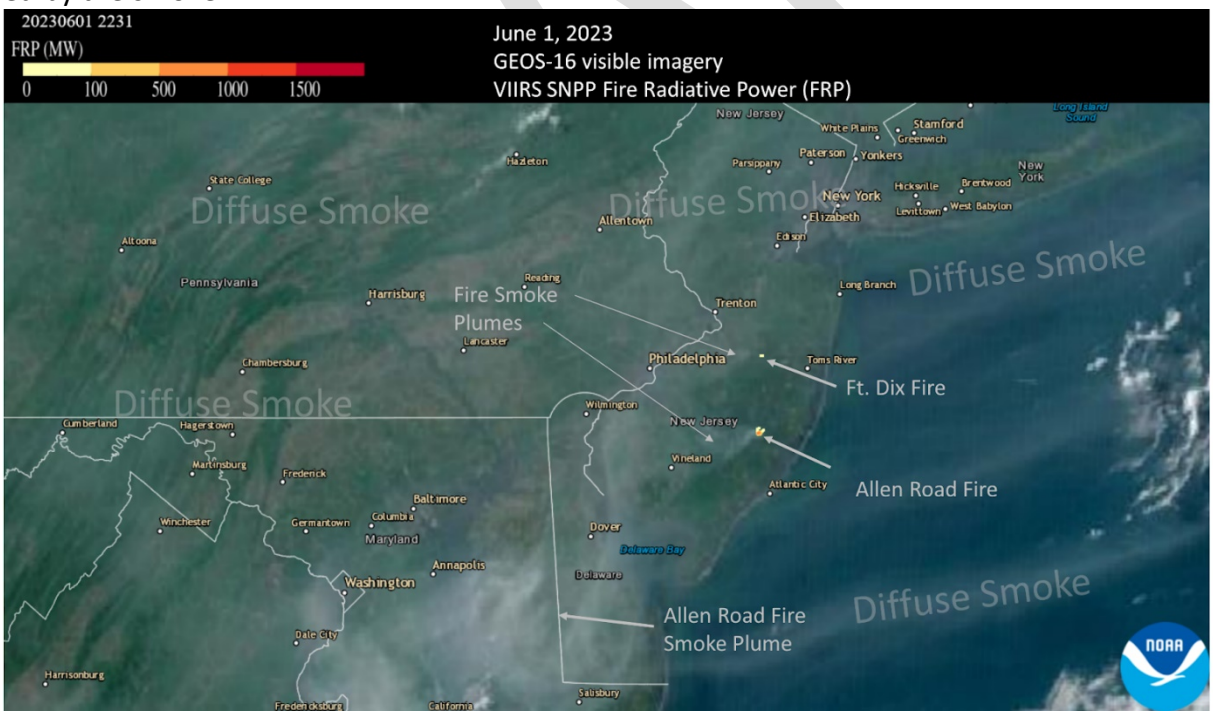

Figure 32: June 1, 2023, GOES-16 visible satellite imagery at 2231 UTC (6:31 pm. EDT) over the northern Mid-Atlantic. Diffuse smoke covers the entire region. Image taken from NOAA AerosolWatch.

Using the values and days burned determined above for the west-central Canada fires, Q/d becomes 318,895 tpd divided by 5,170 km or 7.7 tpd/km (Table 6). This value is well below the EPA recommended level of 100 tpd/km, indicating clear causality. However, we note this is higher than the concurred Exceptional Event Demonstration of similar origins in May and July of 2016. If, instead, we aggressively assumed the single day on May 16 is representative of the smoke arriving in the District from the out-of-control fires, when 311,360 acres burned, the District's Q/d value climbs to 13.7, Still well below 100. A similar test using May 18-20 gives a Q/d value of 8.0. If the emissions per acre burned are allowed to increase to 60 tons/acre in this latter case, the resulting Q/d value is 48.0. If only May 16 were used with the 60 tons/acre emission factor, the Q/d value would be 82.2.

Western Canada Fires May 13-20, 2023

ACRES	Ehc (tons)	Enox	Q	No. days burning	d	Q/d	DESCRIPTION
3,466,255	415,951	69,325	318,895	8	5170	7.7	Standard Q/d
311,360	92,326	15,388	70,784	1	5170	13.7	May 16 only
1,347,522	161,703	26,950	123,972	3	5170	8.0	May 18-20 only
1,347,522	970,216	161,703	743,832	3	5170	48.0	Fuel loading at maximum of 60 tons/arce instead of 10, May 18-20

Table 4: Q/d analysis.

3.3.3 Additive Q/d from Disparate Fire Sources

There is no known guidance for combining Q/d for multiple sources as would be appropriate for the June 1-2 ozone event, when at least three, if not four, different fires all contributed to smoke in the District. Similar methods to those used to create Q/d for the west-central Canadian fires may be applied to the other relevant fires in this event (Nova Scotia, Allen Road, Ft. Dix, Flat Iron). Various scenarios for these fires are presented below, with distances from each of the fires estimated to McMillan monitor in the District. As each of these fires (except for the Flat Iron) was a potential contributor to the District's ozone exceedance on June 2, it seems reasonable that each may be summed to reach a cumulative Q/d impact. In a maximum scenario, where we could assume 60 tons/acre of fuel loading, the summation of all the fire events, starting with May 18-20 from west-central Canada to the maximum scenarios presented below (bottom line of each table) would be 68.4 [48 + 12.5 + 7.7 + 0.2] tons per day per km, a value accepted in other sample cases in EPA guidance (see below) which conveys a clear causal relationship.

Nova Scotia, May 29-31

ACRES	Ehc (tons)	Enox	Q	No. days burning	d	Q/d	DESCRIPTION
43,127	5,175	863	3,968	3	1000	1.3	Standard Q/d
22,620	2,714	452	2,081	1	1000	2.1	May 29 only
22,620	16,286	2,714	12,486	1	1000	12.5	Fuel loading at a maximum of 60 tons/arce instead of 10

Table 5: Q/d analysis, Nova Scotia fires.

Allen Rd Fire New Jersey, May 31-June 1

ACRES	Ehc (tons)	Enox	Q	No. days burning	d	Q/d	DESCRIPTION
2,104	252	42	194	2	127	0.8	Standard Q/d
1,772	213	35	163	1	127	1.3	June 1 only
1,772	1,276	213	978	1	127	7.7	Fuel loading at a maximum of 60 tons/arce instead of 10, May 31

Table 6: Q/d analysis, New Jersey fire, May 31-June 1.

Ft Dix New Jersey Fire, June 1

ACRES	Ehc (tons)	Enox	Q	No. days burning	d	Q/d	DESCRIPTION
77	9	2	7	1	175	0.0	Standard Q/d
77	55	9	43	1	175	0.2	Fuel loading at a maximum of 60 tons/arce instead of 10

Table 7: Q/d analysis, NJ fire, June 1.

Flat Iron New Jersey June 2

ACRES	Ehc (tons)	Enox	Q	No. days burning	d	Q/d	DESCRIPTION
86	10	2	8	1	140	0.1	Standard Q/d
86	62	10	47	1	140	0.3	Fuel loading at a maximum of 60 tons/arce instead of 10

Table 8: Q/d analysis, Flat Iron NJ fire June 2.

3.4 99th Percentiles (June)

As part of demonstrating a clear causal relationship between ozone concentrations and the fire event, monitored concentrations were put in the context of historical observations. Observations at monitors falling at or above the 99th percentile in the past five years established statistical evidence that the event was likely influenced by an exceptional event and are a "Key Factor" used to determine whether a Tier 2 application is appropriate. Following the Exceptional Events Guidance, the 99th percentile was calculated for all District monitors for all days during the months of April – September from 2019-2023. Additional 99th percentiles were calculated using subsets of days as summarized and presented previously in section 3.1 and in Figures 20-21. For convenience, a summary table with comparisons of all the 99th percentiles is given in Table 9.

	99th Percentile ppb					June 1, 2023				June 2, 2023			
Name	**AQSID**	**All Data**	**June Only**	**2022**	**2022-2023**	**All Data**	**June Only**	**2022**	**2022-2023**	**All Data**	**June Only**	**2022**	**2022-2023**
McMillan	110010043	73	79	72.5	75.4	Yes	Yes	Yes	Yes	Yes	No	Yes	No

Table 9: 99th percentile values and comparisons to observations on June 1-2, 2023.

The two District monitors for which DOEE is seeking exclusion due to exceptional event influence have their 99th percentiles presented based on data from April 1 – September 30, 2019-2023, and other subsets as defined in section 3.1. The final four columns highlight which monitors exceed their 99th percentile level ("Yes") for a given data set and day.

3.4.1 Particles

$PM_{2.5}$ can be both a primary pollutant and a resultant secondary pollutant of wildfire emissions downstream, as photochemistry within the plume converts certain species to aerosols. The entire DOEE network showed a correlated increase in $PM_{2.5}$ 24-hour averages from May 27- June 3, which aligned with the onset of the smoke plume in the District (Figure 33). Concentrations climbed from around 5-8 µg/m^3 to 10-20µg/m^3, generally, from after this frontal passage until easterly flow removed smoke from the region late on June 3. Within this four-to-five-day period, PM2.5 concentrations varied as pulses of smoke moved through the region, and active photochemistry sustained PM formation.

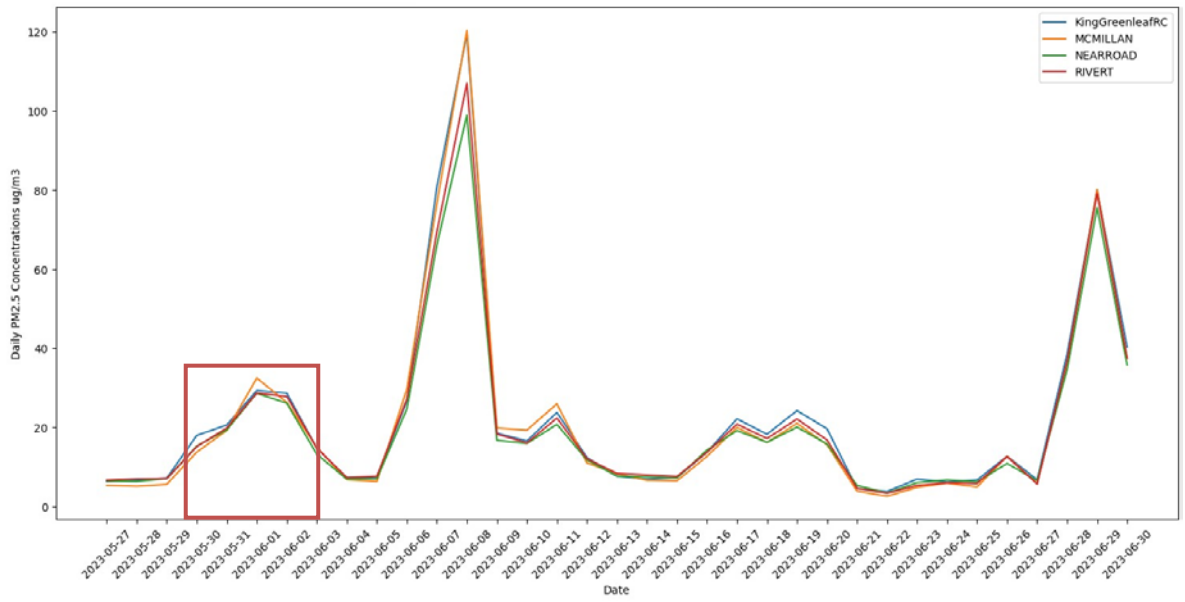

Figure 33: Daily averaged fine particle ($PM_{2.5}$) concentrations for all sites available in the District for the month of June 2023. Starting May 28th, concentrations start to increase with the presence of smoke, which is highlighted by the red box.

3.4.2 3.5.3 Carbon Monoxide (CO)

Satellite retrievals are capable of tracking wildfire smoke visually but also through precursor species to provide irrefutable evidence of the transport of wildfire ozone precursors. CO has been previously identified as a wildfire smoke indicator (Andreae and Merlet, 2001; McKeen et al., 2002; DeBell et al., 2004; Dreessen et al., 2016) and can play a role in ozone production. The conceptual model of the event has a thick plume of smoke being recirculated around central CONUS and the Great Lakes before being transported to the District from the north out of Canada after over a week of aging and transport. CO was observed to follow a pattern of transport similar to that described in the District's ozone exceedance conceptual model (Figure 20) with an identical track to the visual smoke plume as shown below. The mid-tropospheric (500 mb) CO layer observed by the moderate resolution "Atmospheric InfraRed Sounder" or AIRS instrument on the Aqua satellite provided compelling evidence for the smoke influence of ozone chemistry in the District.

As expected, CO concentrations were greatest nearest to the fire source region of west-central Canada in both time and space, generally lessening in intensity as the plume dispersed and aged. However, CO concentrations over central CONUS ebbed and flowed from May 20 through June 1, confirming the supposition that the smoke recirculated several times around the central high-pressure system before reaching the District. The highest CO concentrations were noted with the thickest plume as it continued to enter CONUS on May 21 (Figure 34a). As illustrated in the conceptual model, the plume began to bifurcate at this stage, showing two lobes by May 22, one going south towards Nebraska while the other moved east (Figure 34). General dispersion of the plume began taking place beneath the central ridge.

By May 24, the influence of the cold front, which "cleans out" and pushes smoke back westward, was seen across the northeastern portion of the continent (Figure 34d). This process progresses on May 25, though note how a lobe of CO wraps around to the east across Ontario in accordance with the clockwise circulation around the high pressure (Figure 34e). The thickest CO remains just ahead of the cold front across the lower Ohio River Valley, such as Illinois and Missouri, where ozone exceedances occurred that day (Figures 23e1, 23f1 with Figure 34e).

CO remains locked within the circulation of the central high-pressure system on May 26 and 27 (Figure 34f and g). The densest CO concentrations stretch from Minnesota to southern Quebec on May 27. On May 28, distinct features tied to the narrative model were clear (Figure 34h). First, across central Quebec, a tight gradient in CO concentrations existed, delineating the existence of the cold front, which eventually pushed through the District on May 29. Cleaner air with no smoke north of the front accounts for the lighter shade of red and orange in these areas. South of the front, CO seems to intensify, likely due to the convergence of air along the front as it moves south.

On May 29, the front moved substantially farther south, with a line of higher CO concentrations from New York to western Ontario (Figure 34i). What was particularly striking was the decrease in CO concentrations across Quebec and the northeastern US behind the front. This was due to the subsidence of CO at this altitude towards the surface. This was confirmed by looking at lower altitude analysis (850 mb), where broad increases in CO were observed behind the cold front entering the US between May 28 and 29 (Appendix B, Figures B2 and B3). This confirms residual smoke within the high-pressure system pushed towards the surface behind the cold front, as described in the narrative model. While subsidence reduced CO at the altitude in Figure 35i, an arcing line of higher CO remained clear, associated with the cold front continuing southward.

From May 30 through June 2, CO concentrations diffuse/decrease across the northeastern US, generally dropping in concentration everywhere while generating a nearly uniform concentration within the Mid-Atlantic (Figure 34j-Figure 34m). By June 1 and 2, CO concentrations, even at lower elevations, had continued to drop, likely due to a combination of mixing, leading to uniformly lower concentrations and uptake in chemical reactions.

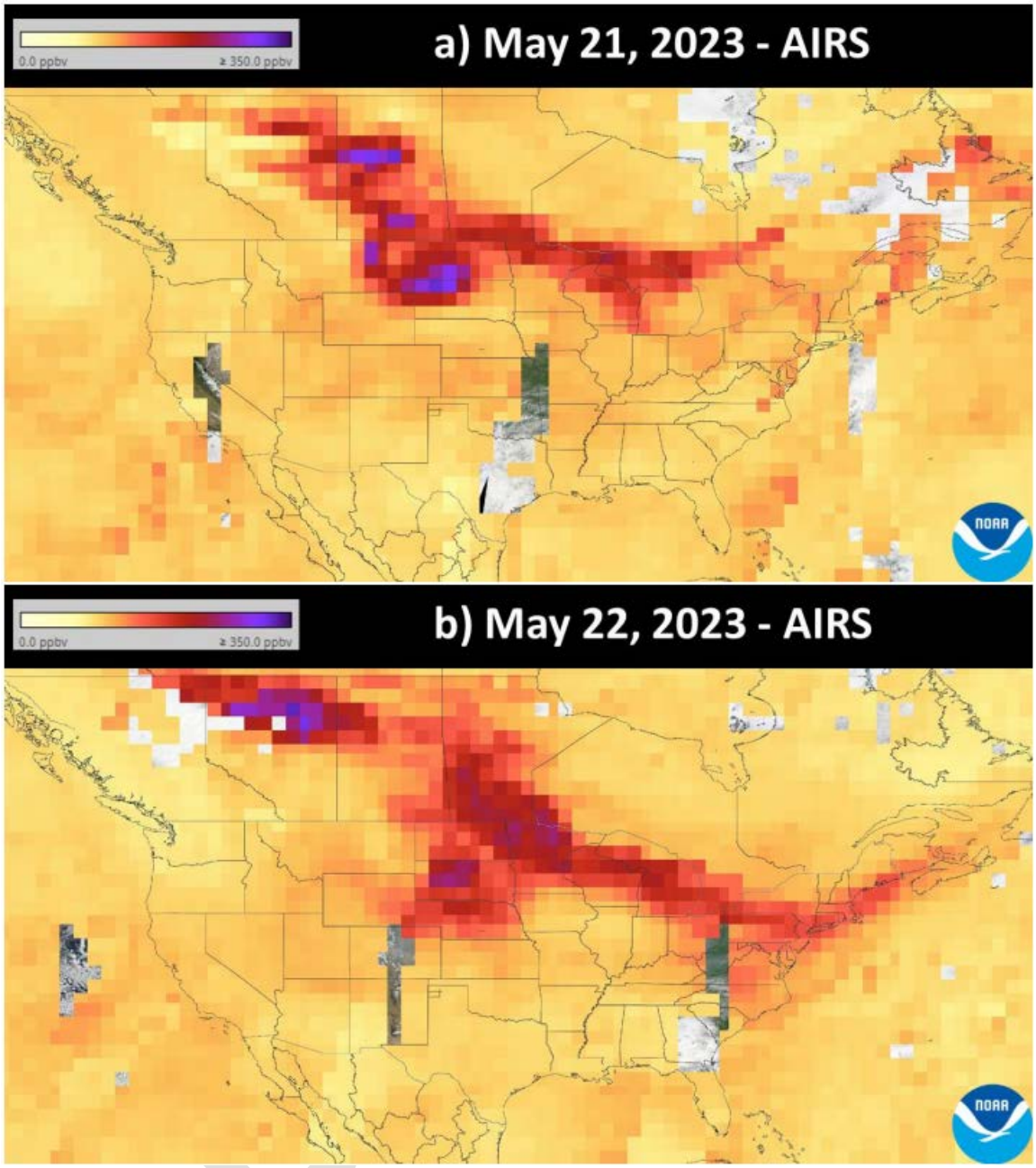
0.0 ppbv
≥ 350.0 ppbv
a) May 21, 2023 - AIRS
NOAA
0.0 ppbv
≥ 350.0 ppbv
b) May 22, 2023 - AIRS
NOAA

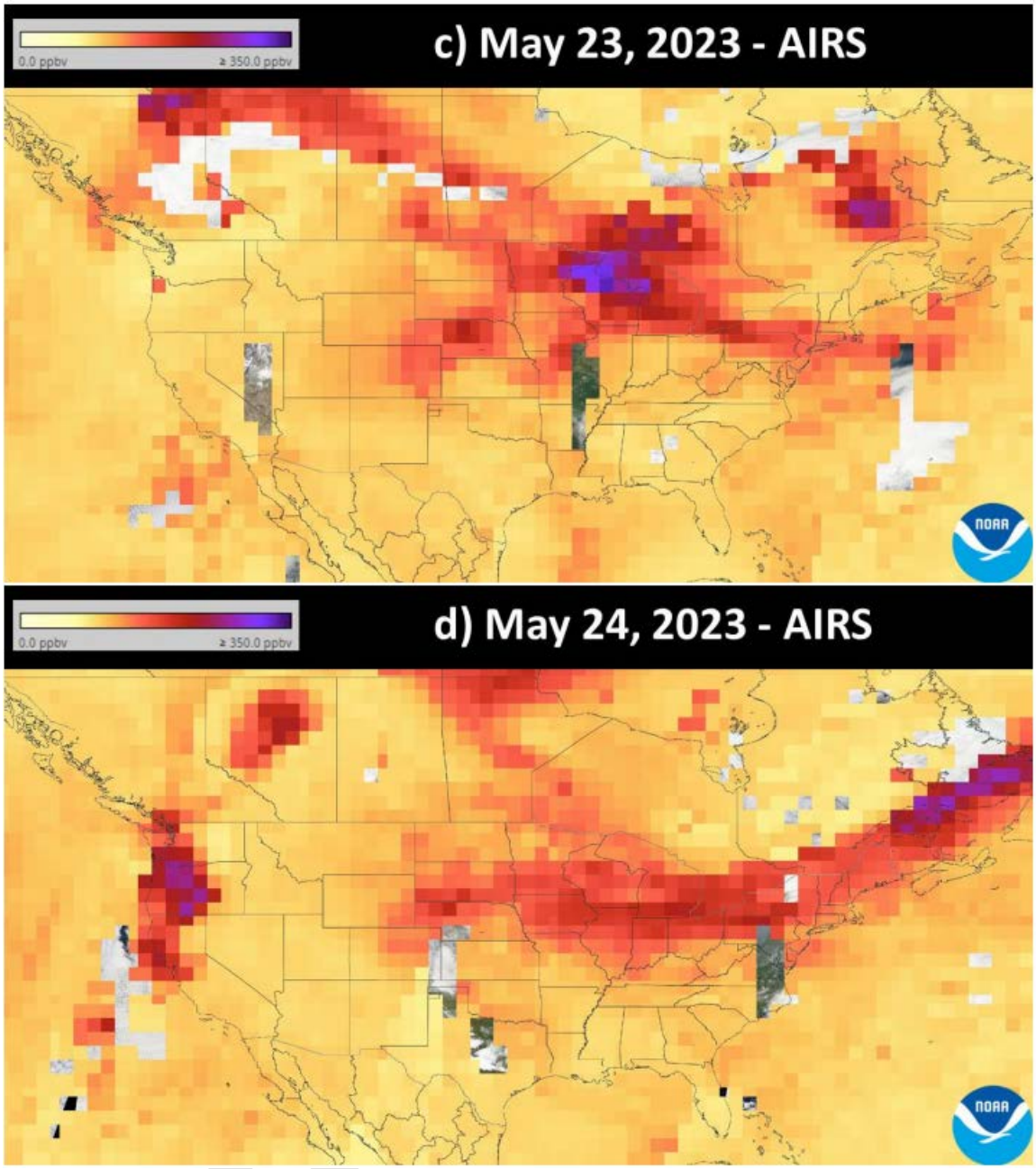
0.0 ppbv
≥ 350.0 ppbv
c) May 23, 2023 - AIRS
0.0 ppbv
≥ 350.0 ppbv
d) May 24, 2023 - AIRS

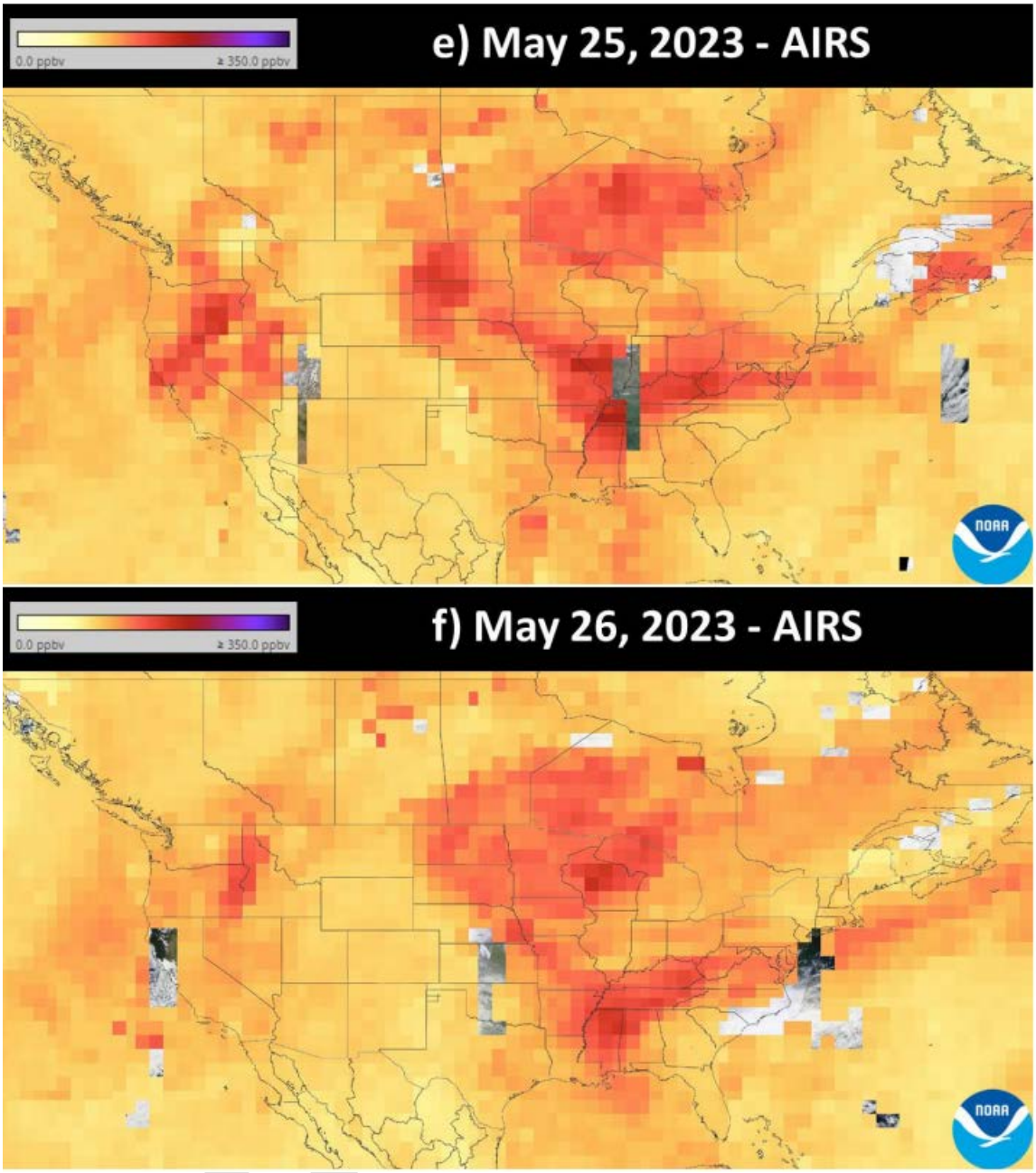
0.0 ppbv
≥ 350.0 ppbv
e) May 25, 2023 - AIRS
0.0 ppbv
≥ 350.0 ppbv
f) May 26, 2023 - AIRS

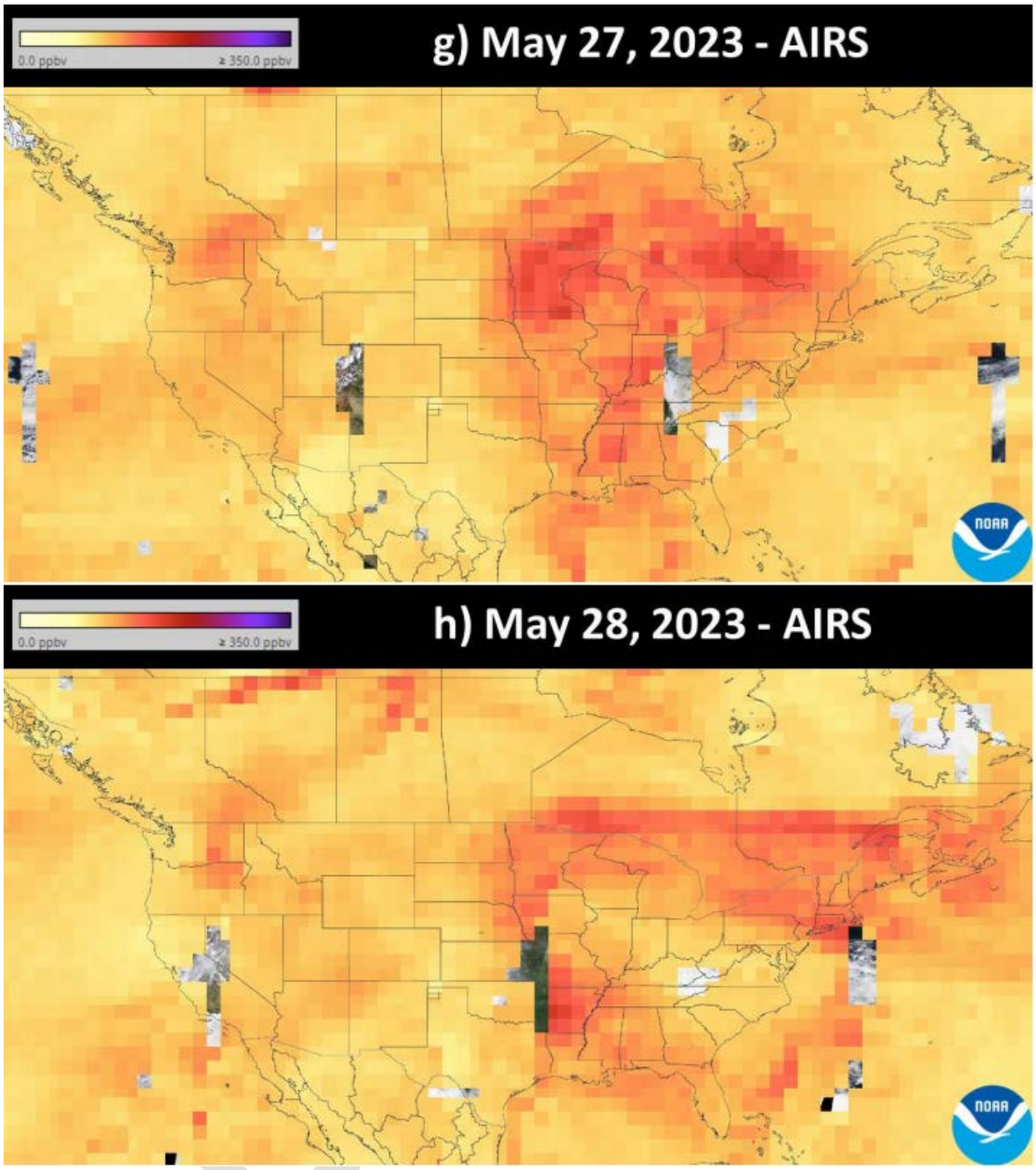
0.0 ppbv
≥ 350.0 ppbv
g) May 27, 2023 - AIRS
0.0 ppbv
≥ 350.0 ppbv
h) May 28, 2023 - AIRS

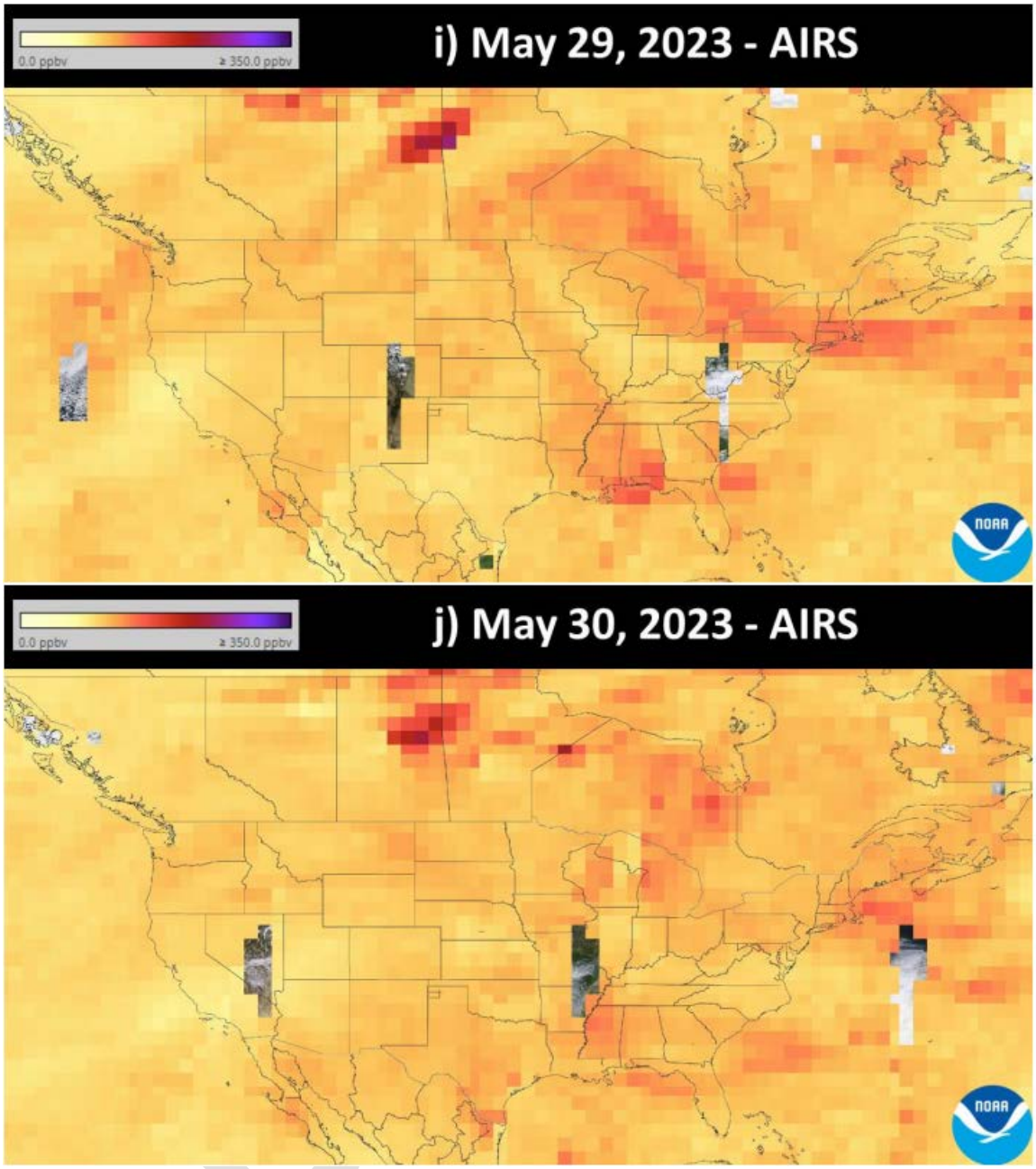
0.0 ppbv
≥ 350.0 ppbv
i) May 29, 2023 - AIRS
NOAA
0.0 ppbv
≥ 350.0 ppbv
j) May 30, 2023 - AIRS
NOAA

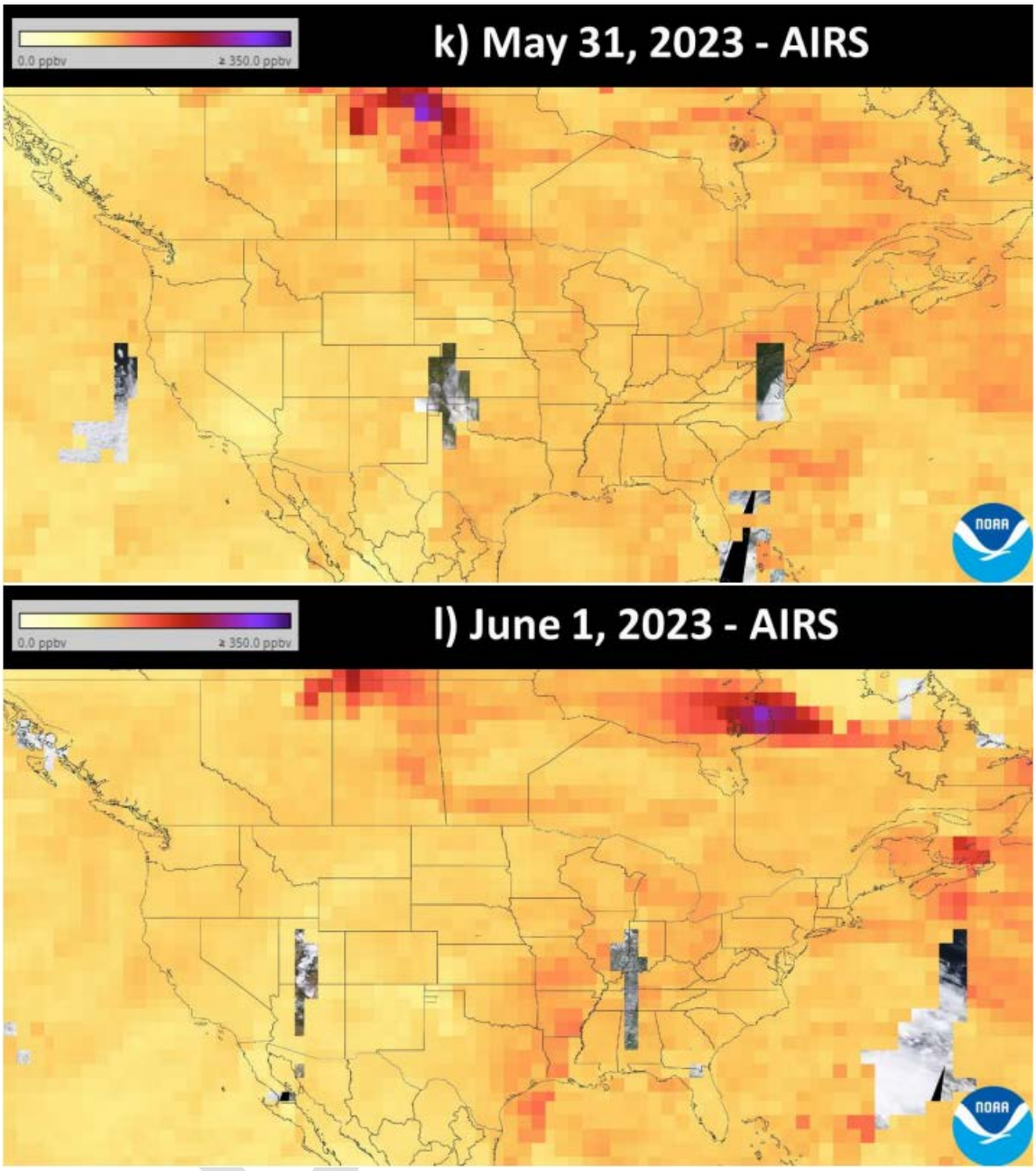
0.0 ppbv
≥ 350.0 ppbv
k) May 31, 2023 - AIRS
0.0 ppbv
≥ 350.0 ppbv
l) June 1, 2023 - AIRS

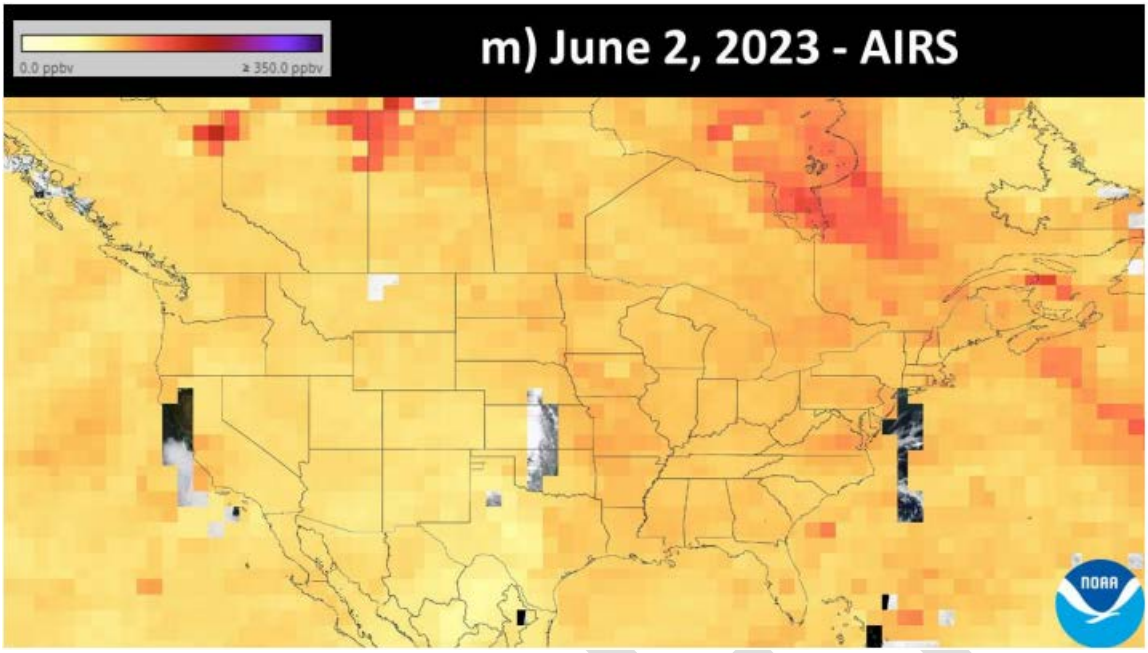

Figure 34: Carbon monoxide from the satellite. AIRS 500 mb retrieval from carbon monoxide images for May 21 - June 2, 2023 (a-m, respectively).
All images are retrieved from https://airs.jpl.nasa.gov/. [vi]Deeper yellows, oranges, reds, and purples indicate higher concentrations of carbon monoxide in ppb through the atmospheric column or layer.

3.4.3 Nitrogen Oxides

Singh et al. (2012) showed that ozone production rates from wildfires in California were dependent upon available NO_x (NO_x = sum of nitrogen oxide (NO) and nitrogen dioxide (NO_2)) and that NO_x from the fires themselves was relatively low. However, NO_x emissions from fires can vary greatly, and research has noted the uncertainties in the influence of wildfire emissions from one to another (e.g., Hu et al., 2008). In the current study, all monitors observing the highest ozone concentrations were near urbanized areas, suggesting the local NO_x contributions from these areas were contributing to ozone concentrations, see Figure 35. Here, hourly ozone concentrations from McMillan and River Terrace were compared to Piney Run (Maryland) and State College (Pennsylvania), both of which are located in rural areas. However, in smoke, ozone production may occur more rapidly than otherwise may occur due to additional precursors being present. As such, NO_x in the District simply augmented ozone production within the smoky and already ozone-laden airmass since ozone concentrations within the smoke plume were already regionally increased, both in rural and urban areas. Ozone would not have reached the MD8AO concentrations observed during the event without the presence of the smoke.

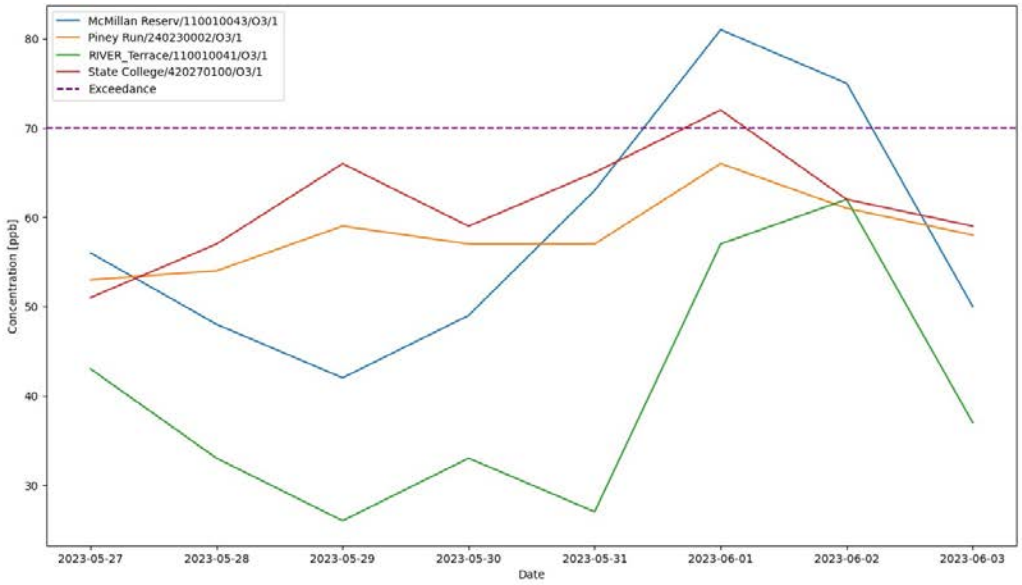

Figure 35: Comparison of hourly ozone concentrations from both urban District monitors vs rural monitors Piney Run (Maryland) and State College (Pennsylvania) from May 27th-June 3rd.

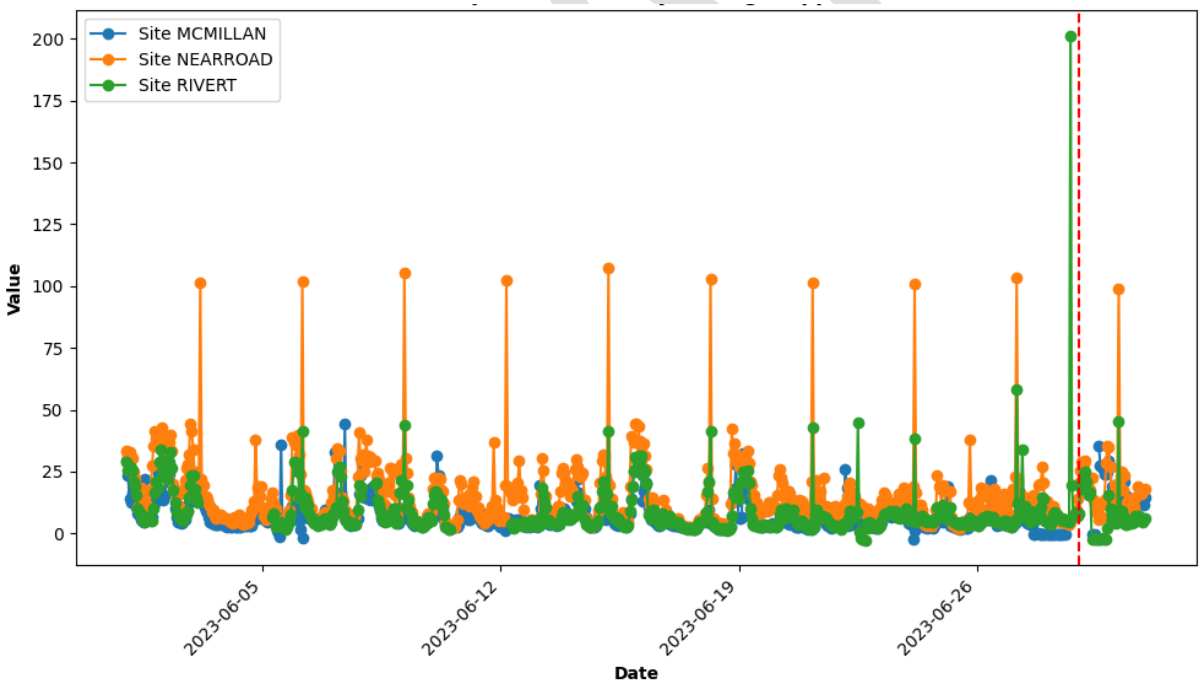

Figure 36: As in Figure 28, except for hourly nitrogen dioxide (NO_2) from available District monitors in June 2023.

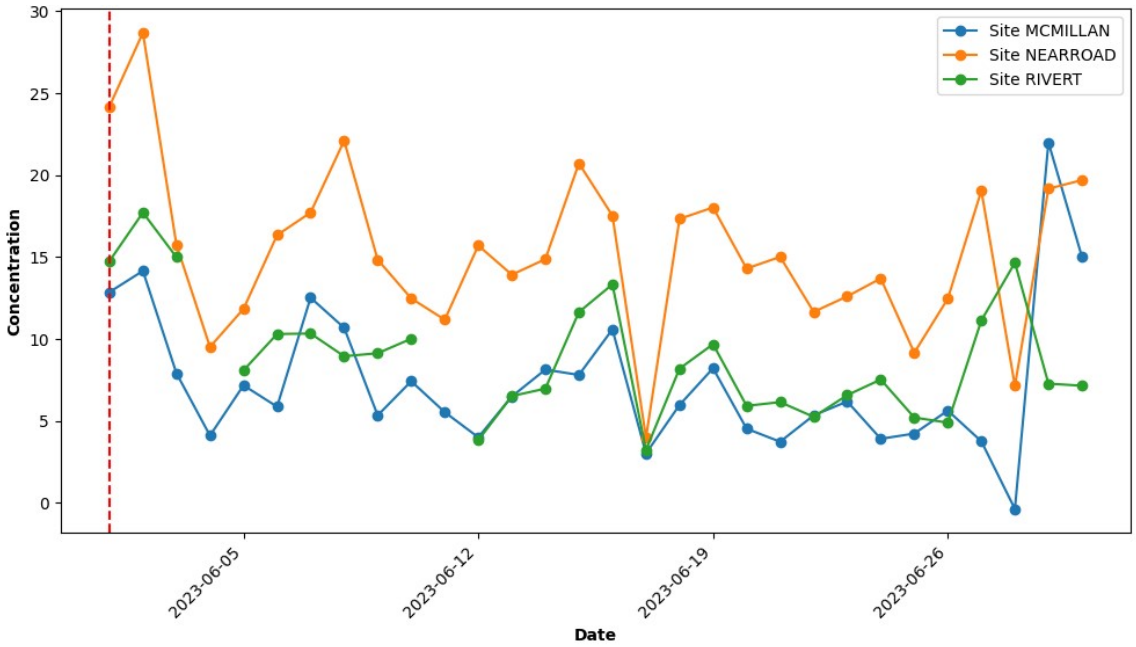

Figure 37: As in Figure 28, except for daily average nitrogen dioxide (NO_2) from available District monitors in June 2023. June 1, 2023, is identified with the red dashed line.

3.4.4 NO_x Historical Context: Local June NO_x, Aged Nitrogen, and Total Reactive Nitrogen

Singh et al. (2012) showed that ozone production rates from wildfires in California were dependent upon available NOx (NOx = sum of nitrogen oxide (NO) and nitrogen dioxide (NO2)) and that NOx from the fires themselves was relatively low. However, NOx emissions from fires can vary greatly, and research has noted the uncertainties in the influence of wildfire emissions from one to another (e.g., Hu et al., 2008). Fire radiative power (FRP), proportional to fire temperature, showed intense temporal increases due to the west-central Canada fires, suggesting the propensity for higher NO emission from these fires. Tropomi column retrievals already shared showed the smoke plume was associated with NO2. The several-day travel time of the smoke plume provided time for nitrogen to age within the smoke plume. Thus, in a similar fashion to Dreessen et al. (2016), NOy, and particularly NOT (NOy - NOx), should be much higher than at other times of the season if an aged plume of NOx traveled with the smoke plume. In essence, in the presence of sunlight, the NOx and VOCs present within the plume should react and "age" the air. NO_T is a measure of the "reservoir" species, a category of nitrogen compounds encompassing nitrogen species that can be transported long distances, indicate aged pollution, and can dissociate (break apart) in sunlight to 138 enhance ozone production by providing additional NOx for chemical reactions. If nitrogen is stored in the plume as the smoke ages, NO_T should be higher during smoke events. As a plume of NO2 was captured by the TROPOMI satellite, we may expect higher NO_T at the surface of the smoke impacted the surface.

Subjective analysis of nitrogen species allows some qualitative source attribution. Generally, it is difficult to distinguish NO_x sources from each other (i.e., point, mobile, wildfire). Fresh NO_x emissions tend to be dominated by Nitrogen Oxide (NO) rather than Nitrogen Dioxide (NO_2) or other non-NOx

speciation (NO_T). NO has a shorter lifetime due to its high reactivity. Thus, an airmass dominated by NO_T tends to indicate aged emissions amid a reactive airmass. The composition of the NO_x was overwhelmingly composed of older and 'storage' nitrogen species on June 1-2. The high levels of NO_2 were indicative of an aged airmass, NO_x transport, and, therefore, non-local emissions. DOEE, therefore, contends the increased NOx observed during the ozone event was a result of efficient NOx storage within the smoke plume sourced from the fire itself and diminutive regional NOx contributions, both of which caused NO_Y and NO_T to be beyond contemporary concentrations in the District, further leading to ozone at statistically extreme concentrations.

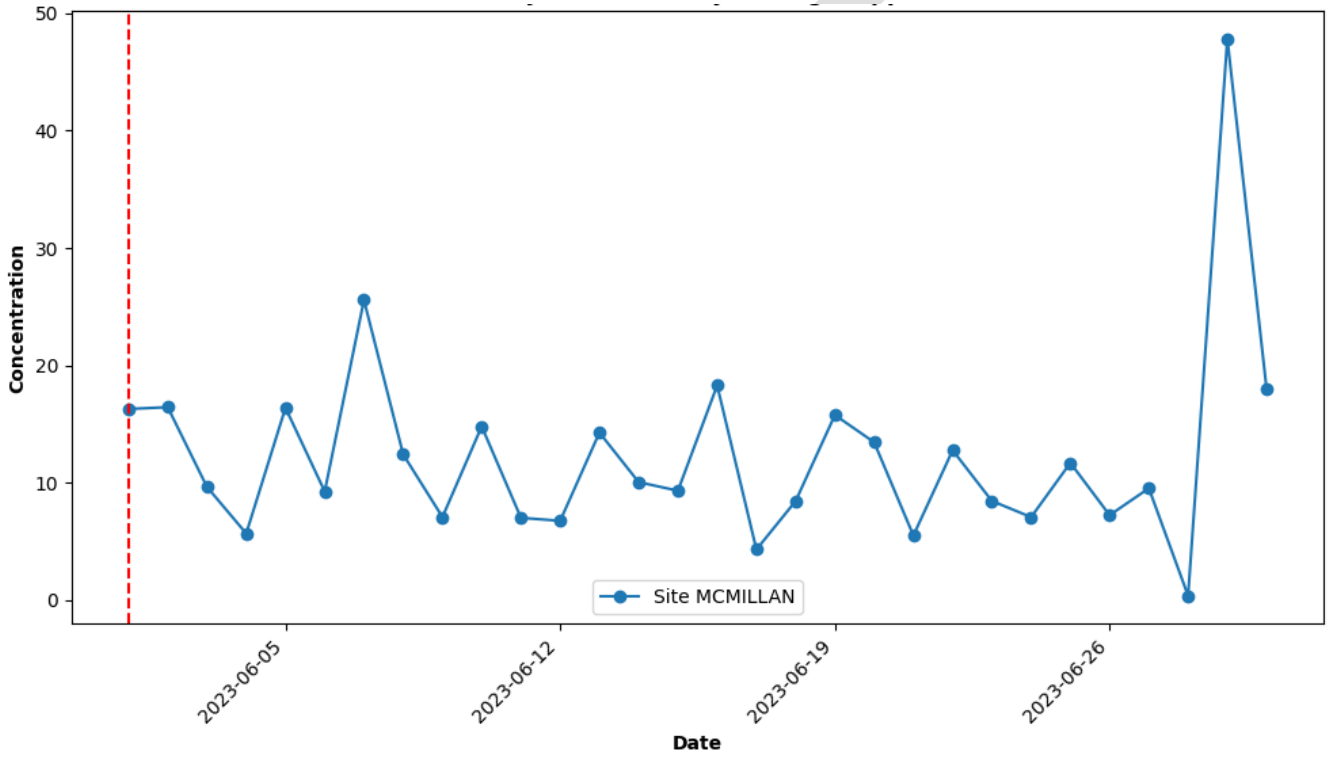

Figure 38: Daily oxides of Nitrogen concentrations at the District's McMillan site for the month of June.

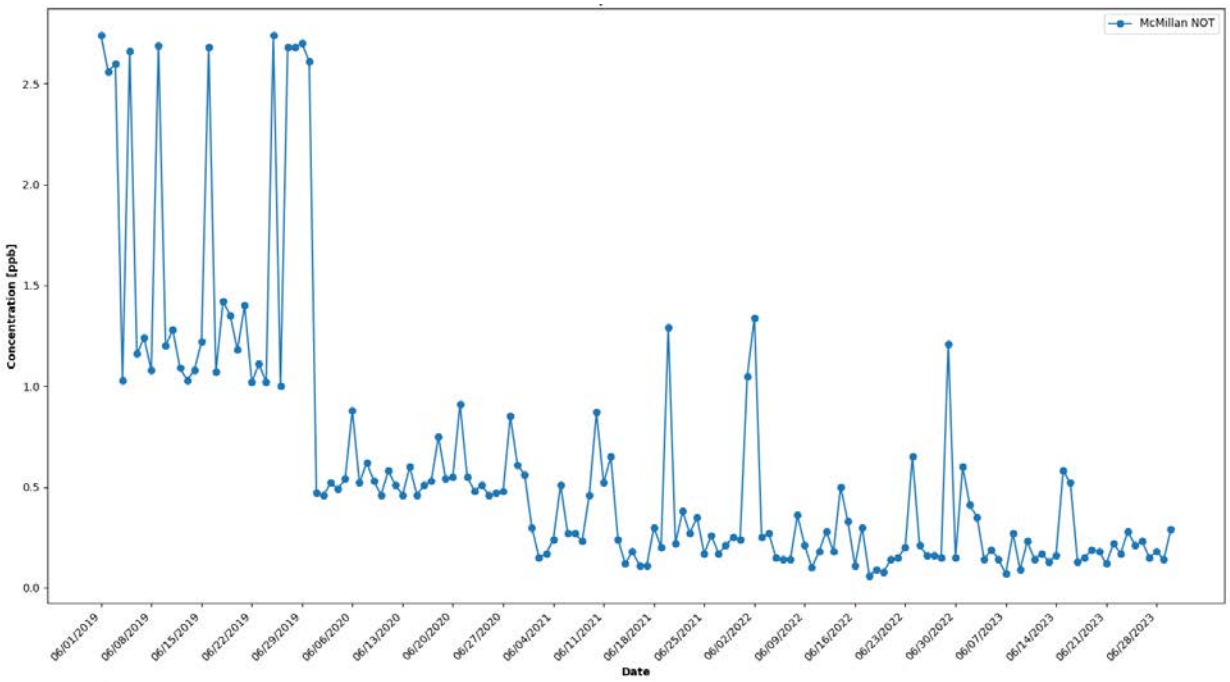

Figure 39: NOT concentrations from McMillan monitor for days in June from 2019 to 2023.

4.0 The Occurrence was a Natural Event

According to the Clean Air Act (CAA)[vii] and the Exceptional Events Rule (40 CFR § 50.14), an exceptional event must be "an event caused by human activity that is unlikely to recur at a particular location or a natural event." The Quebec fires were a "natural event." The Exceptional Events Rule defines a wildfire as "…any fire started by an unplanned ignition caused by lightning; volcanoes; other acts of nature; unauthorized activity; or accidental, human-caused actions, or a prescribed fire that has developed into a wildfire. A wildfire that predominantly occurs on wildland is a natural event." Based on the documentation provided in section 2 of this submittal, which discusses the origin and evolution of the wildfire events, the Quebec fires qualify as a "natural event" because they were unplanned fires on wildland ignited by lightning. EPA generally considers the emissions of ozone precursors from wildfires on wildland to meet the regulatory definition of a natural event as defined in the NAAQS. Accordingly, DOEE has shown that the event is a natural event and may be considered for treatment as an exceptional event.

5.0 The Occurrence was Not Reasonably Controllable or Preventable

Based on the documentation provided in section 2, the fires relevant in this demonstration were due to lightning that caused wildfire events on wildland. These fires were considered natural wildfire events by the EPA, were outside of the United States, and were therefore neither reasonably controllable nor preventable by the District of Columbia. No policy that the District enacted could have prevented the fire, or the smoke which it caused, from entering the United States, or DOEE was not aware of any evidence clearly demonstrating that prevention or control efforts beyond those actually made would have been reasonable. Therefore, emissions from these wildfires were not reasonably controllable or preventable and met the criterion for treatment as an exceptional event.

6.0 Public Comment

This is a draft for public comment. Analysis of the comments will be included in the final document.

7.0 Conclusions

Here, DOEE is focusing on the regulatory significance of ozone during June 1 and 2, caused by the arrival of smoke, starting May 30th. We saw near ozone exceedances on May 31st and exceedances on June 1 and 2. It was evident a clear causal relationship between wildfire smoke and ozone was established prior to the impacts on June 1.

The June 1 and 2 events surpassed the 99th percentile for 2019-2023 for the McMillan monitor. Tracking of smoke from hundreds of fires across west-central Canada, fires in Nova Scotia, and fires locally in New Jersey provided cumulative precursors in the District to push ozone well into the upper tail of the statistical distribution of ozone in contemporary times. The monitored 8-hour ozone concentrations were elevated, reaching as high as 81ppb on June 1. The analysis provided in sections 2 and 3 of this demonstration supports DOEE's position that the May 30th-June 3 wildfire smoke event in the District, the culmination of the regulatorily significant exceedances on June 1 and 2, affected air quality in such a way that there exists a clear causal relationship between the events discussed and the monitored concentrations on June 1 and 2, 2023 and thus satisfies the clear causal relationship criterion for exclusion.

Exclusion of the MD8AO concentrations on June 1 and 2, 2023, directly impacts the design value at McMillan Reservoir, and that brings the site into attainment of 70ppb when considering this event in isolation.

8.0 References

Adam, M., M.Pahlow, V.A. Kovalev, J. M. Ondov, M.B. Parlange, and N. Nair. (2004) Aerosol optical characterization by nephelometer and lidar: The Baltimore Supersite experiment during the Canadian forest fire smoke intrusion. *J. Geophys. Res. Atmos.* (1984–2012) 109: D16. doi:10.1029/2003JD004047

Andreae, M.O., and P. Merlet. (2001) Emission of trace gases and aerosols from biomass burning. *Global biogeochem. Cycles 15*(4): 955–66. doi:10.1029/2000GB001382

Bytnerowicz, A., D. Cayan, P. Riggan, S. Schilling, P. Dawson, M. Tyree, L. Wolden, R. Tissell, and H. Preisler. (2010) Analysis of the effects of combustion emissions and Santa Ana winds on ambient ozone during the October 2007 southern California wildfires. *Atmos. Environ. 44*(5): 678–87. doi:10.1016/j.atmosenv.2009.11.014

Chai, T., H.-C. Kim, P. Lee, D. Tong, L. Pan, Y. Tang, J. Huang, J. McQueen, M. Tsidulko, and I. Stajner. (2013) Evaluation of the United States National Air Quality Forecast Capability experimental real-time predictions in 2010 using Air Quality system ozone and NO2 measurements. *Geosci. Model Dev. 6*(5): 1831–50. doi:10.5194/gmd-6-1831-2013

Colarco, P.R., M.R. Schoeberl, B.G. Doddridge, L.T. Marufu, O. Torres, and E.J. Welton. (2004) Transport of smoke from Canadian forest fires to the surface near Washington, DC: Injection height, entrainment, and optical properties. *J. Geophys. Res. Atmos.* (1984–2012) 109:D6. doi:10.1029/2003JD004248

DeBell, L.J., R.W. Talbot, J. E. Dibb, J. W. Munger, E.V. Fischer, and S.E. Frolking. (2004) A major regional air pollution event in the northeastern United States caused by extensive forest fires in Quebec, Canada. *J. Geophys. Res. Atmos.* (1984–2012) 109:D19. doi:10.1029/2004JD004840

Dreessen, J., Sullivan, J., & Delgado, R. (2016) Observations and impacts of transported Canadian wildfire smoke on ozone and aerosol air quality in the Maryland region on June 9–12, 2015. *Journal of the Air & Waste Management Association, 66*(9), 842-862.

EPA (1997) Peer Review of CASTNet, *Federal Register*, Vol. 62, No. 40 (1997): 9189. http://www.gpo.gov/fdsys/pkg/FR-1997-02-28/pdf/97-4967.pdf

EPA (2006) Air Quality Criteria For Ozone and Related Photochemical Oxidants (Final Report, 2006). US. Environmental Protection Agency, Washington, DC, EPA/600/R-05/004aF-cF, 2006.

Fiore, AM., R.B. Pierce, R.R. Dickerson, M. Lin, and R. Bradley. (2014) Detecting and attributing episodic high background ozone events. *Environ. Manage. 64*: 22.

Flannigan, M.D., and van Wagner, C.E. (1991) Climate change and wildfire in Canada. *Canadian Journal of Forest Research. 21*(1)(Jan,1991) https://doi.org/10.1139/x91-010

Gégo, E.P., S. Porter, A. Gilliland, and S.T. Rao. (2007) Observation-based assessment of the impact of nitrogen oxides emissions reductions on ozone air quality over the eastern United States. *J. Appl. Meteorol. Climatol. 46*(7): 994–1008. doi:10.1175/JAM2523.1

District of Columbia Exceptional Event Demonstration and Analysis of the June 2023 Nova Scotia Wildfires, New Jersey fires and Their Impact on DC's Air Quality on June 1-2, 2023

Hu, Y., M.T. Odman, M.E. Chang, W. Jackson, S. Lee, E.S. Edgerton, K. Baumann, and A.G. Russell. (2008) Simulation of air quality impacts from prescribed fires on an urban area. *Environ. Sci. Technol. 42*(10): 3676–82. doi:10.1021/es071703k

Marlons, J.R., Bartlein, P.J., Walsh, M.K., Whitlock, C. (2009) Wildfire responses to abrupt climate change in North America. *Proceedings of the Nat'l Academy of Sciences 106* (8) 2519-2524, https://doi.org/10.1073/pnas.0808212106

Maryland Department of the Environment, Air and Radiation Management Administration. (2012) Creating a climate for clean air. *e'mde* 5 (4). http://mde.maryland.gov/programs/researchcenter/reportsandpublications/emde/pages/researchcenter/publications/general/emde/vol5no4/article%201.aspx#.VlM-5r_gKPV.

Maryland Department of the Environment. (2022) *Ambient air monitoring plan for calendar year 2023.* https://mde.maryland.gov/programs/air/AirQualityMonitoring/Documents/MDNetworkPlanCY2023.pdf

Maryland Department of the Environment. (2015) Linking weather and air quality using radar. Air and Radiation Management Administration, Monitoring Program. Last modified December 1, 2015. http://www.mde.state.md.us/programs/Air/AirQualityMonitoring/Pages/Radar.aspx

McKeen, S.A., G. Wotawa, D.D. Parrish, J.S. Holloway, M.P. Buhr, G. Hübler, F.C. Fehsenfeld, and J.F. Meagher. (2002) Ozone production from Canadian wildfires during June and July of 1995. *J. Geophys. Res. Atmos.* (1984–2012) 107 (D14): ACH–7. doi:10.1029/2001JD000697

McNamara, D. P., George Stephens, Mark Ruminski, and Tim Kasheta. (2004) The Hazard Mapping System (HMS)—NOAA's Multi-Sensor Fire and Smoke Detection Program Using Environmental Satellites. In *Proceedings of the 13th Conference on Satellite Meteorology and Oceanography*.

Morris, G.A., S. Hersey, AM. Thompson, S. Pawson, J.E. Nielsen, P.R. Colarco, and W.W. McMillan. (2006) Alaskan and Canadian forest fires exacerbate ozone pollution over Houston, Texas, on 19 and 20 July 2004. *J. Geophys. Res. Atmos.* (1984–2012) 111(D24). doi:10.1029/2006JD007090

Pechony, O., Shindell, D.T. (2010) Driving forces of global wildfires over the past millennium and the forthcoming century. *Proceedings of the Nat'l Academy of Sciences 107*, 19167-19170, doi:10.1073/pnas.1003669107.

Putero, D., Landi, T. C., Cristofanelli, P., Marinoni, A., Laj, P., Duchi, R., ... & Bonasoni, P. (2014). Influence of open vegetation fires on black carbon and ozone variability in the southern Himalayas (NCO-P, 5079 m asl). *Environmental Pollution*, *184*, 597-60

Roberts, Sandra, et al. (2022) Multidecadal Trends in Ozone Chemistry in the Baltimore-Washington Region. *Atmopheric Environment, 285.*

Rolph, G.D., (2017) Real-time Environmental Applications and Display sYstem (READY) Website (http://ready.arl.noaa.gov). NOAA Air Resources Laboratory, Silver Spring, MD.

District of Columbia Exceptional Event Demonstration and Analysis of the June 2023 Nova Scotia Wildfires, New Jersey fires and Their Impact on DC's Air Quality on June 1-2, 2023

Ryan, William F. (2004) The low level jet in Maryland: profiler observations and preliminary climatology. *Report for Maryland Department of the Environment, Air and Radiation Administration*. Maryland State Implementation Plan, Appendix-G (2004).

Sapkota, A., Symons, J.M., Kleissl, J., Wang, L., Parlange,M.B., Ondov, J., Breysse, P.N., Diette, G.B., Eggleston, P.A., Buckley, T.J. (2004) Impact of the 2002 Canadian Forest Fires on Particulate Matter Air Quality in Baltimore City. *Environ. Sci. Technol., 39* (1), 24–32 https://doi.org/10.1021/es035311z

Singh, H.B., C. Cai, A. Kaduwela, A. Weinheimer, and A.Wisthaler. (2012) Interactions of fire emissions and urban pollution over California: Ozone formation and air quality simulations. *Atmos. Environ. 56*: 45–51. doi:10.1016/j.atmosenv.2012.03.046

Spichtinger, N., M. Wenig, P. James, T. Wagner, U. Platt, and A. Stohl. (2001) Satellite detection of a continental-scale plume of nitrogen oxides from boreal forest fires. *Geophys. Res. Lett. 28*(24): 4579–82. doi:10.1029/2001GL013484

Spracklen, D.V., Mickley, L.J., Logan, J.A., Hudman, R.C., Yevich, R., Flannigan, M.D., Westerling, A.L. (2009) Impacts of climate change from 2000 to 2050 on wildfire activity and carbonaceous aerosol concentrations in the western United States. *Journal of Geophysical Research, Atmospheres. 114*:D20 https://doi.org/10.1029/2008JD010966

Stein, A.F., Draxler, R.R, Rolph, G.D., Stunder, B.J.B., Cohen, M.D., and Ngan, F., (2015). NOAA's HYSPLIT atmospheric transport and dispersion modeling system, *Bull. Amer. Meteor. Soc., 96*, 2059-2077, http://dx.doi.org/10.1175/BAMS-D-14-00110.1

Westerling, A.L., Hidalgo, H.G., Swetnam, T.W. (2006) Warming and Earlier Spring Increase Western US. Forest Wildfire Activity. *Science 313*(5789): 940-943, DOI: 10.1126/science.1128834

[i] *Guidance on the Preparation of Exceptional Events Demonstrations for Wildfire Events that May Influence Ozone Concentration*s. EPA-HQ-OAR-2015-0229-0130, US. Environmental Protection Agency: https://www.epa.gov/sites/default/files/2016-09/documents/exceptional_events_guidance_9-16-16_final.pdf

[ii] *District of Columbia Calendar Year 2024 Annual Ambient Air Monitoring Network Plan.*
District of Columbia Department of Energy and Environment:
Public Comment Period - 2024 Annual Ambient Air Monitoring Network Plan | doee (dc.gov)

[iii] https://www.ctvnews.ca/canada/nearly-350-firefighters-from-the-eu-will-help-battle-relentless-canadian-wildfires-1.6437130

[iv] *Guidance on the Preparation of Exceptional Events Demonstrations for Wildfire Events that May Influence Ozone Concentration*s. EPA-HQ-OAR-2015-0229-0130, US. Environmental Protection Agency, Section 3.5: https://www.epa.gov/sites/default/files/2016-09/documents/exceptional_events_guidance_9-16-16_final.pdf

[v] Ibid.

[vi] https://airs.jpl.nasa.gov/

[vii] Guidance on the Preparation of Exceptional Events Demonstrations for Wildfire Events that May Influence Ozone Concentrations, Final, EPA, September 2016, page 30: https://www.epa.gov/sites/production/files/2016-09/documents/exceptional_events_guidance_9-16-16_final.pdf , 42 US.C. 7401 et seq,